Project HULK

X-ray dose-rate detector for material irradiation

EEL4914 - Senior Design I
Group 26

Myesha Rahman, EE
Labiba Ibrahim, EE
Madeline Moran, EE
Janani Nagaraj, CpE

Sponsored by Radiation Effects and Reliability Lab (RERL) under Dr. Enxia Zhang
Reviewers: Dr. Enxia Zhang, Dr. Jaesung Lee, Professor Mark Maddox
Mentor: Saleem Sahawneh

Table of Contents

List of Tables

List of Figures

Chapter 1 Executive Summary

In the Radiation Effects and Reliability Lab (RERL), the X-Rad 320 machine is used to deliver precise and repeatable radiation doses within a controlled and shielded environment. Accurate dosimetry—the process of quantifying how much x-ray energy is absorbed by a sample during exposure—is essential for validating experiments, ensuring equipment performance, and maintaining safe operation. Project Hulk is designed to support this need by using a PIN diode to sense the radiation produced by the X-Rad 320. When irradiated, the PIN diode generates a small current that is directly proportional to the dose rate. This current is then transmitted to the Project Hulk system, where it undergoes filtering, amplification, and digital conversion before being represented as a continuously updating graphical display of the measured dosimetry.

Developed in close collaboration with the RERL, Project Hulk was designed, assembled, and tested by engineering students at the University of Central Florida. The system is divided into three primary hardware modules: the diode PCB, which houses and biases the radiation-sensing PIN diode; the signal conditioning PCB, which applies amplification, filtering, and noise mitigation techniques to ensure the integrity of the diode’s output; and the readout PCB, which includes the microcontroller, memory, display, and supporting electronics that interpret and visualize the data. These stages work together to reliably capture the diode’s current, convert it into a dose-rate measurement, and provide real-time updates of the X-ray output as it varies over the course of an exposure.

This documentation serves as a detailed account of the planning, design, and development process for Project Hulk. It includes a thorough discussion of component selection, system architecture, implementation strategies, and testing results, as well as the project’s goals, objectives, and design limitations. The report begins by presenting an overview of the project’s purpose and the engineering motivation behind its creation, followed by a description of the baseline requirements and constraints established during initial planning. It then expands into a comparison of possible hardware and software solutions, providing justification for the selected components and design choices.

Subsequent sections examine the standards, safety considerations, and environmental constraints that influence the system’s design, along with detailed schematics and descriptions of the three major subsystems. The documentation also outlines the testing procedures used to verify proper operation at each stage, the iterative development process that refined the design, and the final PCB layouts and firmware functionality implemented in the readout unit.

The final portion of this report includes administrative content, conclusions drawn from the project’s outcomes, and supporting appendices and references. Altogether, this documentation provides a complete and transparent record of the engineering decisions, challenges, and successes that led to the creation of Project Hulk—a system intended to improve dosimetry visualization and support ongoing radiation research within the RERL.

Chapter 2 Introduction

2.1 Introduction

Radiation research is more critical than ever as we continuously evaluate the effects of ionizing radiation on all types of electronic devices. Radiation is a powerful tool that enables advancements in medicine, security, and electronics testing. X-ray irradiation, in particular, plays a key role in simulating specific environments and testing radiation effects and device reliability. The measurement of absorbed radiation, known as dosimetry, is essential for such studies. Measuring radiation accurately in real-time is essential to protect people, ensure equipment reliability, and conduct meaningful scientific research. Without proper monitoring, researchers and engineers risk drawing incomplete conclusions or, worse, exposing themselves and their equipment to unsafe conditions.

The current industry standard for measuring X-ray dose rates involves ionizing gas chambers . While highly accurate, these systems are bulky, expensive, and require specialized infrastructure such as gas lines, high-voltage supplies, and complex cabling [1]. This makes them inaccessible for many laboratories and impractical for flexible, low-cost setups. As a result, there is a critical need for a simpler, more affordable way to monitor X-ray dose rates without sacrificing accuracy.

At the University of Central Florida, the Precision X-ray 320, which delivers a precise radiation dose with energy up to 320 KV is going to be used for irradiation experiments. But there is currently no integrated system to measure or display real-time dosimetry during operation. This limits the ability to benchmark device degradation under controlled dose conditions.

To tackle this challenge, our project proposes the development of a portable, solid-state X-ray detector based on a silicon PIN photodiode. In order to make it simple, affordable and portable, the project will use low-noise amplification techniques and digital readout electronics. The photodiode will generate a current proportional to the incident X-ray flux [1]. This current will then be converted into a voltage by the precision transimpedance amplifier and read by Raspberry Pi. Raspberry Pi will convert these measurements into dose rates by applying calibration formulas. Finally, the dose rates will be logged and visualized on a PC/display for real-time monitoring [4].

We will use the AXUV20HS1 PIN diode, selected for its fast response, low capacitance, and adequate active area coverage. The diode will be connected with a transimpedance amplifier circuit for current readout, Raspberry Pi for real-time conversion of diode current into dose rate, and a USB interface for PC-based visualization and logging.

The system will further include:

- Filter integration (e.g., 150 μm Al or 2 mm Al + 1 mm Pb) to approximate Co-60 spectra and enable energy-dependent calibration.
- A benchmarking mode to compare diode readings with reference MOSFET degradation data to ensure consistency with industry-standard Co-60 irradiation [4].
- Error-handling features, including saturation detection, baseline zeroing, and range switching, to improve measurement reliability [4].
- Stretch functionalities, such as a handheld display, wireless data transfer, and onboard memory for storing historical dose measurements.

By combining these features, our project aims to close the gap between complicated, high-cost dosimetry methods and the need for a real-time, accessible, and reliable radiation measurement tool for research purposes.

2.2 Goals and Objectives

The goals and objectives are provided below. The goals define our expected outcome from this project and the objectives define the specific means to achieve that.

<u>Basic goal:</u>

Build a safe, portable, real-time radiation dosimeter using a silicon PIN diode that is capable of measuring, displaying, and logging dose rates during X-ray irradiation experiments.

<u>Basic Objectives:</u>

- Build a transimpedance amplifier circuit with precision, low-noise, low-input-bias-current operational amplifiers for diode current readout [1].
- Implement a program on Raspberry Pi to convert diode current into dose rate.
- Log data using a high-resolution Analog-to-Digital Converter (ADC) [5], then process these values with a Raspberry Pi to convert them into dose rates. The dose rates will be stored in a CSV file on a USB drive, which can later be accessed on a PC.

Advanced goals:

Integrate digital calibration curves, compare measurements against reference standards and implement an automated error-checking function.

Advanced Objectives:

- Add digital calibration curves for different filters (no filter, 2 mm Al filter, 2 mm Al + 1 mm Pb) by programming the Raspberry Pi to convert raw diode current to accurate dose-rates.
- Implement a real-time benchmarking mode to compare dosimeter measurements with MOSFET degradation data collected from a parameter analyzer.
- Automate error-checking functions: saturation detection, baseline zeroing, and range switching to ensure the software continuously monitors for hardware disruptions.

Stretch goal:

Increase system portability and usability by adding features that make the prototype standalone and user-friendly.

Stretch Objectives:

- Include wireless connectivity and mobile app to display dose-rates on a real-time dashboard for remote monitoring.
- Use the Raspberry Pi's microSD card to store data that can later be retrieved into a PC to access historical files [5].

2.3 Prior Related Work

2.3.1 Development of a Silicon PIN Diode X-Ray Detector

The Silicon PIN Diode X-Ray Detector is a PCB designed to detect radiation output by monitoring dose rate. As x-ray flux passes through a diode a current is produced. This current can be used to calculate the flux which leads to the calculation of the radiation dose. This project consists of many shared qualities with the PCB we will design.

The PCB consists of an AC and DC circuit to measure the radiation. The end goal for this project is to combine the AC and DC circuits to measure the pulses from the diodes at lower and higher dose rates respectively. The AC circuit was coupled to measure the radiation. A gamma ray is sent to a photodiode creating a photocurrent which is then sent through a high-pass filter coupled with a low-pass filter with a passband of 160 Hz to 18kHz.

In the DC circuit a high pass filter is placed in series with a non-inverting amplifier, two capacitors are also used to filter noise. This circuit worked and the output voltage measurements were taken at different distances from the source of the radiation. Using the Inverse Square Law and the known dose rates (at some of the distances), the dose rates at unknown distances were estimated. [1]

2.3.2 Experimental analysis of a novel and low-cost pin photodiode dosimetry system for diagnostic radiology

The system for diagnostic radiology is a two stage amplifier to measure the photocurrent from the PIN sensor, this current is then processed to be displayed on an LCD screen. The first stage of this amplifier is a trans-resistive amplifier to measure current changes which are then converted to voltages and sent to the second stage, a voltage amplifier, to amplify the first stage output voltage to a range between 0V and 2.5V. The circuit design was found to be very sensitive to noise and was placed in a small metal box to shield it. To evaluate the signal changes a full-wave rectifier was used.

In addition to this circuit, in this project a Digital Processing Unit was used to process the data. The first block of this was an ADC to digitalize the voltage output from the circuit. A signal channel analyzer (SCA) is used to measure the noise sources, this is used as a trigger signal to activate the multichannel analyzer (MCA). When the SCA is active the MCA begins to capture the data from the input signal, when the SCA is not active the MCA uses the data collected to calculate the voltage. [6]

2.4 Required Specifications

Table 2.4.1 Specifications Table

Parameter	**Value/Spec**
Dimensions of Housing	50mm L x 20mm W x 20mm H
X-ray energy limit	<320 keV
Dose rate range	~0.01 → ≥3 Gy/min
Weight	<3lbs
Power supply	5v battery
Cost	$2000

Display time	2-5 seconds
Accuracy	>95%
Display	Onboard 480×320 SPI TFT (3.5inch)
Sensor	Photodiode (AXUV20HS1)

2.5 Prototype Illustration

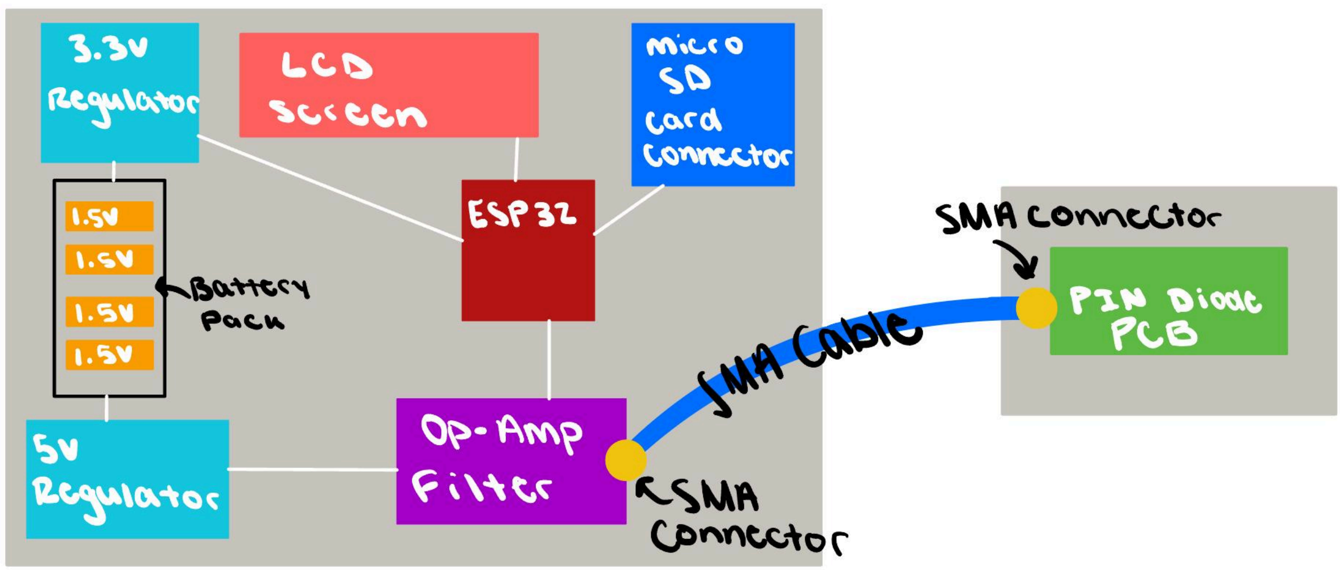

Figure 2.5.1 Prototype illustration

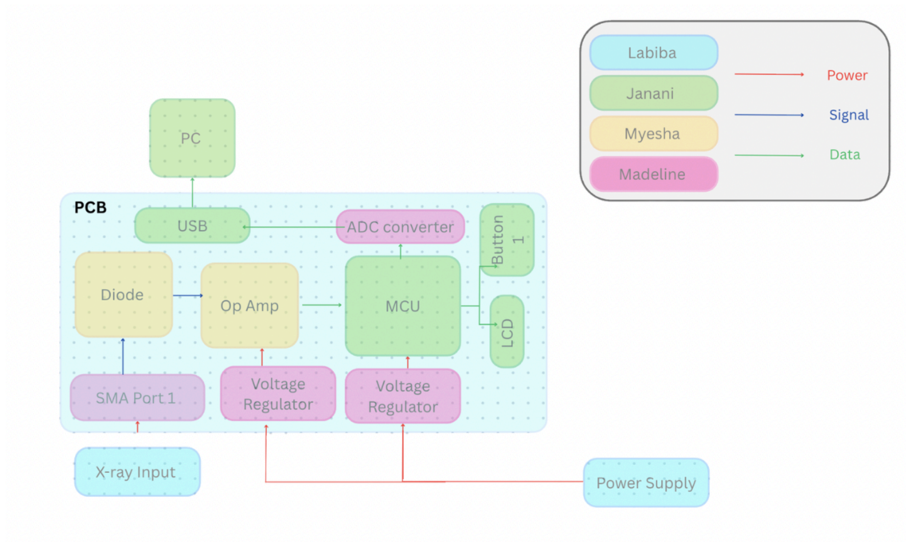

Figure 2.5.2 Hardware Diagram

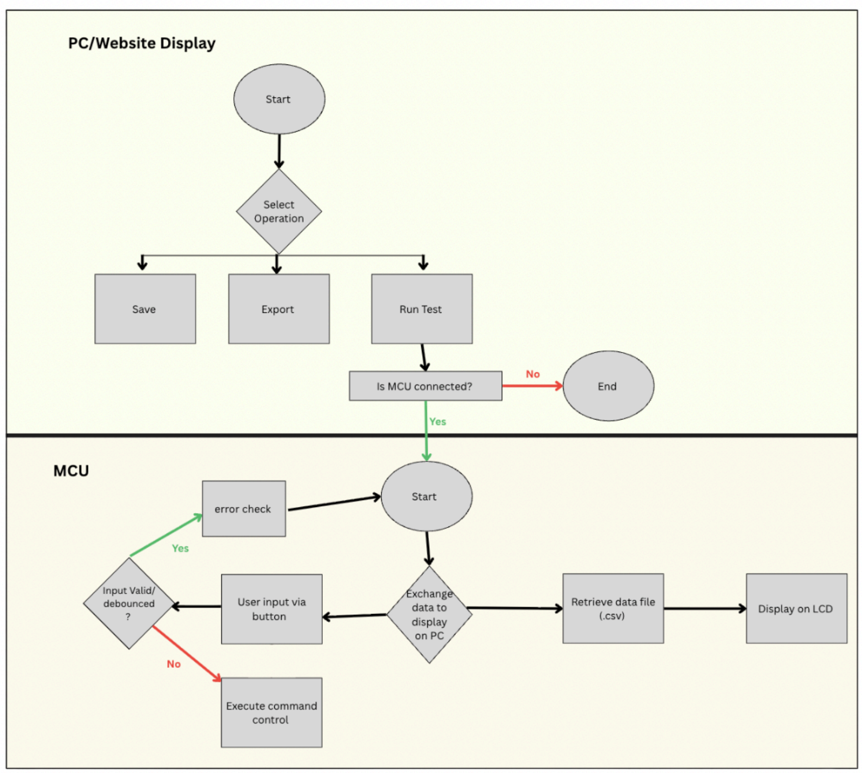

Figure 2.5.3 Software Diagram

2.6 House of Quality

Table 2.6.1 House of Quality

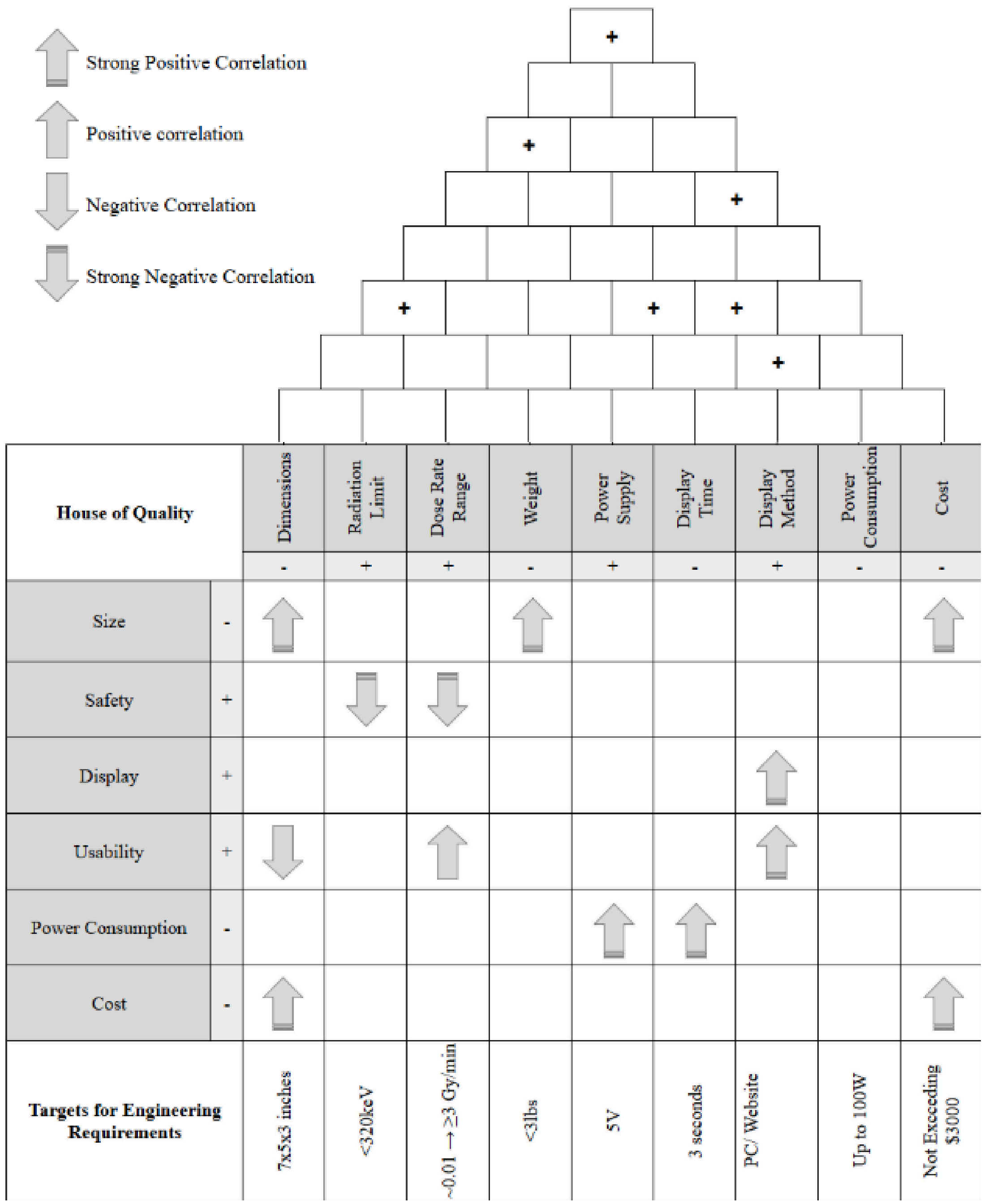

Marketing Requirements	Engineering Requirements
1, 4, 6	7x5x3 inches
2, 4	X-ray energy limit <320keV
2, 4	Dose rate range ~0.01 → ≥3 Gy/min
1, 4	Weight of <3lbs
4, 5	DC power supply of 5V
4, 5	Display time of 3 seconds
3, 4	Display Method
5	Up to 100W power consumption
6	Cost not exceeding $3000
Marketing Requirements: 1. Size 2. Safety 3. Display 4. Usability 5. Power Consumption 6. Cost	

Table 2.6.2 Work Distribution

Task	Primary	Secondary
Voltage Input	Labiba	Myesha
SMA Port 1	Madeline	Janani
Diode	Myesha	Labiba
Op Amp	Myesha	Labiba
SMA Port 2	Madeline	Janani
USB	Janani	Madeline
MCU	Janani	Madeline
LCD	Janani	Madeline
PC	Janani	Madeline

Power Supply	Labiba	Myesha
Voltage Regulator	Madeline	Janani
PCB	Labiba	Myesha

2.7 Milestones

Table 2.7.1 Senior Design 1 Milestones

Senior Design I - Fall 2025		
Milestone	Planned Duration	Status
Project idea	Week 1	Completed
Divide and Conquer Doc	Week 2-3	Completed
Meeting with Advisor (Dr. Sahawneh)	Week 4	Complete
Research and Design	Week 4-7	Complete
Create initial PCB schematic	Week 7	Complete
Select components	Week 8	Complete
Initial PCB Design	Week 9-Week 10	Complete
60 Page Document Submission	Week 10	Complete
Initial prototyping	Week 11	Complete
Troubleshooting	Week 12-15	Complete
Final 120 Page Document Submission	Week 16	Complete

Table 2.7.2 Senior Design 2 Milestones

Senior Design II - Spring 2026		
Milestone	Planned Duration	Status
Order final PCB and parts	Week 1	Incomplete
Design and fabricate housing	Week 2-3	Incomplete
Fabricate/print housing	Week 4	Incomplete
PCB assembly	Week 4-6	Incomplete
Build website	Week 5-8	Incomplete
Configure digital processing unit	Week 6-8	Incomplete
Integration	Week 7-9	Incomplete
Testing and Troubleshooting	Week 8-12	Incomplete
Presentation Prep	Week 12-13	Incomplete
Final Presentation	Week 14	Incomplete

Chapter 3 Introduction

3.1 General Research on X-ray

Research on X-ray radiation has been a relatively new topic. The need for this area of research started around the 1940s-1950s around World War II when nuclear weapons were being built. The earliest research focused on simple vacuum tubes and semiconductor diodes and transistors under gamma and X-ray exposure. Then around the 1960s-1980s, there was more motivation behind the research as scientists were working on space crafts. As there was a critical need to test electronic devices under space conditions, there was a bigger push on radiation research. NASA, U.S. military and Soviet space programs pushed heavily on radiation research. In this era, BJTs and simple MOSFETs were tested heavily and the idea behind Total Ionizing Dose (TID) and Single Event Effects (SEE) were established. Around the 1990s-2000s, semiconductor devices were making good progress and they got smaller. As the scale got smaller, the radiation sensitivity increased (4). Researchers then studied the radiation effect on the latest semiconductor devices under radiation environments. Modern research now focuses on radiation effects of different transistors (FinFET, GAAFET, 3D ICs), wide band-gap semiconductors (GaN, SiC), commercial off the shelf electronics and so on. As technology gets smaller and smaller day by day than ever before, new radiation research is critical to maintain the reliability of electronic devices.

Understanding the importance behind radiation research, our project focuses on finding a method to measure the absorbed radiation, dosimetry, with an X-ray machine accurately. There are a few methods to approach this problem. The current industry standard for measuring X-ray dose rates involves ionizing gas chambers. These methods are complicated, expensive and bulky. They also require specialized infrastructure such as gas lines, high voltage supplies, and complex cabling [1]. Considering the time constraint of this project, budget, and space in the laboratory, these methods are impractical. So, our goal is to find a method that is much simpler, affordable and easy to set up in a laboratory.

Radiation research is more critical than ever as we continuously evaluate the effects of ionizing radiation on all types of electronic devices. Radiation is a powerful tool that enables advancements in medicine, security, and electronics testing. X-ray irradiation, in particular, plays a key role in simulating specific environments and testing radiation effects and device reliability. The measurement of absorbed radiation, known as dosimetry, is essential for such studies. Measuring radiation accurately in real-time is essential to protect people, ensure equipment reliability, and conduct meaningful scientific research. Without proper monitoring, researchers and engineers risk drawing incomplete conclusions or, worse, exposing themselves and their equipment to unsafe conditions.

The current industry standard for measuring X-ray dose rates involves ionizing gas chambers . While highly accurate, these systems are bulky, expensive, and require specialized infrastructure such as gas lines, high-voltage supplies, and complex cabling [1]. This makes them inaccessible for many laboratories and impractical for flexible, low-cost setups. As a result, there is a critical need for a simpler, more affordable way to monitor X-ray dose rates without sacrificing accuracy.

3.1.1 Fundamentals of X-ray generation

X-rays can be produced in a vacuum tube where electrons are accelerated using a high voltage and directed towards a metal target.

When the electrons slow down by colliding with the target, they emit radiation known as Bremsstrahlung. This forms a continuous spectrum of X-ray energies. Additionally, the target atoms may emit distinct X-ray lines when the electrons from the inner shells are replaced by the higher energy electrons. The intensity and energy of the X-rays depend on the accelerating voltage that is measured in kV and current, measured in mA. The voltage and the penetrating beam is proportional to each other [5].

When the X-ray hits a material, they interact through photoelectric absorption, Compton scattering and pair production depending on their energy. These interactions cause the ionization and excitation of the atoms and molecules. If these interactions happen in biological tissues, they can cause DNA damage [5]. Such effects are studied heavily in radiobiology research as they help scientists understand how the cells get impacted by ionizing radiation. They can also help with cancer treatment. In the world of electronics, these interactions are studied heavily to learn how radiation affects semiconductor devices. The research on radiation is particularly relevant to space electronics and defense applications.

3.1.2 X-RAD and its applications

The precision X-ray 320, X-RAD series is one of the most advanced self contained biological irradiators available for laboratory use. It operates at up to 320 kV with a maximum tube power of almost 4200 watts [7]. It offers controlled and reproducible X-ray doses for applications including small animal irradiation, tissue and cell culture exposure and radiation reliability testing of materials and devices. It is designed to provide precise and safe research in biology and electronics. The system has a fully shielded cabinet that prevents radiation leakage and allows users to perform experiments in normal environments without the need for an enclosed radiation vault [8].

The X-ray 320 uses a high voltage generator to power the X-ray tube, a cooling system to maintain the temperature and a control interface called TouchRad. This touchscreen enables users to configure different parameters, such as voltage, current, exposure time, and dose rate with high accuracy. It also has password-protected user accounts to ensure that only authorized users can access the system [8]. The database records all the experiments done on the system and a user can view the history anytime. It also allows users to export all the data to an external software (Microsoft Excel) if they need to be reproduced.

3.1.3 Operational features and modes of control

The X-RAD 320 has several modes of operation that accommodate various experimental needs. Users can independently set the tube voltage, current, and exposure time, providing full control over beam conditions in manual mode. In time mode, X-ray exposures can be terminated automatically after a preset time. This ensures consistency in repeated trials [9]. Dose mode enables the system to automatically stop once a defined radiation dose has been delivered. This is usually measured in grays or centigrays. This mode is particularly useful in biological studies where dose precision is very important. A cycle mode is also available for experiments which require repeated exposures over multiple intervals, such as fractionated irradiation studies or stress testing of materials under cyclic radiation doses.

The system's advanced safety interlock system prevents the emission of X-rays unless all conditions are met. The cabinet doors are equipped with magnetic interlocks that disable X-ray generation when open. An emergency stop button instantly terminates operation if needed. A warning light on top of the cabinet lights up whenever the X-ray tube is active, and the system continuously monitors for cooling flow, tube temperature, and filter positioning. If any fault is detected, the irradiator automatically aborts the X-ray exposure and alerts the user through error messages displayed on the touchscreen [9].

3.1.4 Facility requirements and installation considerations

Despite the X-RAD 320 being a self-contained irradiator, it still requires a properly equipped facility. The system weighs approximately 2,345 kilograms (about 5,170 pounds) and measures roughly 78 inches in height, 57 inches in width, and 41 inches in depth [8]. It requires a dedicated single-phase electrical supply rated at 180-264 volts AC with a 40-ampere circuit and a grounded disconnect box located within three meters of the unit. Adequate cooling and ventilation are necessary to ensure the operation of the X-ray tube and generator as they use several kilowatts of heat. The system can be fitted with either an oil-to-air or oil-to-water cooling system depending on facility infrastructure, and produces roughly 6,000 BTU per hour during extended use. The installation area must have at least 20 centimeters of free space on all sides for maintenance access and proper airflow [8].

Facilities must confirm that the floor can support the system's weight and that access paths such as hallways and doors can accommodate the large cabinet dimensions before installation. During setup, qualified technicians must check alignment, interlock verification, and radiation leakage tests to ensure the system meets federal radiation safety standards. The manufacturer specifies that cabinet leakage should not exceed 0.2 millirem per hour at any accessible surface ensuring that the device can operate safely in standard research environments without exposing users to harmful radiation [9].

3.1.5 Safety protocols and radiation protection

Because the X-RAD 320 emits ionizing radiation, comprehensive safety protocols are very important. System users must complete formal radiation safety training and be certified by their institution's radiation safety officer before using the system. Access to the irradiator room must be controlled, and warning signage must be posted on the wall to indicate when the machine is in operation. Personnel badges or dosimeters are often worn to monitor cumulative exposure over time. The irradiator's cabinet provides adequate shielding but all laboratory staff must follow the rule of keeping exposure "As Low As Reasonably Achievable" (ALARA).

The system incorporates multiple safety redundancies to protect users. The door interlocks, baffle sensors, and key-switch prevent unintentional emission of X-rays. The "X-Ray On" light outside the cabinet provides a visible alert during exposures and the system continuously monitors coolant flow and internal temperature to prevent overheating [9]. In the event of a malfunction the system automatically shuts down and logs the fault for diagnostic review. This can happen when the cabinet door is open, a loss of coolant, or power failure. These features ensure compliance with international and U.S. radiation safety regulations including standards set by the Food and Drug Administration (FDA) and state radiation control agencies.

3.1.6 Maintenance, calibration and quality assurance

Maintaining accuracy and reliability in dosimetry requires routine inspection and calibration of the X-RAD 320. The manufacturer recommends daily visual checks of cabinet condition, door interlocks, warning indicators, and coolant levels [9]. Any evidence of leaks or irregular noises must be reported immediately. Annual maintenance must be conducted by certified service engineers who will inspect the high-voltage connections, verify interlock operation, test cooling performance, and conduct a radiation leakage survey around the cabinet. Calibration of the X-ray output includes measuring dose rates at defined source-to-specimen distances and verifying them against reference dosimetry systems.

Calibration data are very critical for ensuring experimental consistency. For example, the X-RAD 320's nominal dose rate is approximately 3 gray per minute at 320 kilovolts and 12.5 milliamperes with a 50-centimeter source-to-specimen distance and a 1-millimeter copper half-value layer

[7]. Adjustments in distance, filtration, or current will change the dose rate. These changes must be documented carefully. Many research institutions perform monthly constancy checks using dosimeters or ion chambers to confirm that the system's output has not shifted. The instrument's built-in software helps this process by automatically recording exposure parameters that researchers can correlate with dosimetry data to maintain long-term stability.

3.1.7 Applications in biomedical and physical research

The X-RAD 320 is widely used in biological and medical research for its ability to deliver uniform and repeatable radiation doses. In radiobiology, the system is employed to irradiate cell cultures, tissues, or small animals to study DNA damage, repair mechanisms, and radiation-induced carcinogenesis. It also plays a huge part in developing radioprotective drugs and radiosensitizers, substances that modify the biological response to radiation [4]. The precise control over dose and energy spectrum allows researchers to simulate clinical or environmental radiation exposures on a smaller scale. The system acts as a bridge between laboratory experiments and clinical therapy.

The X-RAD 320 has a significant role in the field of materials science and electronics reliability testing beyond biology. Researchers, especially semiconductor researchers, often use the system to study the effects of total ionizing dose on devices such as Schottky diodes, MOSFETs, or GaN-based components. Radiation can change charge distribution in insulating layers, shift threshold voltages, and induce leakage currents, all of which are essential parameters in radiation-hard electronics design. Because the X-RAD 320 enables tightly controlled dose delivery, it can replicate the radiation environments encountered in space or nuclear facilities. For researchers working in university radiation and reliability laboratories interested in replicating space environments, the system provides a compact and precise platform for evaluating electronic degradation mechanisms.

3.1.8 Advantages and limitations

The X-RAD 320 offers several advantages for research laboratories. Its fully shielded cabinet eliminates the need for a separate concrete shielding room. This reduces facility costs. The intuitive touchscreen control system makes the operation simple and minimizes user error. The built-in data logging allows traceability and reproducibility. Optional accessories such as beam-hardening filters, motorized collimators, and rotating specimen platforms allow users to tailor beam geometry and uniformity to specific experimental needs [9]. The modular design also supports upgrades such as dose measurement systems and environmental chambers that maintain controlled temperature and humidity inside the irradiation zone.

Despite the advantages, the system has some limitations. Although 320 kilovolts provides sufficient energy for small animals and thin materials, it may not penetrate larger animals or very dense materials. They might require megavoltage systems unlike the X-RAD 320. The equipment's size and weight require significant floor support and space, and its power and cooling demands may require dedicated electrical and HVAC infrastructure. Additionally, proper regular maintenance and calibration are essential. Otherwise, dose inaccuracy can cause inaccurate research outcomes. Lastly, the equipment must still be operated under institutional radiation permits and subject to periodic safety inspections even though the leakage levels are low.

3.1.9 Conclusion

For laboratories engaged in biological or electronic radiation research, the X-RAD 320 offers a balance of flexibility, precision, and safety that few systems can match. At the University of Central Florida, the Precision X-ray 320 is going to be used for irradiation experiments. But there is currently no integrated system to measure or display real-time dosimetry during operation. This limits the ability to benchmark device degradation under controlled dose conditions. The goal of our project is to build a tool to directly measure the dose-rate or dosimetry. The X-ray machine will be the main focus in this case.

3.2 Diode Selection

The diode is the primary sensing component of our X-ray detection system. A diode allows current to flow in one direction, but when exposed to light or radiation, it can also act as a sensor. Specialized diodes, called photodiodes, generate a current when photons strike the sensitive area of the device. So, the diode will be capturing the incoming X-rays and converting that energy into an electrical signal that we can process and display.

When X-rays strike the active region of the diode, they generate electron-hole pairs that create a measurable current. The size of this current depends on the intensity of the radiation and the physical characteristics of the diode, such as its sensitive area, capacitance, and biasing requirements. This current will be put through an op-amp, filtered, and converted to a readable voltage by the rest of our electronics before being shown on the readout interface.

We researched and compared several diode options based on their electrical and physical properties, as well as their practicality for our project. The results of our comparison and what we valued are shown below.

3.2.1 ARACOR / Quantrad 010PIN025

The ARACOR 010PIN025 was well-suited for total ionizing dose (TID) measurements and its responsivity and calibration data were widely published, which made it a reliable option. However, the diode is now obsolete and no longer commercially available, so it is not considered a viable option. [1]

3.2.2 CERN AXUVHS5

The AXUVHS5 diode was developed for use at CERN facilities and offers ultra-fast rise time of 0.7 ns and very low capacitance (15–50 pF). However, it has a very small active area, which limits the signal strength, and the diode is not readily available through commercial vendors.

3.2.3 AXUV20A

The AXUV20A has a large sensitive area to collect the X-ray signal and low reverse bias, but a significantly slower response time. This would be suitable for slow monitoring systems, but for our project, we want something that would be able to provide real-time monitoring. We intend for the readout machine to adapt as we change the X-ray parameters from the X-rad 320. Slow response time would not be feasible. [2]

3.2.4 AXUV20HS1

After careful consideration, the AXUV20HS1 diode was ultimately chosen for our design. It has a good-sized sensitive area of 20 mm^2 to collect the signal from the X-ray beam, and it will not cause an excess amount of noise and capacitance. Compared to the other options, it has the largest rise time of 3.5 ns; however, it still provides a quick response time when detecting changes in dose rate. It is crucial to have a fast response time because our machine aims to measure dose levels in near real-time rather than averaging values over long periods. The diode has a high reverse bias voltage, which means we need to consider designing a proper biasing network. Another practical advantage of the AXUV20HS1 is its availability. This diode is sold by major electronic distributors on the internet, making it a reliable source for both prototyping and long-term use. [3]

Table 3.2.5 summarizes the main candidates.

Table 3.2.5 Diode Comparison

Attribute	ARACOR/Quantrad	CERN/ AXUVH25	AXUV20HS1	AXUV20A
Sensitive Area	10 mm²	1 mm²	20 mm²	23 mm²
Capacitance	N/A	15–50 pF	300–900 pF	500–1500 pF
Reverse Bias Voltage	~50–100 V	52 V	150 V	10 V
Responsivity	Calibrated vs. Co-60 dose	0.1–0.3 A/W (broadband)	Similar to AXUVHS5	Similar
Rise Time	N/A	0.7 ns	3.5 ns	2 µs (much slower)
Availability	Obsolete	Limited (not sold anymore)	Commercial (DigiKey)	Commercial
Use Case	Designed for TID calibration	CERN X-ray facilities	Suitable for high-speed dosimetry	More suitable for static or slow-scan monitoring
Spectral Match	8–60 keV with Al filter	8–60 keV with Al filter	10–100 keV	10–100 keV
Calibration Curve Availability	Yes (published)	Yes (internal to CERN)	Not directly available; must be generated	Must be generated

3.3 Op-amp

The operational amplifier (op-amp) is the interface between the photodiode sensing element and the microcontroller digital processing unit in this X-ray dosimetry system. The AXUV20HS1 photodiode generates a very small photocurrent that is proportional to the incident X-ray flux that we want to measure. This flux has a magnitude typically ranging from picoamperes to nanoamperes. The microcontroller's analog-to-digital converter (ADC) can not read a current, so the x-ray signal needs to be converted to a voltage. The initial stage of the op-amp design will be a current-to-voltage conversion stage. The op-amp, configured as a transimpedance amplifier (TIA), performs this conversion.

The TIA topology was selected for its ability to convert the photodiode's current output into a proportional voltage while maintaining the diode at a virtual ground. This lessens the effects of junction capacitance and has better response speed. The transfer function of the TIA is defined by the feedback resistor (Rf), where $Vout=-I_{in} \times R_f$. The selection range of the feedback resistor is therefore crucial to the system's sensitivity and dynamic range. The performance of the op-amp within this TIA configuration directly impacts the readout system's overall accuracy.

3.3.1 ADA4530-1

The Analog Devices ADA4530-1 is an excellent option for an op-amp to be used in our project. This op-amp features femtoamp-level input bias current and an integrated guard driver to minimize leakage currents when using very high-value feedback resistors, which we need to use. Although its bandwidth is lower than the OPA140, it remains sufficient for the system’s operational frequency range (below 150 Hz). So, we will conduct testing with this diode as well. [4]

3.3.2 LTC6468

The LTC6268, also by Analog Devices, was also reviewed due to its high speed and low input bias, but it was ultimately deemed excessive and ruled out for the current design. Its high 500 MHz bandwidth is a lot more than the required signal bandwidth for X-ray dose-rate monitoring, and its sensitivity to layout parasitics makes it more difficult to stabilize. [5]

3.3.3 OPA141

After evaluating our options, the Texas Instruments OPA141 was selected as the primary op-amp for the transimpedance amplifier stage. It has a good balance between precision, bandwidth, and cost. With a low input bias current and a gain-bandwidth product of 11 MHz, the OPA141 can handle both low and high dose-rate signals without distortion or oscillation, even when paired with the high-capacitance AXUV20HS1 photodiode. So the OPA141’s low input bias current and 11 MHz bandwidth made it suitable for our use. [6]

Table 3.3.4 Op-Amp Comparison

Parameter	TI OPA141	ADI ADA4530-1	ADI LTC6268
Input Type	JFET	CMOS	CMOS
Input Bias Current	10 pA	20 fA	3 fA
Input Offset Voltage	120 µV	20 µV	200 µV

Gain Bandwidth Product (GBW)	11 MHz	2.9 MHz	500 MHz
Input Voltage Noise	5.1 nV/√Hz	7 nV/√Hz	4 nV/√Hz
Slew Rate	20 V/µs	1.5 V/µs	500 V/µs
Supply Voltage Range	4.5–36 V	4.5–16 V	2.7–5.25 V
Typical Supply Current	1.8 mA	1 mA	16 mA
Package Options	SOT-23-5, SOIC-8	SOIC-8	SOIC-8, DFN-8

3.3 Filters

The purpose of the filter in the X-ray detection circuit is to remove unwanted electrical noise and ensure that the output signal from the transimpedance amplifier (TIA) accurately represents the radiation intensity measured by the AXUV20HS1 photodiode. Filters are essential in signal conditioning because they define which frequency components are preserved and which are attenuated before the signal is digitized by the microcontroller’s ADC. [7]

In the context of this project, several types of filters were evaluated, including low-pass, high-pass, and band-pass, to determine which best fits the characteristics of the signal being measured.

3.3.1 High-Pass Filter

A high-pass filter attenuates low-frequency components while allowing higher frequencies to pass. These filters are often used in AC-coupled systems to remove DC offsets or baseline drift. However, in this system, the signal of interest is a slowly varying voltage proportional to the x-ray dose rate. Removing low-frequency or DC components would eliminate the steady-state radiation signal, leaving only noise and transient fluctuations. Therefore, a high-pass filter would not be appropriate for this application.

3.3.2 Band-Pass Filter

A band-pass filter allows a specific range of frequencies to pass while attenuating both lower and higher frequencies. They're usually used in applications where the desired signal is in a known frequency range, so they can be designed to know what to expect. In the X-ray readout system, there is no intended range of interest, and it is very broad; the signal varies slowly over time as dose rate changes. If we used this type of filter, we would risk filtering out genuine variations in radiation intensity while providing little benefit against broadband electronic noise.

3.3.3 Low-Pass Filter

A low-pass filter allows slow or DC signals to pass while attenuating high-frequency noise. This is ideal for analog sensor applications where the signal of interest changes gradually over time. The photodiode output current that will be converted by the TIA output voltage varies proportionally with X-ray intensity, which is at a low frequency. High-frequency components at the op-amp output primarily come from external environmental sources or noise from the ESP32 microcontroller and LCD.

3.4 Microcontrollers

The microcontroller unit (MCU) is a major component of our system. It will be responsible for acquiring sensor data, performing necessary processing, and driving the LCD. For our project, we considered several factors when evaluating potential microcontrollers. We needed multiple available GPIO pins, compatibility with various communication protocols, fast processing, and it had to meet our power requirements. The chosen microcontroller must reliably handle tasks such as sampling analog signals from the photodiode and op-amp, convert them to digital values, process them into dose rate readings, and update the LCD in real time. [9]

3.4.1 Raspberry Pi

The Raspberry Pi offers the most processing power among the options considered. Its ability to run a full operating system like Linux provides flexibility for advanced tasks, such as data logging, remote access, or creating graphs. The Raspberry Pi does not include a built-in ADC, meaning additional hardware would be required to digitize the amplified photodiode signal. This increases circuit complexity and makes the design harder to implement.

From a power perspective, the Raspberry Pi consumes significantly more current than a microcontroller, which reduces the practicality of running the device on battery power. Although fast processing allows for data manipulation and advanced visualization, it is unnecessary for the scope of our project and could cause more complications.

3.4.2 Arduino

Arduino boards are simple to use and heavily documented. For this system, their accessibility and large set of community libraries could help accelerate prototyping, especially for tasks like driving an LCD screen or writing data to an SD card reader.
However, Arduino is limited in several ways that directly affect our project. The 10-bit ADC included in these boards would not provide the resolution needed for accurately measuring small changes in the diode's signal, which directly impacts dose rate accuracy. Power consumption is another limiting factor. While Arduinos operate efficiently at 5 V, they don't have power-saving modes compared to other microcontrollers, making them less ideal for a battery-powered device like ours. Also, the Arduino platform has mid-level processing speed and memory, which would not be able to efficiently update the display every 2–4 seconds.

3.4.3 MSP

The MSP430 family of microcontrollers from Texas Instruments is what our group is more familiar with using. They are specifically designed for ultra-low-power applications, which aligns well with the project's goal of creating a portable, battery-powered device. Its strong analog performance and flexible ADC configuration make it a strong candidate for an X-ray detector machine. Its 12-bit ADC provides better resolution than the Arduino, so it would have more accurate dose rate measurements. The MSP430 could reliably sample the photodiode's amplified output and process dose rate measurements with minimal energy usage, making it one of the more power-efficient options. [10]

However, the MSP430 falls short in other areas of our project. We aim to implement SD card logging, which the MSP430 could not support without additional design considerations. Development tools for the MSP430 are highly reliable but are less supported in terms of ready-made libraries for displays, SD cards, and advanced peripherals. This means longer development time and more manual implementation.

3.4.4 ESP32

The ESP32 offers a strong balance of the properties we want to focus on for our readout machine. It has strong performance and efficiency. Its dual-core processor provides enough power to simultaneously manage data inputs, real-time filtering, and user interface tasks. The built-in 12-bit ADC provides sufficient resolution for digitizing the amplified diode output, ensuring that small variations in dose rate can be captured and displayed accurately.

In terms of communication, the ESP32 supports multiple communication interfaces such as UART, SPI, and I2C, which allows straightforward integration with the LCD, SD card, and other peripherals required for the system. If we choose to expand on the machine's capabilities in the future, we would be able to consider the built-in Wi-Fi and Bluetooth. [11]

Power consumption is moderate, and with sleep modes available because the machine will not always be in use, the ESP32 can be optimized for battery use. Another advantage of the ESP32 is its strong documentation and assistance. It has numerous open-source libraries for display control, data logging, and wireless communication, which reduces development time and simplifies debugging. For our senior design project, we have limited time, so we want a microcontroller that is highly reliable and easy to troubleshoot, so this community support is a major advantage.

For these reasons, the ESP32 was selected as the microcontroller for the X-ray readout machine. It provides the right combination of processing capability, integrated features, and ease of development, making it the most practical and efficient option for meeting the project's requirements.

Table 3.4.1.1 ESP Comparison

Feature	***ESP32-DevKitC***	***ESP32-WROOM-32***	***ESP32-WROVER***	***ESP32-S3 DevKit***
ADC Resolution	12-bit	12-bit	12-bi	12-bit
Processing Power	Dual-core Xtensa	Dual-core Xtensa	Dual-core Xtensa	Dual-core Xtensa LX7
Memory (RAM/PSRAM)	~520 KB RAM, no PSRAM	~520 KB RAM, no PSRAM	520 KB RAM + 4–8 MB external PSRAM	512 KB RAM + optional PSRAM

Display	Reliable, but limited memory for complex graphics	Library support depends on the clone board	PSRAM allows smoother display updates and data logging	Improved GPIO count and memory help multitasking
Connectivity	Wi-Fi, Bluetooth	Wi-Fi, Bluetooth	Wi-Fi, Bluetooth	Wi-Fi, Bluetooth, USB
Community / Library Support	Strong, official Espressif docs	Very strong, widely used in education/prototyping	Strong but fewer examples than WROOM	Currently expanding

3.5 Debugger for MCU

Another important consideration for our project is to include a debugger for the microcontroller. A debugger would allow us to monitor the system in real time and be able to set break points as well as run the program and track variables simultaneously. This will be particularly useful when checking the photodiode readings as well as making sure that they are updating correctly onto the LCD as expected. The ESP32 supports debugging through the Esp-Prog as well as FTDI adapters connected through JTAG and UART interfaces. This allows for easier troubleshooting without the reliability of serial output which will save us some time during testing and development which given our strict deadline as per Senior Design requirements will be a constraint.

When looking at which ESP32 to use, our group is currently considering the ESP32-WROVER as well as the ESP32-S3 Devkit for testing and prototyping. The WROVER includes a PSRAM which will be helpful for tracking the data as well as quickly updating the LCD. The Devkit, during prototyping for the demo video, will be helpful with an improved GPIO count as well as built-in USB debugging and higher efficiency when running multiple processes. Our final decision will come down to when we do real-time testing and by choosing a variant that is balanced it can make our work easier and keep our detector to be reliable.

3.6 SD Card Reader

3.6.1 SD Card Connectors

For this project we will use an SD card to save the data from our MCU. One of our goals is to allow our design to be easily portable, by adding an SD port this will allow our data to be even more portable and displayed in spaces other than just our PCB. There are some limitations to the portability of our design without the use of an SD card as a way to transport and display the data because of the use of the x-ray machine. The machine cannot be moved from where it is positioned in the lab and we will need to have the filter connected to the output wires from the machine so our PCB will not be able to move too far from where the machine is. Adding an SD card will allow for our calculated values and graphs to be viewed even from across campus from the Radiation Effects and Reliability Lab. In addition the data we are recording from the x-ray machine will change

There are two different options for SD cards we can use and will compare to choose the best option for our design. MicroSD cards and full-sized SD cards are the two most common types of SD cards that we will decide between using for this design. Full-sized SD cards have dimensions of 32mm x 24mm. These cards are usually used in cameras and most laptops and computers have an SD card reader built in, the readers are usually sized for a full-sized SD card and can easily use an adaptor to fit a microSD card instead. These microSD cards are 15mm x 11mm and are typically used in cell phones and embedded systems. [25]

For our application it makes the most sense to utilize a microSD card connector to store data. One concern we had with this choice was the need of an adaptor to connect the card to standard sized SD card readers; however, they are smaller and more compact which will help to keep size and cost down for our design. We will still be using the microSD card because most of these SD cards will come with adaptors to allow the cards to be easily connected to different devices regardless of the type of connector they have.[26] In addition, microSD cards can typically store up to 32GB of data which is more than enough to store the graphs we will be saving.

3.6.1.1 Catalex MicroSD Card Adapter

This is an arduino module that is capable of connecting to our MCU and saving data to a microSD card. The operating voltage of this part is 3.3V which will allow for the device to be directly connected to the same power supply as the ESP32 which also runs on a 3.3V supply. There are eight pins on the SD card, six of which are used in this design. Chip select, controller-out, positive supply, serial clock, ground, and controller-in. This option is 11mm x 15mm and 1mm thick, this is not a significant amount of space however we can still look at smaller options. [27]

3.6.1.2 AdaFruit MicroSD Card Breakout Board+

This module is designed by AdaFruit Industries and also uses SPI to share data. Since there is an onboard regulator the connector can support either a 5V or 3.3V input voltage and would work with our input 3.3V regulator. The actual SD card port on this board requires a 3.3V input so the regulator can switch off allowing the 3.3V to enter the board without modification. When the microSD card is connected the DET pin is pulled up to the 3.3V input and is otherwise connected to ground. When using SPI logic, the serial clock pin is used along with the serial out pin. For this setup a serial in and chip select pin are also enabled to share data between the chip and ESP32 using 3.3V logic. The board connects to our PCB using male header pins which can easily be soldered onto our design. This option is slightly larger than the Catalex, 31.85mm x 25.4mm and costs $7.50. [28]

3.6.1.3 Adafruit MicroSD SPI or SDIO Card Breakout Board

This third option for our SD card connector is also from AdaFruit and can work with 3.3V power only. One major difference between this option and the previous option from AdaFruit is the requirement of SDIO pins for the most ideal operation. The ESP32 that we are using does function at 3.3V however it uses SPI. This board can use SPI to function however it will be slower and it will no longer achieve the speed and ideal functionality it would have if SDIO was used. It is also much more difficult to connect the SPI wiring when this board is used in the SPI setup. This board is however smaller and cheaper than the breakout board+ at 25.4mm x 22.8mm and $3.50 which is ideal for the sizing and cost goals of our project. [29]

3.6.2 SD card connector comparison

For our design we will be using the AdaFruit MicroSD Card Breakout Board+ because it meets all of our functionality requirements. This option will be able to function at the 3.3V input we will be able to provide as well as communicate with our ESP32 easily in SPI. This option is slightly larger and more expensive than the other options however, the other options had very little documentation to help with designing our project using these boards. The breakout board+ will be the simplest option for our design and the easiest to purchase and test so it will be the option we are using in this project.

3.7 Display

3.7.1 PC vs. LCD:

A personal computer (PC)'s general purpose is to perform as a computing device that provides a power platform for processing data, running software, and interfacing directly with hardware. In the context of our project, the PC would serve a centralized display where our sensor would be able to display measurements, graphs and sensor outputs that can be further collected and analyzed. It uses a full operating system and has flexibility to run specialized programs such as data visualization suits, dashboards, and scripts perfect for radiation detection systems. A PC also brings in storage capabilities, displays, easy connectivity to external devices via USB and wireless interfacing.

From a project perspective, the PC is not just an end-user interface but also a backend that is able to run computations. It can handle the heavy workload being able to store long experimental logs, performing calibration calculations and can support remote data access. Another positive to PC's are their versatility, they are adaptive to evolving making it easy to use specifically in a research environment. In addition to their ability to handle a heavy workload and be versatile, PC's include processing power, compatibility with almost all software ecosystems and salability for complex tasks like high volume data logging, and real time graphing (like dose-rate vs. time graphs) for our project that the LCD may not be able to support.

A liquid crystal display (LCD) is a thin, low power visual interface that provides feedback directly to users. An LCD is often integrated to display only the most essential information perfect for sensor readings, dose rates, and error messages (for error checking). The LCD differs from the PC in the way it is not general-purpose, it is more specific to its dedicated interface meaning it must be programmed to connect to the device. An advantage to an LCD is its lightweightness, portability, and lighter in terms of resources. This is important in places where size, power, and mobility of the device.In respect to our project, an LCD offers the ability to present results directly on the hardware without relying on an external computer. Additionally the use of an LCD would make our device self-contained and portable whereas a PC could be impractical and make the device less accessible. Although the capabilities of the display are a bit more limited than a PC, the LCD will align well with a project such as the PCB where the prototype is a standalone, this could ensure that the user can monitor with dose rates with minimal setup, leading to quicker results and minimal set up.

Our X-ray detector requires a display to communicate real-time measurements to its users. Without a display (PC or LCD), the system would produce raw data with no way for researchers to be able to interpret and visualize the results during experiments. Incorporating one of these displays is the best way to allow researchers to interpret results and be able to visualize the measurements from the diode and our understanding. Additionally, using a display will allow for the system to be practical, safe, and align with our goal of real-time dosimetry. It’s important to compare the PC to the LCD to figure out the most effective solution for our project. The PC is far more powerful with an unlimited amount of storage and computation resources as well as the ability to advance data visualization relevant to the project. Its advanced capabilities makes it ideal for a large-scale project like ours where high-resolution graphs, calibration comparisons and data logging is required. A PC can also integrate with external tools making it easier to export data for papers interested in research as well as remote monitoring. These capabilities are beyond the scope of an LCD. From a programming aspect, programming on a PC allows for full software environments with advanced visualization, processing, and multiple applications giving it a much broader scope.

On the other hand, the LCD prioritizes practicality in its portability as well as its integration. It consumes way less power and requires no external set-up and can be embedded directly into the device’s housing, making it better for quick monitoring when it comes to viewing dose-rates. The low cost of an LCD would also align well with our budget, however, the limitations with an LCD are way more with the lack of having extensive logs, complex calculation abilities and interfacing with advanced external systems. Programming an LCD is limited to displaying numeric outputs whereas a PC allows for a broader scope for researchers to be able to analyze.

Another key factor between the PC and the LCD is user experience. A PC allows for more flexibility, for example, the ability to export the data with the option of a CSV file. An LCD is limited to showing simple outputs without the option to export files; this makes it less suitable for detailed research but perfect for quick outputs. The choice to choose between a PC and LCD is dependent on the scalability of the project as well as its use between computational value or embedded usability.

For our project, we have chosen to use an LCD display. Our main reasoning for this being portability, real-time device monitoring as well as the advantage this has for our project financially. Our objective is to build a compact dosimeter that researchers can use directly in the lab, having a PC adds the constraint of the device not being portable and affordable for researchers to use directly in the lab.

We did not choose the PC because it would require additional cost, power requirements, and complexity in terms of set up. While it does offer advanced capabilities, relying on a PC would make the device less portable. Since we are ultimately trying to create a self contained device the PC became unnecessary for the scope of the project.

3.7.2 LCD Selection

When it comes to choosing an LCD, we had a couple key considerations in mind which included display size, the ability for the display to be a touch screen, and the number of required pins making it compatible with our MCU. Table 3.7.2.1 summarizes our choices of displays.

Table 3.7.2.1 LCD Comparison

Feature	Parallel TFT LCD	Character LCD	SPI TFT LCD	I2C TFT Touch LCD
Screen Size	3.5–5.0 in., full graphics	16×2 or 20×4, text only	2.4–3.5 in., graphics	3.5–4.0 in., graphics + touch
Resolution/ Output	High (320×480+)	Limited to text characters	240×320 – 480×320	320×480, interactive
Interface Complexity	High (many GPIO lines)	Low (simple but limited)	Moderate (4 to 5 pins)	Only 2 data lines
Integration with ESP32	Difficult, heavy routing	Easy but non-scalable	Good, requires optimized drivers	Minimal wiring, easy PCB integration
Data visualization	Supports plots and graphics	Only numeric text	Supports plots and graphics	Full graphics + touch interaction
Power Consumption	Moderate	Very-low	Moderate	Moderate
Cost Range	$20-40	$8-15	$15-25	$30-50
Touchscreen options	Optional (resistive or capacitive)	None	Resistive or capacitive panel option available	Capacitive panel built in

3.7.3 Parallel TFT LCD

The Parallel TFT displays provide high resolution and have fast refresh rates, but they require a large number of GPIO pins and complex wiring. In terms of compatibility with the ESP32, this heavy pin usage would limit flexibility for other peripherals. While it would be capable to use, the unnecessary complexity of the hardware would make it impractical for our project.

3.7.4 Character LCD

The common 16×2 or 20×4 character LCDs are inexpensive, simple to drive, and have excellent library support. However, they can only show text and numeric values, which wouldn't be enough for the scope of our project which includes plotting and visualizing dose-rate data. Due to the fact that we would like our system to present the radiation graphically, this option was not feasible for our project.

3.7.5 SPI TFT LCD

The SPI TFT would be perfect for wiring simplicity given its need for only 4-5 pins and performance given its capability to display graphics. However, the SPI has multiple dedicated pins that have a slower throughput than parallel which could create bottleneck issues when dealing with other SPI peripherals.

3.7.6 I2C Touch Display

The I2C touch display is the perfect display for our project simplified wiring and performance capabilities. It requires only 2 lines of data (SDA/SCL) which simplifies the wiring process on the ESP32 and frees up pin space for other sensors and interfaces. The panel supports capacitive and graphic input allowing for us to be able to visualize doserates. Though it is slightly more expensive, the easy integration process and capabilities make it the best option for our project.

3.8 Power Supply

Based on our calculations on the selected parts, the power output of the device is calculated between 0.045W - 68W. The battery selection for this device is going to be based on this. We will focus on efficiency, reliability and cost when comparing and selecting different power supplies.

Table 3.8.1 Power Distribution

Component/Part	Power Requirement	Power Usage
Op amp	±4.5V - ±20V, ±10mA	0.045W - 0.2W
Regulator	3V - 17V, <4A	12W - 68W

ESP32	2.2V - 3.6V, 250mA	0.55W - 0.9W
I2C Touch Display	3.3 - 5V, <200mA	0.66W - 1W

There are lots of different power supply sources available on the market. We will compare different power supplies here and select the one that's most suitable for our project.

3.8.2 Alkaline batteries

Alkaline batteries are the most common type of disposable battery used at home. You can find them in many sizes, like AA, AAA, C, D, and 9V. They work by using zinc and manganese dioxide with an alkaline liquid inside. Each battery gives about 1.5 volts of power. Alkaline batteries store a fair amount of energy. They last between 5 and 10 years when kept on a shelf [4]. They work best in things that do not use much power all at once, such as remote controls, wall clocks, flashlights, and many toys. These batteries are cheap and easy to find in stores around the world. This is why most people choose them for single-use needs. AA alkaline batteries cost less than many rechargeable types when you buy them. However, alkaline batteries have some problems. They do not work well in devices that need a lot of power or work for a long time without stopping. In these cases, the voltage drops and they run out faster. They also do not perform as well in cold temperatures. Since they are single-use, you have to throw them away, which creates waste.It is easy to use alkaline batteries because you do not need a charger. But for devices you use a lot, rechargeable batteries save more money in the long run and are better for the environment.

3.8.3 Zinc-carbon batteries

Zinc-carbon batteries were made before alkaline batteries. They are cheaper and still sold for devices that do not need much power. These batteries have about 1.5 V and less energy and capacity compared to alkaline batteries. Their low price matters only for the cheapest products. They do not last long if the device uses much power. They also do not work well with higher current or last long in storage, as they lose charge quickly. Because of these problems, they are mostly used in cheap toys or as emergency backups, where cost is more important and little power is needed [4]. More people now use alkaline or rechargeable batteries because zinc-carbon batteries do not perform well and are not good for the environment when thrown away.

3.8.4 Silver Oxide batteries

Silver-oxide cells are small batteries shaped like buttons or coins. People often use them in wristwatches, some calculators, hearing aids, and special instruments that need accuracy. These batteries usually give about 1.55 volts of power [4]. Some other coin batteries, like lithium types, can give a bit more voltage. Silver-oxide batteries are known for steady power and high energy for their size. They also last a long time on the shelf. This is why they are a top choice for devices that need reliable power for long periods without changing batteries, such as watches. These batteries are more expensive than many others. This is because they contain silver, which costs a lot. They are usually not rechargeable, meaning you use them once and then throw them away. These batteries can be found in stores that sell electronics or watch parts. But, their higher price and environmental concerns limit their use to special cases where small size and steady power are very important. There are some rechargeable button batteries, such as silver-zinc or lithium rechargeable cells, but these are not as common as the regular, non-rechargeable silver-oxide cells.

3.8.5 Zinc-air batteries

Zinc-air batteries are mostly used in hearing aids and other small devices that need a lot of power in a tiny size. These batteries work by mixing zinc with oxygen from the air. Because they get oxygen from outside instead of keeping it inside the battery, they can store a lot of energy for their weight and size. They have great energy density for small button-shaped batteries. They also cost less than some other types. But once a zinc-air battery is opened and it touches air, its life starts to run out. These batteries can only last for a limited time after being exposed to air. They also do not work as well if it is too humid or too dry, or if the weather is very hot or cold. Most zinc-air batteries for consumers cannot be recharged. Scientists are working on special rechargeable types, but these are not common. Zinc-air batteries can usually be found in places that sell hearing aid supplies. They are great for small devices that need to work a long time on one battery. However, they must be handled very carefully to make sure they last as long as possible.

3.8.6 Lithium batteries

Primary lithium batteries, such as lithium manganese dioxide coin cells (CR series), lithium thionyl chloride ($Li\text{-}SOCl_2$), and lithium iron disulfide types, have high energy density and a long shelf life. These batteries also work well in cold temperatures. Lithium coin cells like the CR2032 are very common in small electronics and sensors because they are small and provide steady power. Larger primary lithium batteries, such as Li-SOCl2, are often used in industrial sensors, memory backup, and remote telemetry. These applications need batteries with very low self-discharge and a long life, sometimes lasting many years without being replaced. The typical voltage for these lithium batteries is around 3.0 volts, which is higher than other types like alkaline batteries [4]. Their energy density is also much higher. Primary lithium batteries usually cost more than alkalines, but the higher price is worth it for devices that need long battery life or that must work well in very cold conditions. Most lithium primary batteries cannot be recharged. Special rules are in place for shipping and handling these batteries, and some types, such as those with thionyl chloride, need extra safety measures. These batteries are easy to find through electronics stores and industrial supply companies.

3.8.7 Lithium-ion batteries

Lithium-ion batteries are the most common rechargeable batteries for many uses, such as phones, laptops, electric cars, and even storage for buildings. This type of battery comes in different forms, including lithium cobalt oxide (LCO), lithium nickel manganese cobalt (NMC), and lithium iron phosphate (LFP). Most lithium-ion cells provide about 3.6 to 3.7 volts each. They can store a lot of energy for their size and weight, usually between 150 and 260 Wh/kg for standard types, and even more for some high-energy versions [4]. Lithium-ion batteries work efficiently when charging and discharging. They do not lose much energy when not being used and can last for hundreds or even thousands of cycles, depending on the type and how they are used. These batteries are used in devices like smartphones, laptops, electric vehicles, and even for storing energy linked to the power grid. Prices for lithium-ion batteries have dropped a lot over the years, but battery packs still make up a large part of the cost of electric vehicles. Special battery management systems (BMS) are needed to keep these batteries safe by watching over charging, preventing overcharging or deep discharge, and balancing all the cells. Problems can happen if the batteries are damaged or overheated. There are also concerns about collecting materials for these batteries, especially lithium, cobalt, and nickel, which can have environmental impacts. Lithium-ion batteries are easy to find in both stores and industry. They are easy to use when paired with proper safety electronics. Each subtype has strengths and weaknesses. LCO batteries have high energy but don’t last as long. NMC types balance power and energy well and are popular in electric cars. LFP has a bit less energy, but lasts longer, is safer, and usually costs less [5].

3.8.8 Nickel-metal hydride batteries

Nickel-metal hydride (NiMH) batteries are a popular type of rechargeable battery. They replaced nickel-cadmium batteries in many products because they are safer and more efficient. Each NiMH cell gives about 1.2 volts. These batteries can hold more energy than nickel-cadmium but less than most modern lithium-ion cells [4]. NiMH batteries are often sold in familiar AA and AAA sizes. They are used in items where low cost, easy recharging, and safe operation are important, such as toys, cordless phones, and older digital cameras. NiMH batteries lose charge faster when not in use compared to lithium-ion types, but some special versions lose power more slowly. They can be charged several hundred times before wearing out. Prices and availability are both moderate, so finding replacements is usually easy. The main problems with NiMH batteries are that they can lose their charge more quickly and don't store as much energy as lithium-ion cells. Because of this, they are not ideal for devices that need a lot of power or where weight and size matter most. However, they are still useful anywhere standard voltage is necessary and where lithium-ion batteries are not safe or not a good fit.

Table 3.8.9: Alkaline battery comparison

Battery	**Power supply**	**Energy Density (Wh/kg)**	**Lifespan**	**Cost**	**Size and Portability**	**Disadvantages**
Alkaline	1.5V/9 V	80-150	Single use	$0.3-$5	, AA, AAA, C, D sizes	Not rechargeable, not proper for high power devices and causes waste
Zinc carbon	1.5V	30-80	Single use	$0.2-$1	Portable, AA, AAA sizes	Low-energy density, short shelf life and high internal resistance
Silver oxide	1.55V	100-180	Single use	$1.5-$5	Very small (button)	Expensive compared to other batteries, not rechargeable
Zinc-Air	1.4V	100-300	Single use	$1-$5	Very small	Short active life, humidity sensitive
Lithium	3.0V	200-300	Single	$1-$10	Compact and	Not rechargeable,

			use		lightweight	costly
Lithium-ion	3.6V	150-250	Recharg eable	$1-$180 +	Portable for phones and EVs	Costly, thermal runaway risks
Nickel-meta l hydride	1.2V	60-120	Recharg eable	$2-$6	Portable, AA, AAA sizes	Lower energy than Lithium-ion

3.9 Battery selection

For our project, we have decided to go with simple alkaline batteries. They are easily accessible, low cost and have a wide variety to choose from.

The 1.5V alkaline battery is a common type of battery. It can be found in many sizes, such as AA, AAA, C, and D. All of these sizes give the same voltage: 1.5V. Bigger batteries, like C and D, hold more energy and last longer than smaller ones. This means larger sizes are better for devices that use more power, while smaller ones fit better in compact gadgets.

These batteries use a chemical reaction inside. Zinc and manganese dioxide produce electricity through this reaction. It is a more reliable system than older zinc-carbon batteries. Because of this chemistry, alkaline batteries give a steady voltage. They also last longer and perform better, especially in devices that need ongoing power. Clocks, radios, and remotes work well with these batteries.

Alkaline batteries can be kept in storage for a long time. Many brands say they last five to ten years without losing much power. This is good for people who buy in bulk or use batteries for emergency supplies. They work in many different environments. Their temperature range of operation is from -18°C to 55°C [29]. This makes them useful both indoors and outdoors, in cold or hot places. However, they do not work as well in extreme cold. The battery’s power drops when it gets very cold. These batteries are also affordable. You can usually buy one for $0.30 to $1.00 per cell. Price depends on the brand and package size. Buying a lot at once is often cheaper. Because of this, alkaline batteries are common in homes and offices. People trust them for their reliability and long shelf life.

3.9.1 AA Alkaline batteries (1.5V)

AA alkaline batteries are the most common type of 1.5V battery. They are present in almost every household. Each AA battery measures 50.5 mm long and 14.5 mm wide. These batteries usually offer a capacity between 2,000 and 2,800 mAh under normal use [29]. People use them to power remote controls, game controllers, wall clocks, wireless mice, and flashlights. AA batteries are available in different types. The standard models are used for everyday devices. High-drain and professional-grade versions work better for items like digital cameras or toys that need a quick boost of power.

In stores, there are many brands available. Duracell Coppertop and Energizer MAX are known for lasting a long time. They cost more but provide steady performance and a long shelf life. Rayovac and AmazonBasics are the budget-friendly brands. They can perform almost as well as the big brands in low-drain devices. A 24 pack of AmazonBasics AA batteries costs about $10 to $12. The same amount from Duracell might cost $15 to $20. Although premium brands are more expensive, both types work similarly in devices like remotes and clocks.

AA batteries are popular because of their size and power balance. Their energy density is high for their small size. This means they fit many devices without being too big or bulky. However, these batteries are not perfect. When used in high-drain devices, like cameras or powerful flashlights, the voltage drops quickly. In these cases, rechargeable NiMH or lithium batteries work better. They last longer and keep their voltage even when the device needs more power.

3.9.2 AAA Alkaline batteries (1.5V)

AAA alkaline batteries use the same chemical setup as AA batteries. They are just smaller in size. Each AAA battery is 44.5 mm long and 10.5 mm wide [30]. This compact shape makes them perfect for slim or lightweight devices. People commonly use them in remotes, wireless keyboards, small flashlights, and thermometers. Their energy storage, or capacity, is usually between 800 and 1200 mAh [30]. The exact amount depends on the battery brand and how quickly the battery is drained. While AAA batteries have less energy than AA versions, their small size is a big advantage in devices where space and weight are important.

AAA batteries cost about the same as AA batteries per battery. However, since they hold less power, their cost per amount of energy is a little higher. For instance, a 24 pack of Energizer MAX AAA batteries often costs about $15. The same pack from AmazonBasics usually costs $10 to $11. The best things about AAA batteries are their lightness and convenience. They are easy to handle and fit in small gadgets. Their downside is they don’t last as long, especially in devices that use a lot of power. Despite this, for normal uses like remote controls and LED lights, AAA batteries give enough power. They also keep a steady voltage across most of their life, making them reliable for everyday items.

3.9.3 C Alkaline batteries (1.5V)

C-size alkaline batteries are bigger than AA and AAA batteries. They deliver more power, with a typical capacity between 6000 and 8000 mAh. Like the others, they also provide 1.5V per cell. Because they are larger, they fit more active material inside. Each C battery is 50 mm long and 26.2 mm wide [31]. This allows them to run devices for a much longer time before needing to be replaced.

C batteries work well in medium powered devices. Common uses include radios, large flashlights, children's toys, and some medical tools. Their steady voltage and high energy capacity are useful where changing batteries often would be a hassle. You can buy C-cell batteries from top brands like Duracell and Energizer. These are available in packs of 2, 4, or 12, with prices from $1.50 to $2.50 per battery. Less expensive brands, like Rayovac or AmazonBasics, cost under $1 each when bought in large packs.

The best thing about C batteries is their ability to hold a lot of energy and keep a stable power output. Their size and weight are the main downsides. This makes them tough to use in small gadgets or slim devices. Also, not as many modern products need C batteries. That means stores may not always keep them in stock, especially compared to AA or AAA batteries.

3.9.4 D Alkaline batteries (1.5V)

D-size alkaline batteries are some of the biggest cylindrical batteries one can buy. They provide the same 1.5V as smaller batteries, but their capacity is much higher- usually from 12000 to 18000 mAh. Their larger size gives them more power to run high-drain devices for a long time. Each D battery is 61.5 mm long and 34.2 mm thick [33]. This makes them good for things like industrial flashlights, large radios, motorized toys, and backup power supplies.

D batteries are great for situations where you need energy to last a long time without changing batteries often. They are popular for use in emergency kits and field gear. Top brands like Duracell and Energizer are trusted for their quality, but they are more expensive. A pack of four from these brands usually costs $12 to $15. Generic brands like AmazonBasics or Rayovac are more affordable, priced at $6 to $8 for a 4 pack.

The main benefits of D batteries are their large power capacity and long run time. However, they are also heavy and bulky. This makes them hard to use in small or handheld devices. Because demand for D batteries is lower now, stores do not always keep them in stock. Even so, D batteries remain common in industrial gear and for emergency use because of their reliability and strong power output.

3.9.5 9V Alkaline batteries

The 9 volt alkaline battery is easy to spot because of its rectangular shape. Inside, it holds six small 1.5V cells wired together to give a total of 9 volts. This higher voltage is useful for many electronic devices. Some common uses are smoke detectors, portable radios, guitar pedals, and testing tools like multimeters. The usual capacity for a 9V battery is between 400 and 600 mAh [34]. This is less energy than larger cylindrical batteries, but the 9V shape is perfect when one small battery needs to give higher voltage.

Premium brands like Duracell and Energizer sell 9V batteries for about $3-5 each. Cheaper options from AmazonBasics or Rayovac usually cost around $2 each in big packs. The biggest advantage of the 9V battery is its high voltage in a compact size. This makes building simple circuits easy for devices that need more voltage. 9V batteries also fit in small spaces. The main downside is their lower capacity, so they won't last as long in devices that use a lot of power. These batteries also lose power faster when stored or used in high-drain products. Because of this, modern devices often switch to AA batteries or rechargeable lithium-ion packs for better efficiency and longer life.

Table 3.9.6: Alkaline battery comparison

Batteries	Capacity (mAh)	Nominal voltage	Weight	Operating temperature	Market availability	Cost
AA alkaline (1.5V)	2000-2800	1.5V	~24 g	-18°-55° C	Very high	$0.75-$2
AAA alkaline (1.5V)	800-1200	1.5V	~12 g	0°-60° C	Very high	$0.40-$1.50, higher is rechargeable
C alkaline (1.5V)	6000-8000	1.5V	~65 g	-18°-55° C	High	$1.5-$5

D alkaline(1.5V)	12000-18000	1.5V	>65 g	-18°-55° C	High	$1.5-$5
9V alkaline	400-600	9V	~45-50 g	0°-50° C	Moderate	$5-$7

For our project, we need a battery with a voltage range of 5V to 10V. We have two main choices: use a 9V battery or connect 1.5V batteries in series. We decided to use four AA 1.5V alkaline batteries connected in series to provide a total of 6V. Selecting more than four batteries could make the pack too large for our PCB, and since battery holders often hold two batteries each, using four is ideal.

Four AA batteries in series provide about 6V, which is suitable for circuits that use 5-10V. The voltage will gradually decrease as the batteries discharge, making it easy to monitor how much power is left. AA batteries are widely available and inexpensive, and buying four costs only a few dollars, much less compared to lithium packs. Each AA alkaline cell typically provides 1800-2800 mAh at low-to-moderate loads, so a four-cell pack will deliver plenty of capacity for our device. This means long run times, especially for low-power projects. Compared to a single 9V alkaline battery, which usually has only 400-600 mAh, four AA cells offer higher capacity and more stable voltage during use. One downside is that AA batteries are not rechargeable, so they will need to be replaced, creating some waste. However, replacing batteries is easy and less complicated than regular recharging.

3.10 Voltage Regulator

Voltage regulators are essential components in electronic systems because they provide a stable and nearly constant output voltage regardless of variations in the input supply or changes in load conditions. Without regulation, fluctuations in the input voltage—such as those caused by battery discharge, inconsistent power sources, or sudden current demands—can propagate through the system, leading to unreliable behavior or even permanent damage. A voltage regulator prevents these issues by maintaining the output voltage within a narrow, predefined range, ensuring device safety, improving performance, and protecting sensitive components. [35] For this project we have two uses for voltage regulators. The first is supplying the microcontroller (MCU) with a consistent voltage level. Our ESP32 requires a stable 3.3 V input to operate correctly. However, our power source is a 6 V battery, which is significantly higher than what the ESP32 can tolerate. Exposing the MCU directly to 6 V would damage it, so a regulator is needed to step the voltage down to the safe and precise 3.3 V level required for proper operation. The second use of a voltage regulator in our system is to power the analog signal-conditioning circuitry—specifically, the operational amplifier used in our filter design. The op-amp we selected requires a clean and stable 5 V supply rail for optimal performance. Just as with the ESP32, this voltage must also be derived from the same 6 V battery. Therefore, a second regulator is used to convert the 6 V supply into a regulated 5 V rail for the analog filter. This ensures that the amplifier operates within its specified voltage range, maintains linearity, and produces accurate, low-noise output signals for further processing. Together, these two regulators allow the digital and analog portions of the system to operate reliably from a single power source while meeting their different voltage requirements.

3.10.1 Linear Regulator

Linear regulators are integrated circuits that function like controlled, variable resistors. Their main purpose is to maintain a constant output voltage even when the input voltage or load current changes. They accomplish this by continuously adjusting their internal pass element to “burn off” the excess input voltage as heat. This is fundamentally different from switching regulators, which rapidly switch energy on and off and use inductors or capacitors to efficiently convert voltage levels. In contrast, linear regulators achieve regulation purely through dissipation, which makes their operation simpler but also less efficient.

Because linear regulators do not require inductors and use only a few external components, they are attractive for designs that prioritize simplicity, low noise, and quick implementation. They are very stable, introduce minimal electromagnetic interference (EMI), and work well in sensitive analog circuits. Linear regulators can perform only step-down conversions, which fits the needs of our design since both required voltages—3.3 V for the ESP32 and 5 V for the operational amplifier—are below the 6 V battery supply.

However, the major drawback of linear regulators is heat generation. Since the device reduces voltage by dissipating the difference as thermal energy, large drops between input and output voltages significantly increase power loss. This effect becomes more pronounced at higher load currents. In our case, stepping down from 6 V to 3.3 V represents a substantial voltage drop, meaning the regulator would need to dissipate nearly half of the supply voltage as heat. As a result, the regulator would exhibit low efficiency and may require additional thermal management such as heat sinking to prevent overheating. [35] The efficiency of a linear regulator is calculated as the ratio of output power to input power. For simple step-down conversions, efficiency approximates Vout / Vin, which in our case is 3.3 V / 6 V ≈ 55%, even before considering current losses. This is significantly lower than what a switching regulator could achieve, especially under battery-powered conditions where efficiency directly impacts runtime. Because linear regulators rely entirely on power dissipation to reduce voltage, they are typically far less efficient than switching alternatives in applications with large input-to-output voltage differences. [36]

Linear regulators can only work to produce an output voltage that is lower than the input voltage. For our design we will be looking at dropping voltage with both of our regulators so this aspect of a linear regulator design will be possible for our system, however, it may not be ideal.

3.10.2 Switching Regulator

Switching regulators are also integrated circuits used to convert an input voltage to a desired output voltage. As their name suggests, switching regulators operate by rapidly turning internal switching elements on and off, controlling the flow of current into an energy-storage component such as an inductor or capacitor. Instead of dissipating excess energy as heat, switching regulators store and transfer energy in discrete packets, making them far more efficient than linear regulators. In a switching regulator, the output voltage is controlled through pulse-width modulation (PWM). The regulator continuously monitors the output voltage and adjusts the duty cycle, the fraction of each switching period during which the switch is turned on. The average voltage delivered to the output is approximately equal to the input voltage multiplied by this duty cycle. When the averaged output reaches the target voltage, the regulator reduces the duty cycle or temporarily stops energy transfer until the output begins to drop again. This switching process allows the regulator to supply only the amount of energy needed, precisely when it is needed.

One of the main reasons a switching regulator is preferred to a linear regulator is efficiency. Switching regulators tend to have much higher efficiency than linear regulators. Because switching regulators convert the input power rather than dissipating the unused portion, very little energy is wasted as heat. In the ideal case, input power equals output power, resulting in a theoretical efficiency of 100%.[36] In real designs, efficiencies around 85–95% are common depending on load, switching frequency, and component selection. As a result, switching regulators generate far less heat than linear regulators—an especially important consideration in battery-powered systems where thermal buildup and energy waste must be minimized.

Another advantage of switching regulators is their versatility. Unlike linear regulators, which can only reduce voltage, switching regulators can perform step-down (buck), step-up (boost), or even inverting conversions depending on their topology. Although our project requires only step-down conversions (from 6 V to 3.3 V for the ESP32, and from 6 V to 5 V for the op-amp rails) the broader capability of switching regulators highlights their usefulness in more complex or future system expansions.

3.10.3 Comparison

One of the key goals of our system design is to achieve high overall power efficiency. Because the efficiency difference between linear and switching regulators is substantial—especially when the input-to-output voltage drop is large—it is most practical and energy-conscious to use switching regulators throughout the design. Switching regulators allow us to maximize battery life, minimize heat generation, and ensure stable performance even as the battery voltage decreases over time. Since the same 6 V battery supply must be converted into both 5 V and 3.3 V rails, using two separate switching regulator stages allows each subsystem to receive clean, well-regulated power optimized for its specific needs.

For the 3.3 V power rail, we determined that the regulator must be capable of supplying approximately 1.5 A. This value was calculated by summing the estimated current consumption of all components powered from this rail, including the ESP32 microcontroller, the LCD display, and the microSD card interface, and then applying a 50% design margin. This margin accounts for transient spikes, future feature expansion, and variations in component power consumption, ensuring that the regulator will remain stable under worst-case conditions.

The 5 V regulator, which powers only the operational amplifier used in the analog filter stage, requires significantly less current. The op-amp's supply current is approximately 1.8 mA, making the load extremely light. Although this rail does not require high current, using a switching regulator still allows us to maintain a consistent and efficient conversion from the shared 6 V supply, keeping thermal dissipation low while ensuring the analog circuitry receives a clean and stable voltage.

By selecting switching regulators for both voltage rails, our design maintains high energy efficiency, reduces unnecessary heat, and ensures reliable operation across all parts of the system.

3.10.4 Boost vs. Buck vs. Buck-Boost

Having selected switching regulators as the most efficient solution for our power-conversion needs, the next step is to determine which specific type of switching topology is appropriate. Switching regulators generally fall into three categories: buck, boost, and buck-boost converters. Each topology serves a different purpose, so it is important to match the regulator type to the voltage conversion requirements of the system. In our design, we must convert a 6 V battery supply into two regulated outputs (3.3 V at 1.5 A and 5 V at 1.8 mA) meaning both regulators must be capable of stepping the input voltage down.

Boost regulators are designed to step up a voltage from a lower input to a higher output. They accomplish this by storing energy in an inductor while a switch is closed and then releasing that energy to the load when the switch opens, causing the inductor current to flow through a diode to the output. During the “on” phase, current in the inductor ramps up; during the “off” phase, this energy is transferred to the output, increasing the voltage above the input level. Like all switching architectures, their efficiency is calculated by the ratio of output power to input power. However, since boost regulators can only increase voltage and our design requires voltage reduction, this topology is not applicable.

Buck regulators are designed specifically to step down voltage, making them well suited to our needs. They operate similarly to boost converters but reverse the roles of the inductor and diode. When the switch closes, current flows through the inductor and into the load, causing the inductor to store energy. When the switch opens, the inductor continues to supply current to the load through a diode or synchronous switch, maintaining a stable output voltage. Because the output voltage of a buck converter is approximately equal to the input voltage multiplied by the PWM duty cycle, it efficiently scales down higher input voltages. Like boost regulators, efficiency is evaluated by the ratio of output power to input power. Since buck converters are optimized for step-down operation, they are ideal for converting our 6 V supply into both 5 V and 3.3 V rails.

The third topology, the buck-boost regulator, can either increase or decrease voltage depending on the configuration and operating conditions. This makes buck-boost designs highly flexible, especially when the input voltage might vary above and below the desired output. However, this versatility comes with drawbacks: buck-boost converters are generally more complex, require additional components, and occupy a larger PCB footprint. Because one of our project goals is to maintain a compact, portable device with a simplified PCB layout, choosing a buck-boost topology would introduce unnecessary complexity without providing any benefits, given that our input voltage will always remain above both target output voltages.

For these reasons, buck regulators are the most logical and efficient choice for both the 3.3 V and 5 V power rails in our design. They offer high efficiency, appropriate voltage conversion, and a compact footprint aligned with our system goals.

3.10.5 LM Regulators

When we began evaluating regulator options for our design, our initial focus was on the TPS series of switching regulators from Texas Instruments. These devices, particularly the TPS564252, were an excellent match for our requirements. They provided the necessary voltage and current capabilities, offered compact form factors suitable for a portable system, and operated with high efficiencies in the range of 90–95%, which aligned well with our efficiency goals. Based on electrical specifications alone, the TPS family seemed to be the most technically sound choice.

However, in our research, we found that the TPS regulators had a noticeably lower success rate in previous Senior Design projects. Many teams reported difficulties such as sensitivity to PCB layout, instability due to layout noise coupling, challenges in achieving reliable startup behavior. Switching regulators in the TPS family often require strict adherence to layout guidelines and careful selection of external components, tasks that can be error-prone in academic prototyping environments.

In contrast, the older LM-series regulators, although less efficient (typically around 60% efficiency), consistently demonstrated higher reliability and ease of implementation across past projects. These parts tend to be more forgiving of non-ideal PCB layouts, have simpler external component requirements, and are generally easier to debug when issues arise. The proven track record of the LM regulators in educational and prototype settings gave us greater confidence in their ability to function reliably in our design, despite their lower efficiency compared to the TPS devices.

Because reliability and project robustness are critical goals, especially in a system that must operate predictably during testing and demonstration, we decided to shift our focus toward the LM-series regulators for the final design. Their higher real-world success rate outweighed the theoretical efficiency advantages of the TPS parts, leading to a more practical and dependable regulator choice for our application.

3.10.5.1 LM25575

This regulator option is a step-down switching regulator from Texas Instruments. This regulator operates with an input voltage between 6V and 42V. Since our design will utilize a 6V input from the batteries, this input voltage range will work, however it is worth noting that the minimum input voltage allowed is 6V which will not give us any flexibility with our design. These ICs will cost $3.63 from DigiKey, since we will need two, the total price for the regulators will be $7.26.

Using WEBENCH a design of this regulator operating at 6V input with a 3.3V and 1.5A output was made. Note: this design is made with a 1.5A output current because this is the maximum. Since the output current was determined to be 2A for additional protection, the 1.5A output will work for the design but it could cause some issues if more current is needed for our components. In this design the regulator operates with 83.7% efficiency and has an output voltage tolerance of 2.76% making it an efficient option with low variation in output voltage. The design will require $320mm^2$ space on the PCB and has a BOM count of 15 parts.

When designed for the 5V and 1.8mA output, the regulator will have very low efficiency of 29.5% and the actual output voltage will be around 5.02V with a tolerance of 3.02%. This design will require a BOM count of 14 parts. This design is very inefficient and could generate an unpredictable and unfavorable outcome to the design, however this is expected when using the less efficient LM style regulators. [38]

3.10.5.2 LM2592HV

The LM2592HV regulator, also from TI, is capable of producing an output voltage between 1.2V to 60V. The recommended supply voltage of the regulator is a minimum 4.5V and a maximum 60V. While on the lower side of this, the voltage we will be supplying of 6V does fall into the ideal range. On DigiKey, these regulators are $6.97 per IC, the total cost of this option would be $13.94.

According to the datasheet when operating with an input voltage in the ideal range, the typical output voltage is 3.3V with a range from 3.168V to 3.432V. In this setup, the regulator has an efficiency of 76%, this is lower than the previous option however, it is not too low for effective operation.

While this option would work for the 3.3V regulator, the 5V regulator design requires an input voltage between 7V and 60V. For our design we will be using a 6V input from our batteries, lower than the required range. Since this regulator will not work for our 5V regulator design we will not be using it in the project. [39]

3.10.5.3 LM20242

This regulator from TI is able to take in an input voltage between 4.5V and 36V to generate an output voltage as low as .8V. This option is also very efficient and depending on the design can have an efficiency of up to 93%. These basic conditions of this regulator make it a feasible option for our design. DigiKey sells these regulators for $4.90, we will need two for our design so the total cost for the regulators will be $9.80.

Using WEBENCH to design the 3.3V regulator with a 2A current, the efficiency of the regulator would be around 88.8%, making this a highly efficient option. The design will create a 3.3V output with 2.35% output voltage tolerance. The footprint for this design is around 277mm^2 with a total BOM count of 16.

Looking at a design on the 5V regulator using the LM20242, the efficiency for a regulator using this design is 11.5%, much lower than other options. This setup for the regulator will generate an output voltage of 5V with an output voltage tolerance of 3.22%. It will operate with the correct output current of 1.8mA and it has a smaller footprint of 267mm^2 with a BOM count of 14. [40]

3.10.5.4 LM22680

One final regulator option to compare is the LM22680 also from Texas Instruments. This regulator operates with an input voltage range from 4.5V to 42V. It has efficiency of more than 90% in some cases and will be able to support both our 3.3V and 5V regulator designs. The maximum output current for this regulator is 2A which does meet the design requirements and is a potential option for our design. The LM22680 ICs from DigiKey cost $4.80 per unit, the total cost for using these regulators would be $9.60

According to the WEBENCH designer, when the 3.3V regulator is designed, the regulator will have an efficiency of 84.2% making this a generally efficient design option. The actual output voltage will be 3.32 with an output voltage tolerance of 2.73%. The LM22680 in this design will be able to produce a 2A output current, which is required for the power of our design. This regulator will have a footprint of 272mm^2 with a total BOM count of 13.

For the 5V regulator design, the output voltage will be 5.06V with a tolerance of 3.01% and the output current will be 1.8mA, both of these will meet the requirements. This regulator will perform with a 29.8% efficiency, while still low this is the highest of the four options. The total footprint for this design is 140mm^2 with a total BOM count of 12. [41]

3.10.6 Regulator Comparison

When comparing these four regulators, several key factors guided our decision-making process. These included each regulator’s ability to meet the required input and output voltage ranges, whether it could reliably supply the necessary output current, and the overall efficiency of the device. Because our project relies on battery power, efficiency is especially important: a more efficient regulator ensures that the available energy is used effectively, reduces heat generation, and helps maintain stable performance across the entire system. Reliability and output accuracy also played a significant role, since consistent power delivery is essential for both the digital and analog portions of the design. In evaluating the regulators for the 3.3 V rail, the LM20242 initially emerged as a strong candidate. It provided high efficiency and demonstrated excellent output regulation performance, making it well suited for the higher-current 3.3 V supply. However, when the same device was evaluated for the 5 V rail, its efficiency dropped significantly due to the extremely low load current required by the operational amplifier. This made the LM20242 an impractical choice for the 5 V portion of the design.

The LM22680, on the other hand, delivered the best efficiency when configured for the 5 V rail and still performed as the second-best option for the 3.3 V rail. Although it is not the absolute top performer for the 3.3 V supply, its consistently strong performance across both voltage rails offers a major advantage: it allows us to standardize the design using a single regulator type. This simplifies component selection, reduces design complexity, and increases the likelihood of reliable performance during testing and final integration.

For these reasons, the LM22680 provides the best overall balance between efficiency, accuracy, and practicality. Therefore, it is the regulator we have chosen to implement for both the 3.3 V and 5 V power stages of our final design.

Table 3.10.6.1: 3.3V Buck Regulator Comparison

3.3 V Buck Regulator	Input Voltage Range	Output Voltage	Output Voltage Tolerance	Output Current Operating Point	Efficiency	Price
LM25575	6V-42V	3.3V	2.76%	1.5A	83.7%	$3.63
LM2529	4.5V-60V	3.3V		2A	76%	$6.97
LM20242	4.5V-36V	3.3V	2.35%	2A	88.8%	$4.90
LM22680	4.5V-42V	3.32V	2.73%	2A	84.2%	$4.84

Table 3.10.6.2: 5V Buck Regulator Comparison

5V Buck Regulator	Input Voltage Range	Output Voltage	Output Voltage Tolerance	Output Current Operating Point	Efficiency	Price
LM25575	6V-42V	5.02V	3.02%	1.8mA	29.5%	$3.63
LM2529	7V-60V	N/A	N/A	N/A	N/A	$6.97
LM20242	4.5V-36V	5V	3.22%	1.8mA	11.5%	$4.90
LM22680	4.5V-42V	5.06V	3.01%	1.8mA	29.8%	$4.84

3.11 Housing

In the paper *Experimental Analysis of a Novel and Low-Cost PIN Photodiode Dosimetry System for Diagnostic Radiology*, the authors present a design approach that closely resembles aspects of our own system. Their PCB incorporated a metal housing around the photodiode to minimize the effects of ambient temperature fluctuations while the detector was positioned inside the X-ray chamber. Thermal stability is important because PIN photodiodes are sensitive to temperature variations, which can introduce measurement drift and affect dose-rate accuracy.

In our design, the overall system is divided into two separate PCBs. The first PCB contains the PIN photodiode and is placed directly inside the X-ray machine where the radiation measurements are taken. The second PCB, located outside the chamber, contains the analog filter circuitry and the ESP32 microcontroller, which processes the dose-rate data and displays the results. Since only the photodiode board is exposed to the radiation environment, it is the only part of the system that requires protective housing. Similar to the referenced study, we will need to provide appropriate shielding or enclosure for the diode PCB to mitigate temperature effects and ensure accurate, reliable measurements during operation.

3.11.1 Housing requirements

The primary purpose of the protective housing is to shield the circuit components from direct exposure to ionizing X-rays, since prolonged exposure can damage electronic parts or introduce unwanted noise into the measurement system. To achieve this, the enclosure must cover as much of the PCB as possible while still allowing the photodiode to function properly. The housing must be fabricated from a material that is both structurally suitable for machining and capable of attenuating X-rays effectively. The X-Ray Calibration Lab has chosen aluminum for this purpose, and the enclosure will be manufactured in the UCF machine shop to meet our design specifications.

In addition to protecting the circuit from the ionizing x-rays, the housing has to also have a section that will leave the PIN diode exposed so it is able to actually sense the radiation to generate the current we will be measuring. There is a small window on top of the housing box, this will be used to place the diode which will be exposed to the radiation. There is also a small circular cutout on two of the sides of this box. These are used to connect the PCB to a coaxial cable which sends the generated current to our main PCB board outside of the machine. This design is 50mm long x 20mm wide x 20mm tall. This specification will play a role in our final design of the PIN diode PCB which will need to fit inside of the box.

3.12 Coaxial Cable

3.12.1 Coaxial cable connection

The PCB board containing the PIN diode will be placed inside the Precision Xray 320 and connected to our second PCB for data analysis through the coaxial cable on the machine. For our design we will need to select a coaxial cable connector for both the diode and main PCB boards to allow the current generated from the sensor to flow to the filter and MCU.

There are three different designs of coaxial cables that we will be looking between, through hole, surface mount, and edge mount. Through holes are mounted onto the PCB and inserted through holes that are drilled into one side of the PCB and are then soldered to pads on the other side. Surface mount connectors are designed to be soldered directly to the PCB, similar to how we will solder resistors and capacitors onto our board. Finally, edge mount connectors are similar to surface mount but instead of being soldered to the top of the board they are soldered to the side.[42] In the X-Ray Calibration lab the housing was designed using the measurements of a through hole coaxial cable connector.

3.12.2 SMA Connectors

In addition to the lab requiring a through hole connection, the cable in the precision x-ray needs an SMA connector which is best for signal integrity. SMA is typically able to operate in a frequency range of 12-18GHz however for a lab use the frequency is typically up to 26.5GHz. Because of this, the connectors we will be looking at are those that are able to operate in the range of around 18-26.5GHz and with an impedance of 50ohms. In looking for different options for this connector I found three that stood out as they had a mechanical design that matched the requirements of our design.

3.12.2.1 RFPC-SMA27-F

This connector is SMA through hole with a right angle for the soldering pins, meeting the requirements we are looking for. It also operates with a 50ohm impedance. This part has a maximum frequency of 6GHz and a unit cost of around $2.26. Since we are looking for parts that will operate with a maximum frequency between 18GHz and 26.5GHz, this part will not be suitable for our design as its maximum frequency is significantly lower than this value. We will not be using this part for this main reason.

3.12.2.2 SMA-J-P-H-ST-EM1

This is another SMA through hole connector that we will be considering for this design. Similar to the previous option, this connector uses through hole soldering at a 90° angle that is required for our design. This option has a maximum frequency of 20GHz and an impedance of 50ohms making it a better choice for our system as it will be able to operate at a frequency that is more precise for our usage. This part has a unit price of $2.43 making it slightly more expensive than the previous part however it is still a better option due to the frequency requirements.

3.12.2.3 SMA-J-P-H-RA-TH1

The final SMA through hole connector we looked at was this option. This connector, also sold at digikey, is also connected to the PCB at a right angle making the physical design appropriate for our usage. In addition, this option also has a maximum frequency of 20GHz with an impedance of 50omh. This part will also meet the electrical requirements of our design but it has a unit price of $3.40 which is significantly more than the previous option. Because of this, we will be using the SMA-J-P-H-ST-EM1 for our design.

3.12.3 SMA Connector Comparison

For this design we will be using the SMA-J-P-H-ST-EM1 for our connections between the x-ray machine and our main PCB. This option is the correct size and shape for our design. In addition it has a maximum operating frequency of 20GHz which is in our ideal range of 18-26.5GHz. Since the first option looked at

(RFPC-SMA27-F) is not in this range it will not be the one we choose. Compared to the SMA-J-P-H-RA-TH1 at a price of $3.40, the SMA-J-P-H-ST-EM1 which costs $2.43 is a more cost effective option for our design and will be what we use in this project.

Table 3.12.3: SMA Connector Comparison

Part	Impedance	Maximum Frequency	Center Contact Materials	Price
RFPC-SMA27-F	50	6GHz	Brass	$2.26
SMA-J-P-H-ST-EM1	50	20GHz	Beryllium Copper	$2.43
SMA-J-P-H-RA-TH1	50	20GHz	Beryllium Copper	$3.40

3.12.4 SMA Cables

In addition to needing to find SMA connectors we will also need to look for cables to use in our design. Based on our selection for the connectors we will be using, the cables we will look at will be simple male to male SMA cables with 50 ohm impedance and since our PCBs will likely be relatively close to each other, we will not need too long of a cable. We would like this cable to be able to work to at least a 20GHz frequency, matching that of the connector.

3.12.6 SMA Cable Comparison

The first option for the cable is the Pasternack RG402 Semi-Rigid SMA. This cable is male to male and has an impedance of 50 ohms. This cable is pretty short, only 6 inches long which could cause issues for our design. It is also a bit more expensive, costing $91.03 from DigiKey. [43]

The next option available is the Amphenol RF SMA Coaxial Cable Assemblies 135101-03. This male to male cable is three feet, a more suitable length for our design, and has a 50 ohm impedance. This is a less expensive option from DX Engineering costing $34.99. [44]

The final SMA cable option is HA141AL-S1-S1-06 from Hasco Components. This cable has male to male connections and an impedance of 50 ohms, which both meet our designs requirements. This cable is however 6 inches long, this could cause issues in our design as the distance between the two PCBs that are being connected will likely be more than 6 inches long. This cable costs $57.99 but will not be a possible option for us as it is not long enough. [45]

Comparing these three options for our SMA cable, it is clear that our best option for the design is the Amphenol RF SMA Coaxial Cable Assemblies 135101-03 from DX Engineering. This cable is the option we will be using for our design.

Table 3.12.6 SMA Cable Comparison

Part	Impedance	Length	Price
Pasternack RG402 Semi-Rigid SMA	50 ohms	6 inches	$91.03
Amphenol RF SMA Coaxial Cable Assemblies 135101-03	50 ohms	3 feet	$34.99
HA141AL-S1-S1-06	50 ohms	6 inches	$57.99

3.13 Software Comparison

The software for the Silicon PIN Diode X-Ray Dose-Rate Detector plays a critical role in ensuring accurate data acquisition, conversion, visualization, and logging of radiation dose measurements. Because the detector relies on a photodiode–amplifier interface that produces continuous analog signals, the software must efficiently manage real-time data conversion and transmission from the microcontroller to the display or web dashboard. The selected software must therefore balance performance, flexibility, scalability, and ease of implementation, ensuring accurate measurements while remaining accessible for development and future modification.

To determine the most suitable software environment, multiple software frameworks were examined based on their compatibility with the Raspberry Pi 4 and the ESP32 microcontroller, which act as the system's digital processing and data-handling units. Specifically, this section compares (1) LAMP, (2) MERN, and (3) PERN web development stacks for visualization and data logging, as well as (4) embedded programming frameworks including Arduino IDE, Visual Studio Code (VS Code), and Espressif IDE for hardware control. The objective is to select an ecosystem that supports both reliable embedded operation and accessible user-interface development.

3.13.1 Web Development Stack Comparison

The system's front-end interface must display real-time radiation levels, historical dose-rate data, and hardware diagnostic messages. Since the detector outputs continuous readings through the ADC-Raspberry Pi pipeline, the web stack must provide high-speed asynchronous updates and seamless database integration.

3.13.1.1 LAMP Stack

The LAMP (Linux, Apache, MySQL, PHP/Python) stack is one of the most established solutions for server-side development. Its open-source nature and strong community support make it a reliable option for stable, low-complexity web applications. LAMP excels in structured data management through MySQL, which offers relational data storage and easy integration with CSV logging from the Raspberry Pi. Additionally, Linux-based servers provide security and strong uptime, ensuring that dose-rate logs remain consistent and protected from corruption. However, LAMP's front-end limitations, its primarily static HTML pages, restrict interactivity, making it less suited for modern, real-time dashboards that require dynamic data refresh.

Advantages: mature ecosystem, low setup cost, simple implementation, stable database management

Disadvantages: limited real-time visualization capability, less dynamic UI options

3.13.1.2 MERN Stack

The MERN (MongoDB, ExpressJS, ReactJS, NodeJS) stack introduces a more modern, JavaScript-based approach. ReactJS allows real-time data visualization through reactive components that update instantly when new dose readings are received. NodeJS and ExpressJS provide robust back-end routing for handling HTTP requests and WebSocket communication, enabling the Raspberry Pi to continuously stream dose-rate data without page refresh. MongoDB's flexible NoSQL schema suits unstructured datasets which is ideal for storing timestamped dose readings, calibration logs, and error messages. The MERN stack is also highly scalable, supporting potential future extensions such as remote web access or wireless dashboard monitoring.

Advantages: real-time UI with ReactJS, scalability, full-stack JavaScript development

Disadvantages: higher development complexity, more system resources required than LAMP

3.13.1.3 PERN Stack

The PERN (PostgreSQL, ExpressJS, ReactJS, NodeJS) stack combines MERN's JavaScript interactivity with the robust structure of SQL databases. PostgreSQL offers advanced querying, data integrity, and relational modeling which is useful for calibration records and multi-user access control. Compared to MongoDB, PostgreSQL's consistency ensures that each radiation reading corresponds to a unique timestamp, preventing duplication and maintaining experimental traceability. PERN thus serves as an ideal compromise, providing real-time performance while retaining data consistency critical for radiation research.

Advantages: real-time visualization, relational database consistency, cross-platform compatibility

Disadvantages: slightly higher configuration time, moderate learning curve

3.13.1.4 Stack Summary

Table 3.14.1.2 Software Stack Comparison

Criteria	LAMP	MERN	PERN
Real-time capability	Low	High	High
Database type	Relational (MySQL)	Non-relational (MongoDB)	Relational (PostgreSQL)
Complexity	Low	High	Moderate
Resource demand	Low	Moderate/ High	Moderate
Recommended for project	Low	High	High

3.13.2 Embedded Programming Frameworks

The embedded software governs the data acquisition pipeline, including analog-to-digital conversion, baseline correction, and error detection. The chosen programming language and framework must maximize hardware efficiency on the ESP32 and enable seamless communication with the Raspberry Pi.

3.13.2.1 C/C++

C/C++ was selected as the primary embedded programming language due to its compatibility with both Arduino and ESP-IDF frameworks. The language provides low-level access to hardware peripherals, essential for precise timing in ADC reads and interrupt-based sampling. C/C++ ensures low memory overhead and high execution speed, reducing latency between diode signal acquisition and digital conversion. While Python offers easier syntax, its higher abstraction introduces unnecessary computational overhead, which can distort real-time readings.

Advantages: high speed, memory efficiency, full ESP32 library support

Disadvantages: steeper learning curve, manual memory management

3.13.2.2 Python / MicroPython

MicroPython offers ease of prototyping and scripting flexibility but lacks the deterministic timing control required for radiation-rate measurement. Its slower execution makes it suitable only for high-level data parsing, not time-critical ADC sampling. Thus, it was considered a second choice, reserved for optional integration scripts running on the ESP32 side for post-processing.

3.13.3 Integrated Development Environment Comparison

Table 3.13.4.1IDE Comparison

IDE	Familiarity	ESP-IDF Support	Abstraction level	Advantages	Disadvantages
Arduino IDE	Moderate	No	High	Simplified libraries with rapid prototyping	Limited low-level control
VS Code	High	Yes	Moderate	Integration with ESP-IDF, debugging	Requires set-up time

				tools	
Espressif IDE	Low	Yes	Low	Full framework control	Heavy learning curve

3.13.4 Containerization Frameworks

To simplify deployment across development environments, containerization tools such as Docker and Podman were compared. Docker remains the industry standard, offering well-documented image repositories and configuration through Dockerfiles. However, Podman’s rootless execution enhances security which is a key advantage for devices exposed to network interfaces. For this project, Podman was selected for its lightweight footprint and reduced system overhead, aligning with the ESP32 resources.

3.13.5 Final Software Selection and Rationale

After comprehensive comparison, the following software environment was selected for implementation:

• Embedded Layer (ESP32): C/C++ using Arduino IDE for low-latency control and ADC interfacing.

• Processing Layer (Raspberry Pi): Python and NodeJS backend to collect, convert, and forward dose-rate data.

• Web Layer: PERN stack for database storage (PostgreSQL), ExpressJS API routing, and ReactJS-based dashboard for visualization.

• Containerization: Podman for deployment security and reproducibility.

This configuration offers the best trade-off between real-time performance, scalability, and maintainability. C/C++ on the ESP32 ensures deterministic sensor sampling; NodeJS and PostgreSQL provide reliable cross-platform data management; and React enables a responsive and intuitive interface for researchers monitoring experiments in real time.

The software design of the Silicon PIN Diode X-Ray Dose-Rate Detector emphasizes reliability, modularity, and extendibility. By integrating a PERN-based visualization layer with C/C++-driven embedded control, the system provides a unified architecture that captures radiation data, processes it with minimal latency, and displays it in a modern, accessible format. The selection balances proven stability from traditional stacks like LAMP with the flexibility of modern JavaScript frameworks, ensuring a sustainable path for future upgrades such as wireless monitoring and cloud data logging. Ultimately, this architecture enables a seamless bridge between hardware-level sensing and user-level visualization, critical for achieving real-time radiation dosimetry.

Chapter 4 Standards

Standards and design constraints are used to ensure engineering projects are safe, reliable, and compatible with other products. These principles help to allow components designed by different manufacturers to function together effectively while also establishing guidelines that maintain quality across industries. In this section, we discuss the relevant standards and design constraints that guided the development of our X-ray dose rate readout machine.

4.1 Safety Standards

4.1.1 Occupational Safety Standards (OSHA)

The Occupational Safety and Health Administration (OSHA) establishes regulations designed to protect individuals working with electrical systems, laboratory equipment, and ionizing radiation. For our project, these standards ensure that the design, development, and testing maintain our health and safety. [46]

4.1.1.1 Radiation Safety Compliance

OSHA sets strict limits on occupational exposure to ionizing radiation, which are relevant when working with the Precision X-ray 320 machine in the lab. These standards require engineering controls such as shielding, administrative controls such as restricted access, and personal protective equipment to reduce exposure. Warning signs, interlocks, and controlled usage protocols align with OSHA's requirements for laboratories working with X-ray sources. [46] By adhering to these guidelines, our project minimizes the likelihood of unsafe radiation exposure to team members or bystanders during testing. We as a team will not be interacting with the machine itself. Under the direction of our sponsor, we will have additional support from her lab in using the X-ray machine.

4.1.1.2 Electrical Safety Standards

The photodiode detector and readout device involve PCB design, power regulation circuits, and battery operation, which fall under OSHA standards. OSHA requires that all electrical systems be designed and handled in ways that prevent hazards such as shock, short circuits, or overheating. This means using proper insulation, grounding, and protective enclosures for exposed wiring. [46]

4.1.1.3 Grounding and Bonding Requirements

OSHA emphasizes proper grounding and bonding of all electronic systems to reduce the risk of electrical shock and equipment failure. For our device, this means ensuring that the PCB includes ground planes and protective grounding of any exposed conductive parts. [46]

4.1.1.4 Enclosures and Accessibility

According to OSHA standards, all components that have energy must be housed in protective enclosures that prevent accidental contact by users. For our project, we are exploring various non-conductive housing materials to create a custom enclosure with limited openings for displays and connectors. Sharp edges, exposed wires, or protruding solder joints must be avoided to reduce the likelihood of user injury. [46] OSHA further requires that labels and hazard markings be placed on enclosures to indicate voltage levels or potential risks.

4.1.1.5 Laboratory and Workplace Practices

Beyond radiation and electrical safety, OSHA standards extend to general laboratory practices, including emergency preparedness, equipment labeling, and safe handling of electronic components. For instance, all testing setups must be clearly labeled with hazard warnings, and equipment must be operated in environments free of clutter or unnecessary personnel. Furthermore, OSHA requires that emergency procedures be in place, including access to fire extinguishers, first-aid kits, and spill-control materials in laboratory environments.

4.2 IEEE

The Institute of Electrical and Electronics Engineers (IEEE) is a widely known organization that develops international standards that establish best practices in the design, testing, and operation of electrical and software systems. For our X-ray dose rate detector, several IEEE standards directly apply to both the hardware and software components. [47]

4.2.1 IEEE 315 – Graphic Symbols for Electrical and Electronics Diagrams

IEEE 315 defines a universal set of schematic symbols for electrical and electronic components. By following this standard in all design documentation, our schematics become unambiguous and easily interpretable by engineers, manufacturers, and reviewers. This is particularly important for multidisciplinary projects like ours, where the PCB design incorporates a mix of analog front-end circuitry (op-amps for current-to-voltage conversion), digital logic (MCU interfaces), and peripheral components (LCD and SD card). Compliance with IEEE 315 ensures that our circuit diagrams are consistent. [48]

4.2.2 IEEE 1057 / IEEE 1241 – Standards for ADC Performance Characterization

Since our design relies on converting the diode's current into a digital signal via the ESP32's analog-to-digital converter, IEEE has established performance parameters for that component. Applying these standards ensures that the readout system produces reliable dose rate measurements, reducing the risk of misinterpretation caused by ADC inaccuracies. This is especially critical in radiation detection, where small variations in measured signal may correspond to significant differences in dose rate. [49]

4.2.3 IEEE 12207 – Software Lifecycle Processes

IEEE 12207 establishes guidelines for the planning, development, testing, and maintenance of software systems. In our project, the embedded firmware on the ESP32 is central to system functionality, handling sensor interfacing, real-time signal processing, data logging, and LCD updates. By following IEEE 12207, we can structure our development process to include requirements definition, modular coding, version control, and systematic testing. This ensures that the software is maintainable, extensible, and reliable, reducing the risk of undetected bugs in critical data acquisition routines.

4.2.4 IEEE 829 / ISO/IEC/IEEE 29119 – Software Test Documentation Standards

When developing this system is it crucial to test it extensively. IEEE 829 provides a standardized framework for test plans, test cases, and result reporting. Applying this framework to our project means that every subsystem is comprehensively verified.

4.3 PCB Design Standards- *IPC-2221A*

The IPC-2221A standard is a standard that covers generic requirements for printed circuit board design. The standard covers board design, component selection and mounting, and other important design requirements. This standard is applicable to PCBs with through-hole, and surface mount components, both of which will be used in our design. By using this standard, there is less room for error and miscommunication when transferring a PCB design from the designer to the manufacturer. It is also necessary to follow as it sets standards that will help keep our board operable and functioning correctly if followed. In using these standards while designing our PCB we can ensure that we will be able to effectively select and place our parts to allow for proper testing, and usage of each component within their requirements. [50]

4.3.1 Board Layout Design

The layout of the PCB should be designed so specific areas of the board are reserved for sections of the design. For example, in our board, we should have a section for the power supply and voltage regulators, and a section designed for the filter and op-amp. It is also a requirement that the components have testable points accessible to allow us to test their functionality effectively. In order to meet this standard and have a successful design we must also ensure that the layout accurately shows the size and locations of all components. We also must ensure that there is at least 1.5mm between our components and the edge of our board to allow proper space to solder and test the parts. [51]

Our board must have a 0.8mm to 2.4mm thickness, this is to prevent warping and to allow for more ease in soldering with through-hole components. In addition, there are PCB parameters that need to be taken into account when using manual assembly. The PCB size (if using automatic assembly) must be able to fit the manufacturers’ equipment specifications. When using pick and place machines we need to ensure that orientation of components is clear on the design. [51]

4.3.2 Component Selection

In our design we must select components that are able to withstand thermal stress, humidity, temperature cycling and all environmental conditions it may face during installation and its usage. Our design will likely use both surface mount and through-hole soldering so it is important to consider components that will be capable of handling the stresses of both assembly methods. [51]

4.3.3 Thermal Management

In ISP-2221A thermal management is used to ensure all components are able to function within their allowable limits. In addition the correct trace width must be measured based on the current carrying capacity and acceptable temperature rise. This is important to remember for design as failure to meet this requirement could cause the board to overheat, which could cause damage to our PCB or the parts being used on it. [51]

4.4 Requirements for Soldered Electrical and Electronic Assemblies- IPC J-STD-001J

This standard is focused on the materials, methods, and criteria for soldering in electronics. It mentions specific solders, fluxes and cleaning agents that can be used in the design of a PCB. This standard is in accordance with IPC-2220, the previously mentioned standard, meaning that the standards mentioned in this will align with the standards mentioned in IPC-2220. The use of this standard will allow for safety of both the components and circuit board and also of the designers who are using the standardized soldering materials. [52]

4.4.1 Soldering Requirements

In J-STD-001J the general soldering process requirements are covered, these are used to prevent damage to both the board and components being soldered onto the board. For hand soldering it is required to control and monitor the tip temperature which should be kept between 340-380°C. When using reflow soldering complete wetting to allow for the components to be fully mounted onto the board. [52]

4.4.2 Material Requirements

Material requirements play a vital role in ensuring the reliability, safety, and overall performance of electronic assemblies. The materials selected for soldering, flux application, and cleaning directly influence the electrical integrity, thermal stability, and lifespan of the system. In our design, maintaining proper material quality is essential to ensure consistent conductivity, corrosion resistance, and long-term durability under varying environmental and operational conditions. Establishing clear material guidelines helps prevent contamination, weak solder joints, and premature failure, allowing the device to perform reliably throughout its intended use. [52]

4.4.2.1 Material Requirements- Alloys

In IPC J-STD-001J, the main material requirements focus on solder alloys, fluxes, and cleaning agents. The solder alloy used must align with J-STD-006, another standard focused on the requirements of solder alloys. These alloys can be either Sn-Pb or lead-free, in our design we will be using lead-free alloys. [52]

4.4.2.2 Material Requirements- Fluxes

The standard J-STD-001J requires the solder fluxes used to meet another standard J-STD-004 which describes the requirements for fluxes used in the soldering process. This standard covers different types of flux including liquid flux, and paste flux. These flux residues used must be non-corrosive and should be able to be removed according to the cleaning requirements (typically $<1.56 \mu g/cm^2$ NaCl equivalent). [52]

4.5 SD Association

The SD Association is responsible for many standards relating to the design and use of SD cards. SD cards are widely used and because of their functionality, it is extremely necessary for the cards to meet specific standards. Since these cards are designed with the purpose of collecting data from one device and sending it to another, they need to be designed in a way that will allow the card to effectively connect with many devices. One of the main ways this is ensured is through standards of size and layout of the SD cards. [53]

SD cards must all use the same pinout to effectively communicate with different devices. In SPI mode- which we will be using- there are two pins for transferring data, pin 3 is used as the data input and pin 7 as the data output. Pin 2 is also used for chip selection, allowing communication to the SD card, pin 5 is used as the serial clock to synchronize data transfer. The final two pins which are used in SPI design are the power supply (pin 4) and ground (pin 6). It is vital that all SD cards use the same pinout design for effective communication and data transfer to take place between multiple devices.

In addition to the pinout of MicroSD cards needing standards, the physical and sizing elements of MicroSD cards need to be consistent as well. These cards are required to have the dimensions of 11 x 15 mm with a 1mm thickness.[54] There are also standards for memory on these cards, standard SD cards (both SD and microSD) have up to 2GB of memory available. Bus speed for these cards is also standardized for both a default mode and high speed mode. This uses two lanes for data transfer and a bus speed of 12.5MB/s for default speed and 25MB/s for high speed SD cards. Through standards of embedded SD’s, the engineering of the system is simplified since all of these devices should be designed with the same input/output interface. [54]

4.6 Communication Standards

4.6.1 Serial Peripheral Interface (SPI)

Serial Peripheral Interface (SPI) is a widely used synchronous communication protocol that enables fast, full-duplex data transfer between a central controller and multiple peripheral devices. Originally introduced by Motorola, SPI has become a staple in embedded systems due to its simplicity, reliability, and high-speed performance therefore making it ideal for applications like our detector system, which requires quick and consistent communication between the microcontroller, ADC, and supporting sensors [55].

Compared to other serial protocols such as I²C, SPI offers higher data throughput and lower latency, which is particularly useful when transmitting continuous analog-to-digital data. Unlike I²C, which relies on shared addressing across devices, SPI uses individual chip-select lines to communicate directly with each peripheral. This point-to-point approach allows faster and more deterministic control of timing and data flow, both of which are crucial in our system's real-time data acquisition.

Although SPI does not have a single governing standard under organizations like IEEE, it is well-defined by industry practices and manufacturer documentation. Companies such as Texas Instruments, NXP, and STMicroelectronics publish detailed SPI guidelines in their datasheets and application notes, which serve as de facto standards for electrical characteristics, timing, and compatibility. Over time, enhanced versions like Dual, Quad, and Octal SPI (QSPI/OSPI) have emerged, improving the bandwidth by transmitting multiple bits per clock cycle. These variants are often used for fast memory interfacing or large data transfers [56].

SPI operates over four key signal lines:

- SCLK (Serial Clock): Synchronizes communication.
- MOSI (Controller Out, Peripheral In): Transfers data from the controller to the device.
- MISO (Controller In, Peripheral Out): Sends data from the device back to the controller.

- CS (Chip Select): Activates specific devices for communication.

The controller generates the clock and manages device selection, ensuring data is transferred predictably. In multi-device systems, additional logic or multiplexing may be used to reduce the number of dedicated select lines, simplifying wiring while maintaining data integrity.

SPI is highly configurable through its clock polarity (CPOL) and clock phase (CPHA) settings, which define how data is sampled relative to the clock edge. This flexibility allows SPI to adapt to a wide range of peripheral requirements. Communication typically occurs in 8-bit frames, though implementations may vary depending on device capabilities. Operating voltages are defined by the hardware, commonly 3.3V or 5V for embedded applications, with manufacturer timing diagrams specifying setup and hold times for stable operation.

For our X-ray detector project, SPI provides the necessary speed and simplicity to relay converted photodiode data from the ADC to the microcontroller with minimal delay. This deterministic timing is essential for ensuring that measurement results accurately reflect the radiation exposure in real time. Additionally, because the system runs in a controlled hardware environment, the short wiring distance minimizes noise and helps maintain data integrity.

While SPI excels at speed and design simplicity, it lacks built-in error detection and acknowledgment mechanisms. Designers typically address this through software-level solutions, such as adding cyclic redundancy checks (CRC) or redundant sampling routines. Another design consideration is scalability since each peripheral requires its own chip-select line, adding more devices can increase pin usage. Nonetheless, in systems like ours with only a few key components, SPI remains an efficient and dependable choice.

Overall, SPI continues to be one of the most practical communication standards in embedded hardware design. Its straightforward architecture, broad industry support, and adaptability make it a perfect fit for compact systems requiring high-speed, low-latency data exchange. Reference materials from manufacturers such as Texas Instruments, STMicroelectronics, and NXP provide detailed best practices for implementing robust SPI communication in both prototype and production-level designs [57].

4.7 Constraints

4.7.1 Health and Safety (X-Ray)

Health and safety represent some of the most critical constraints in the development of an X-ray dose rate detector, as the project involves both ionizing radiation and electronic hardware. Unlike many embedded systems, this device must be developed and tested in close proximity to a highly powerful X-ray source, which creates specific risks that must be managed.

4.7.1.1 Radiation Exposure Risks

The most significant safety consideration is ionizing radiation exposure. Even though the detector itself does not emit radiation, its testing environment places team members in potential proximity to x-ray beams. This requires strict adherence to laboratory safety protocols, including limited access, use of lead shielding, radiation warning signage, and appropriate personal protective equipment (PPE). In addition, the system must be designed to minimize unnecessary operator interaction with the source during measurement.

4.7.1.2 Electrical Safety Risks

The system includes sensitive analog front-end circuitry, high-current op-amp stages, and a battery power supply. Improper wiring, poor insulation, or overloading could result in electric shock or overheating. These risks constrain the design to include proper grounding, fuses, protective enclosures, and heat management. Furthermore, since the device may be used in a laboratory with other sensitive instruments, electromagnetic interference (EMI) must be minimized to prevent cross-system hazards.

4.7.1.3 False Readings and Ethical Safety

Another health-related constraint lies in the accuracy of measurement. If the detector produces false negatives or positives, operators may unknowingly expose themselves or others to unsafe conditions. This elevates the importance of calibration against known radiation standards, redundancy in measurement verification, and well-documented testing procedures.

4.7.2 Manufacturing PCB

Custom PCB fabrication requires lead time for design, ordering, and assembly. Errors in the layout may necessitate reorders, increasing both cost and time pressure on the team. Since the senior design schedule is fixed, this creates a constraint where PCB errors cannot be easily recovered without significant project disruption.

4.7.3 Economic

For many senior design projects, cost represents a primary limiting factor. However, in our case, direct financial constraints are minimized because our sponsor is funding the acquisition of necessary components, fabrication services, and testing equipment. This sponsorship allows us to prioritize technical performance and reliability without being forced to compromise based on price alone.

4.7.3.1 Component Availability and Supply Chain Factors

Even with funding secured, the availability of specialized components such as the AXUV20HS1 photodiode or specific op-amp models can pose economic challenges. Global supply chain fluctuations, semiconductor shortages, or shipping delays may still impact the timeline of the project. For example, if the photodiode becomes back-ordered, alternative sourcing options could increase costs or extend delivery times, potentially disrupting our schedule.

4.7.3.2 Tariffs and Import Considerations

Another factor that remains outside of our direct control is the potential impact of tariffs or international trade regulations. Many electronic parts are manufactured overseas, and changes in tariff policies could increase overall project expenses. It also makes it harder to obtain because of supply chain uncertainty and shipping. While these additional costs would be absorbed by our sponsor, they nonetheless represent an economic constraint that could influence budgeting and procurement planning.

4.7.3.3 Long-Term Commercialization Considerations

Although sponsorship covers this prototype phase, scaling the design for widespread use would introduce significant financial considerations. Certification for radiation measurement devices, compliance with safety standards, and mass production would all require substantial investment. Thus, while immediate financial pressures are alleviated, the project must still be designed with economic scalability in mind should it be pursued beyond the academic setting.

4.7.4 Time

One of the biggest constraints our group is going to face when working on this project is the time limitation given by the design of the course. We have two semesters to write our paper, design our prototype, develop it as well as test the system before presenting it at the final showcase on top of taking other classes and extracurriculars. This constraint makes it crucial for us to make smart decisions with quick thinking as well as making sure we are making deadlines on time as we don't want to compromise our performance or part of the project.

An additional challenge to this project is that this project is sponsored. We had to make sure to take our Sponsor's time and schedule into consideration too to make sure that we are keeping our sponsor updated while meeting the requirements, standards, and specifications led by her and the rest of the team. Working alongside our own time constraints as well as hers had made it crucial for our team to have a disciplined schedule set very early on in the beginning of the first semester. We made sure to form our group early on, meet with our sponsor and the research team to work on the project specifications and standards as well as set strict timelines for our group to meet recurring only once a week just as a group and another time to meet with our sponsor to provide updates. Setting this time as well as framing deadlines early on has aimed to mitigate the time pressures that may come up later in the project and the semester begins to ramp up.

Another issue stemming from having a time constraint is the amount of time needed for manufacturing our device. We need time to build, test, and debug our device which can be quite challenging with such a short timeframe to complete the project. Errors in system design are expected and almost inevitable when designing a device at the scope of which we are. Each problem requires time to resolve and debug and we need to account for that when making milestones/deadlines so that we don't heavily disrupt our progress and ultimately compromise on the performance of our project. Additionally, having a sponsor who is in charge of our finances can also add to unexpected delays when it comes to ordering parts. It is important for us that we are asking for parts to be ordered in advance and strict about when we need them to make sure that our workflow is not impacted but also make sure that it is done in time for our sponsor's needs as we are also working simultaneously to meet their deadlines.

Shipping delays could also impact our work especially when ordering PCB's, and our photodiode which is a crucial piece for our project. WIth that in mind, it is imperative that we are not only ordering things in a timely fashion but making sure that we also have ordered backups so that time isn't working against us if one component is not working and we have extra to rely on.

Proper communication is also necessary to make sure that we are not slowing our progress especially when we are communicating with our team, our sponsor, and the research team that we are working closely with. Collaborating with essentially 10 people (between our 4 person team, our sponsor, and her 5 person team) makes scheduling difficult and makes having multiple meetings and documentation important when working on our in person collaboration.

The effect of this constraint could result in a compromised, rushed, final product if we don't properly manage our project. We have made weekly meetings a priority, as well as organized an extensive Google Drive for us to document all our work and progress to make sure that the project is on track and ensure that time is not against us when completing this project, rather for us during our project completion throughout this semester and the next.

4.7.5 Power

One of the most important parameters to consider in this project is power. Without sufficient power, the components will not operate, while excessive power can damage them. We must also ensure power consumption stays within acceptable limits since heat generated from power loss may harm the components. This constraint affects our battery choice, voltage regulator selection, thermal management solutions, run time, and safety margins. As indicated in Figure 3.8.1, the power consumption of the electrical components ranges from 0.045W to 68W, with total system consumption between 13.26W and 70.10W. The total power consumption will dictate our selection of efficient power sources.

We plan to use four 1.5V AA alkaline batteries in series for a 6V supply, which meets the components' 5-10V requirement. However, we need to check the batteries' runtime and peak current capabilities before finalizing the hardware design. Assuming a battery capacity of 2000 mAh, a 6V system drawing 13.26W requires about 2.21A (13.26W/6V), resulting in an estimated runtime of 0.9 hours (2000 mAh/2.21A) or 54 minutes. At maximum load (70.10W), the current draw rises to 11.68A, reducing runtime to just 10 minutes (2000 mAh/11.68A ≈ 0.17 hours). Actual runtimes may differ from these estimates due to ideal condition assumptions.

Our selected buck regulators operate at approximately 90% efficiency. Factoring this in, the system at 13.26W will actually draw (13.26/0.9)/6V ≈ 2.46A, resulting in a runtime of about 49 minutes. At maximum load, the current increases to roughly 12.98A with a runtime of around 9 minutes (0.15 hours). As we can see, higher power consumption decreases runtime.

Both batteries and regulators generate heat, emphasizing the need of proper thermal management such as heatsinks, airflow, or thermal vias on the PCB to protect the components. The hardware design should include a 20%-30% safety margin above the peak expected power usage. Our project aims to build a power-efficient, reliable system. By implementing safeguards against power overconsumption, planning for unforeseen circumstances, and ensuring effective thermal management, we can create a stable, energy-efficient, and dependable device.

Chapter 5 Comparison of ChatGPT and Similar Platforms

5.1 Introduction of LLMs and Comparison

Generative artificial intelligence (AI) chatbots and large language models (LLMs) have become increasingly prevalent over the past several years. Models such as ChatGPT, Microsoft Copilot, and Deepseek are built on massive datasets and deep learning architectures capable of summarizing information, predicting text, and generating original content. These LLMs are used in many people's daily lives, and individuals rely on AI to access an abundance of information, making their lives easier and more efficient. By providing a prompt and expecting an original response, people are able to boost productivity and have access to information faster than ever before. Some may use AI for creativity, such as story writing, while others use it in technical research settings. Regardless of the application, there is a need to identify the strengths and weaknesses of these LLMs and how they are relevant to our project and report writing.

5.1.1 ChatGPT

ChatGPT, developed by OpenAI, quickly became one of the most recognized and widely used LLM platforms. As of October 2025, the most recent architecture is GPT-5 with more reasoning and faster processing than previous models. In research, it is frequently used for tasks such as condensing information, design brainstorming, data interpretation, and code prototyping. Its integration with features such as browsing, memory, and image analysis makes it even more convenient to use. The platform also has “memory” and “Deep Research” modes, which enable the model to recall past prompts and search for information with citations. This can make long-term research projects much easier.

Despite its versatility, ChatGPT has its limitations. While its responses are coherent, they can occasionally overstate findings or merge unrelated concepts.

This can cause confusion or simply misinformation for researchers, which can be detrimental. There is an emphasis on how to prompt the chatbot, which is crucial in getting the output one would want. It may oversimplify complex models or misinterpret experimental data if not guided by carefully structured prompts. Due to these drawbacks, most researchers treat it as an assisting tool rather than a primary source, ensuring that all AI-assisted outputs are verified.

5.1.2 Microsoft Copilot

Microsoft Copilot is an LLM integrated into Microsoft's productivity suite, which includes Word, Excel, PowerPoint, and Outlook. Rather than serving as a standalone chatbot, Copilot acts as an assistant that provides contextual recommendations, document editing support, and task automation directly within the user's workflow. It should be noted that Copilot is powered by OpenAI's models. So some answers that Copilot generates may resemble ChatGPT. Its integration allows it to interpret and manipulate existing documents, summarize large data sets, and even generate content. This makes it especially valuable for people who mainly use Microsoft Office products for daily productivity. Another benefit of Microsoft Copilot is that it is considered safer than other LLMs in terms of data security. Because it operates within Microsoft's ecosystem, it has those safeguards in place for your data, ensuring that research data remains private and traceable. This can be an advantage when working on a project that is more classified, such as defense research, medical trials, or semiconductor design projects.

However, Copilot does have its drawbacks. It is not as flexible as other AI platforms because it is confined to Microsoft's ecosystem. This poses an issue for cross-functional applications. Also, while Copilot can synthesize content and summaries from documents, it does not clearly indicate where specific pieces of information come from within those files. This makes it difficult for users to verify or trace statements back to their original context, a serious limitation for technical documentation and legal or compliance work where citations are critical.

5.1.3 Deepseek

DeepSeek is a newer LLM that is rising in popularity for focusing on technical tasks like coding, data analysis, and precise research. DeepSeek LLM 67B surpasses LLaMA-2 70B on various benchmarks, particularly in the domains of code, mathematics, and reasoning [citation number]. This LLM allows full access to its architecture and training parameters, making it appealing to research institutions that want reproducibility and transparency about the model's behavior. Since the model's code and training parameters are publicly available, it can be adapted for specialized use cases. In academia, where resources may be limited, the ability to run on standard GPU setups without heavy cloud infrastructure is preferred. Another advantage is its customizability. Because it is open-source, users can fine-tune the model with their own data or modify its architecture to better align with their research needs.

However, DeepSeek also has several disadvantages that limit its usability. Since it is newer and less widely tested, it lacks the extensive user support that you can find in systems like ChatGPT or Microsoft Copilot. Furthermore, safety systems are still developing, which is challenging in environments where strict data control is needed.

5.2 Project Impact

Upon examining various LLM options and weighing their pros and cons, we will discuss how our team has used LLMs in our project development. Some of the main advantages we valued were accessibility, multi-modal capabilities, and organization.

Throughout the development of our project, our team actively utilized ChatGPT as a tool to enhance our decision-making. We selected ChatGPT primarily for its accessibility and adaptability, as it could be applied to multiple phases of the design process. One of the most significant ways it supported our work was during component selection and standards research. Finding reliable information on electronic components and applicable safety or IEEE standards typically requires extensive research across numerous datasheets and websites. Using an LLM consolidated this information, allowing our team to compare specifications more efficiently.

However, we also considered the limitations of using ChatGPT and refrained during certain tasks. We avoided using it for numerical analysis, circuit simulations, or code generation, as the model's mathematical reasoning is not always precise. ChatGPT has been shown in several independent evaluations to produce inaccurate or inconsistent mathematical results, particularly in tasks requiring symbolic computation or multi-step quantitative reasoning [X] (Bang et al., 2023).

5.3 Case Studies

In this section, we compare how different Large Language Models, including ChatGPT, Microsoft Copilot, and DeepSeek respond to the same set of prompts to see how they perform in technical and explanatory contexts. Our goal is to get a better sense of each model's organization, depth, and efficiency, especially when applied to engineering-related topics. By looking at their responses side by side, we can identify where each model excels, where it falls short, and what responses we would prefer to help us with our project. All LLMs were familiar with the context of our project and we only asked the prompt one time with no follow up questions.

5.3.1 Case Study 1

We prompted the LLMs: “What are some electrical engineering standards related to PCB design?”. Refer to Appendix E, [1a], [1b] and [1c] for the Case Study 1 outcomes from ChatGPT, Microsoft Copilot, and Deepseek. This was a question we asked aiming to have a list of standards we can further explore to integrate into chapter 4 of our paper.

ChatGPT provided an extensive list of standards that covered many aspects of PCB design. It also provided a summary table at the end including all the standards and their key focuses. This was helpful in selecting what was relevant to us. The only minor drawback is that it focuses primarily on design-oriented standards and briefly touches on fabrication or assembly guidelines, which would have given a more broad overview. Having a more diversified list would allow for our standards to be more comprehensive.

Microsoft Copilot gave a much shorter list of standards and did not explain what they were or why they were relevant. It was a more condensed version than the ChatGPT response, this can be understood because they come from the same model. One thing that Copilot did that was appreciated was that it included a link to where it got this information to use as a reference.

Deepseek output the longest list of standards and broke down what the standard is and why it is important. It lacked consistency in its answer because some standards had explanations for why they were important, and some simply had a list of key focuses. Regardless, this answer gave us lots to choose from.

5.3.2 Case Study 2

We prompted the LLMs: “What does an MCU do?”. Refer to Appendix E, [2a], [2b] and [2c] for the Case Study 2 outcomes from ChatGPT, Microsoft Copilot, and Deepseek. We aimed to understand how the LLMs do with explaining the functionality of a component in simple, digestible terms.

ChatGPT’s explanation of the MCU is detailed and structured. It shows a connection between theoretical understanding and real-world application. One of its biggest strengths is how it integrates the MCU’s internal functions with specific project relevance, such as how the ESP32 would operate within an X-ray dose rate detector. This applied context makes it particularly valuable for us writing a technical document. However, for someone that does not know anything about technical jargon with electronics this might be too excessive for someone looking for a quick summary.

Microsoft Copilot gave a lot of irrelevant information in its response. It did not do a good job at answering what an MCU does but dumped information about MCUs in general. It also does not relate anything to our project so it is not as relevant of an answer to use when trying to understand how it fits into building our x-rate dose rate detector. The response was not concise and provided a lot of fluff, like how they differ from microprocessors. The answer provided was not efficient in teaching someone what an MCU does.

The response from Deepseek was very detailed and touched on how the MCU would fit into our project and integrating components. This answer allows one to easily understand what an MCU is and in great detail explains what the MCU will do while maintaining an easy-to-understand structure.

5.3.3 Case Study 3

We prompted the LLMs: "If I want an output voltage of 2.5V and the AXUV20HS1 photodiode produces 2.5 microamps of photocurrent at any given x-ray intensity, what feedback resistor should I use when constructing the TIA?". Refer to Appendix E, [3a], [3b] and [3c] for the Case Study 2 outcomes from ChatGPT, Microsoft Copilot, and Deepseek.This question assists us in the design of the circuitry as well as tests the LLMs ability to perform computations. This is a simple enough computation to perform by hand using Ohm's law so it can easily be checked.

The ChatGPT answer is the only one that includes the negative sign in the transimpedance amplifier (TIA) equation: Vout = -Iphoto x Rf. That's a crucial detail because, in a standard TIA configuration, the circuit inverts the signal. While all models get the correct magnitude of 1 MΩ, ChatGPT explicitly explains the inverting signal that if you want a positive 2.5V output, you'll need to either add a non-inverting stage after the TIA or reverse the photodiode's orientation.

The Microsoft Copilot answer is the most straightforward and the least detailed. It gives the formula, and the direct calculation to get to the answer. It's good if you just need the number and a quick justification. The calculation it uses to solve for the resistor is Rf = Vout/Iphoto. However, in the process of simplifying the calculation, it fails to mention the inverting aspect of the TIA. It's efficient, but it leaves out important details that could trip you up when actually building the circuit.

The Deepseek answer is the most technically advanced and goes above just doing the calculation. The initial calculation also misses the negative sign, simplifying the equation to Vout = Iphoto x Rf. But what makes this response stand out is continuing to turn a simple resistor calculation into design advice for implementation. The practical concerns include: Op-Amp selection, stability and bandwidth, resistor specifications, and diode biasing. From an engineering standpoint, it is the most thorough and I don't feel the need to ask for more follow-up questions because they were already answered.

5.3.4 Case Study 4

We prompted the LLMs: “Describe the main sources of noise in a low-current photodiode readout circuit and how they can be minimized through op-amp design and PCB layout.”. This was a good question to ask the LLMs because it tested their ability to condense complex technical information and tested their practical application ability.It required the models to go beyond simple definitions and demonstrate how different factors interact in a real engineering context. It also helped highlight differences in how each model structures information and what details they prioritize. It could also show the accuracy of the information because if the same answer is repeated, there is a chance it is valid.

The ChatGPT response is the most organized and compact with information. It concisely breaks down the noise sources into four main categories: thermal, shot, flicker, and op-amp V/I and proceeds to make a three-part guide focusing on op-amp selection, circuit design, and PCB layout. The solutions it provided were easy to understand and doable. ChatGPT commonly provides a table at the end of each prompt when there is a lot of information provided, which is appreciated because it can be viewed over, and the more detailed explanation is right above.

Microsoft Copilot’s response does a decent job of breaking down the technical aspects of noise in a low-current photodiode readout circuit, but it’s very short and not informative. The bullet points make it easy to skim, but they limit flow and depth. In a research or design context, I’d prefer the content to have more background that connects ideas like explaining why each noise source matters and how the minimization techniques interact with one another. However, the information was similar to ChatGPT as it correctly identifies thermal, shot, flicker, and op-amp noise, and it highlights practical design considerations like guard rings, feedback capacitors, and low-bias op-amps. This response was similar to ChatGPT which shows how they use the same model.

The Deepseek response does a great job breaking down noise sources in transimpedance amplifier design. It talks about the thermal and shot noise and parasitic effects and then transitions deep dives into practical noise-reduction strategies. It offers good advice for op-amp selection, bandwidth control, and PCB layout. I especially like how it connects theoretical equations with practical design practices. This is helpful in getting background for why we choose components and why they work. The way the layout section is explained was more conversational than the other LLMs. I personally liked this flow because it made it much easier to read while still maintaining organization. The other versions, while more concise, do not really provide the answer one would want when doing such a technically advanced project.

5.3.5 Case Study 5

We prompted the LLMs: "What factors should be considered when selecting and integrating software for an embedded system in an engineering project?". Refer to Appendix E, [5a], [5b] and [5c] for the Case Study 5 outcomes from ChatGPT, Microsoft Copilot, and Deepseek. This was a question we asked to aim for a list of factors we can explore to directly integrate when working on the software selection and comparison of packages part of our paper.

5.3.5.1 ChatGPT

ChatGPT gave a detailed breakdown of the factors to consider when selecting software for an embedded system. It emphasized areas such as hardware compatibility, real time performance, security and maintainability. The response explained how software choices must align directly with processing power, memory limitations, and communication interfaces which is useful in our case for understanding how to match the software to our project's hardware. It also mentioned real-time considerations and the use of operating systems for performance purposes. The answer was strong in terms of holisticness and its organized manner. It covers both the technical side and implementation side of things, but generally leaned more toward principles than software examples upon first search. This probably can be expanded on with more questions but it is a little limited to direct application to our system set up.

5.3.5.2 Microsoft Copilot

Microsoft Copilot gave a more concise response that focused mainly on language selection and efficiency in terms of the software. It mentions compatibility with the hardware and real-time considerations briefly but does not go into detail when explaining the integration process or testing methods which are essential to the project. The benefit to copilot was that it gave examples of tools and frameworks which makes it easier to see how things would be implemented. Nonetheless, there is a lack of depth when it comes to answering the list of factors and the answer is less useful for system set up compared to Chat GPT.

5.3.5.3 Deepseek

Deepseek offered the most technical response of the 3 AI models. It broke down embedded softwares into firmware development, communication protocols, and debugging workflows. Additionally, it provided some insight into common conflicts experienced which the other 2 models lacked information on. Some of these included interrupt management, modular programming as well as how one can go about mitigating this. Although these were some great benefits, the model's answer still lacked implementing how the project will be managed which Chat was successful in mentioning. The detail in explaining the technical stuff makes it a valuable application for our design however, it needs more of a holistic response.

ChatGPT provided the most holistic and organized answer. While Copilot offers a very clear answer and Deepseek provides strong technical insights, a combination of these helped us understand how software should be selected and integrated within an embedded system.

Chapter 6: Hardware Design

At the start of the hardware design phase, we organized the X-ray Dosimetry System into several functional sections to better understand its operation and interconnections. We broke down the system into subsections and analyzed the requirements needed for those sections as well as chose components. This assists us with understanding how each subsection will be connected and interact with each other to create the overall readout system.

6.1 Subsystem Overview

The X-ray Dosimetry System was divided into several key subsystems. Each subsystem fulfills a specific role in the measurement, processing, and output of X-ray radiation. The main subsystems include the X-ray source machine, diode, op-amp, microcontroller, and LCD display. Figure 6.1 illustrates the overall subsystem block diagram, showing how data flows through the device.

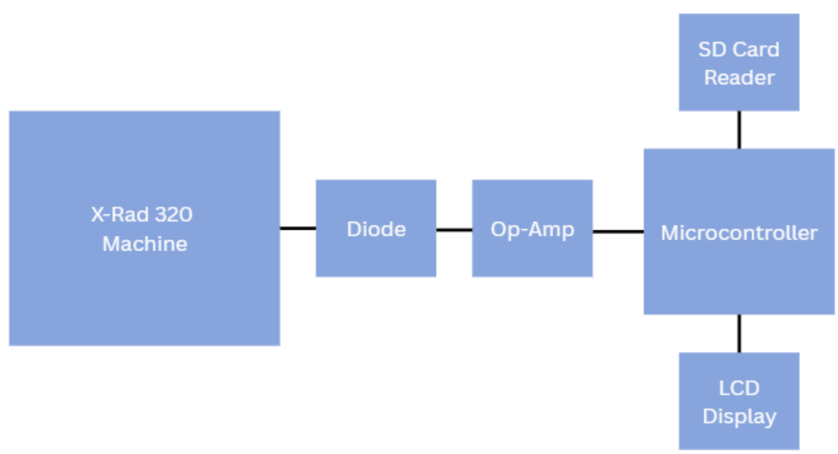

Figure 6.1.1

6.2 Diode PCB

The AXUV20HS1 photodiode did not exist in Fusion 360's default component libraries, so I had to create it manually. This process involved designing a custom schematic symbol to represent the diode's anode and cathode terminals, building a corresponding PCB footprint with two through-hole pads spaced 2.54 mm apart, and adding a 5 mm silkscreen outline to match the diode's physical body. Afterward, I linked the symbol and footprint together into a new component within my personal library, mapping each pin to its corresponding pad. This ensured the AXUV20HS1 could be accurately placed in both the schematic and PCB layout for our project.

Figure 6.2.1 PIN Diode

The diode PCB was designed to securely hold the AXUV20HS1 photodiode and provide a clean, low-noise interface between the X-ray source and the second PCB board that will be used to amplify and filter the signal. It will be a compact 20 mm × 50 mm layout that fits within the X-ray chamber housing and ensures minimal parasitic effects. A reverse-bias resistor and decoupling capacitor were placed close to the diode to maintain a stable bias voltage and reduce high-frequency noise.

To preserve signal integrity, a ground plane and guard trace were implemented around the photodiode and input node, minimizing leakage currents and stray capacitance that could distort the intended signal. An SMA connector provides a shielded path for transmitting the signal to the secondary board and we included a low-capacitance TVS diode to protect the circuit from transient voltage spikes during operation.

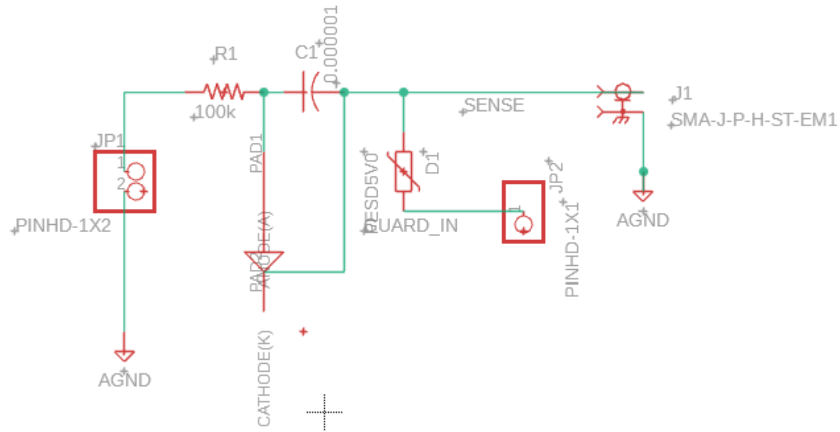

Figure 6.2.2 Diode and TIA Schematic

6.3 Op-Amp Filter

The secondary PCB was designed to further condition the output voltage from the transimpedance amplifier and prepare it for analog-to-digital conversion by the ESP32 microcontroller. This board implements a two-stage passive RC low-pass filter followed by a unity-gain buffer using the precision OPA141 operational amplifier.

The filter being implemented is a two-stage RC low-pass filter with buffering used to condition the transimpedance amplifier (TIA) output. The input signal enters the circuit through the FILTER_IN header and first passes through a 16 kΩ resistor (R1) and a 100 nF capacitor (C1) connected to the mid-supply reference voltage (VREF). This forms the first RC network, establishing a cutoff frequency near 100 Hz. The filtered signal then feeds the non-inverting input (pin 4) of the OPA141 operational amplifier, which is configured as a unity-gain voltage follower by directly connecting its output (pin 1) to its inverting input (pin 3). A second 100 nF capacitor (C2) is connected at the output node to further smooth residual high-frequency noise. Finally, a 100 Ω series resistor (RISO) is placed between the op-amp output and the ADC_IN header to protect the op-amp from transient current spikes generated by the ADC's internal sampling capacitor during conversion.

The +VS and –VS pins correspond to +5 V and AGND, respectively. The VREF net (approximately 2.5 V) biases the signal around mid-supply, ensuring proper operation in a single-supply configuration. [4]

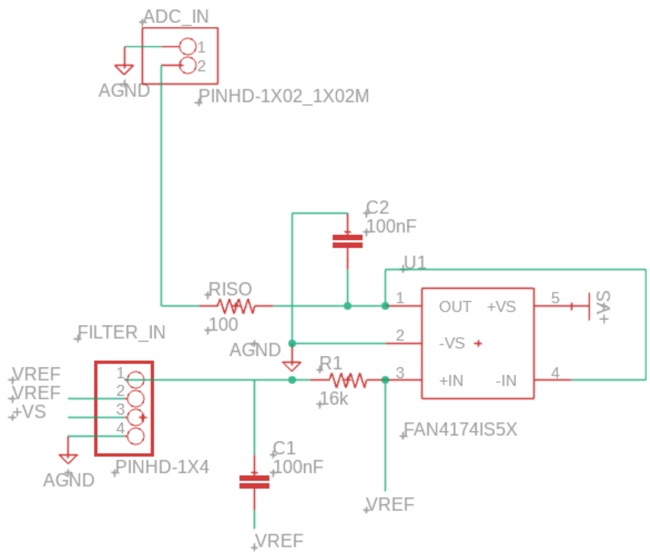

Figure 6.3.1 Low Pass Filter Schematic

6.4 Voltage regulator design

There are two voltage regulators being used in this system, the first is the regulator which will be connected to the battery pack for the input voltage and the output voltage will be connected to the V_{cc} port of the MCU. To design this regulator the equations and schematics from the datasheet were used along with the WEBENCH Power Designer.

The datasheet of the LM22680 explains the design process of the regulator with some schematic examples and equations for finding the impedance of different components in the regulator design.

6.4.1 3.3V Regulator

In the typical input range with an output of 3.3V at 2A, the regulator circuit will need 5 capacitors (labeled C1-C4 and C6), 3 resistors (labeled R_{FBB}, R_{FBT}, and R3), an inductor, and a diode. The inductor is found using equation 12 in the datasheet, using this equation the inductor value is found to be 4.7uH. Using equation 14 the input capacitor value can be found. From this equation, the input capacitor must be 10uF and 1uF. To find the output capacitor equation 16 is used, from this we find that the output capacitance must be 47uF, this value meets the requirement from the datasheet of the output capacitor of being at least 100 uF or more. A voltage divider is used to find the values of R_{FBT} which are found using equation 19, 1K and 1.58K, and a 1K value for R_{FBB}, the sum of these two resistor values should be at a maximum of 10K to maintain an accurate output voltage.

These values are consistent with the values shown in the WEBENCH design of the LM22680. The CAD schematic created in KiCad of this design is shown below.

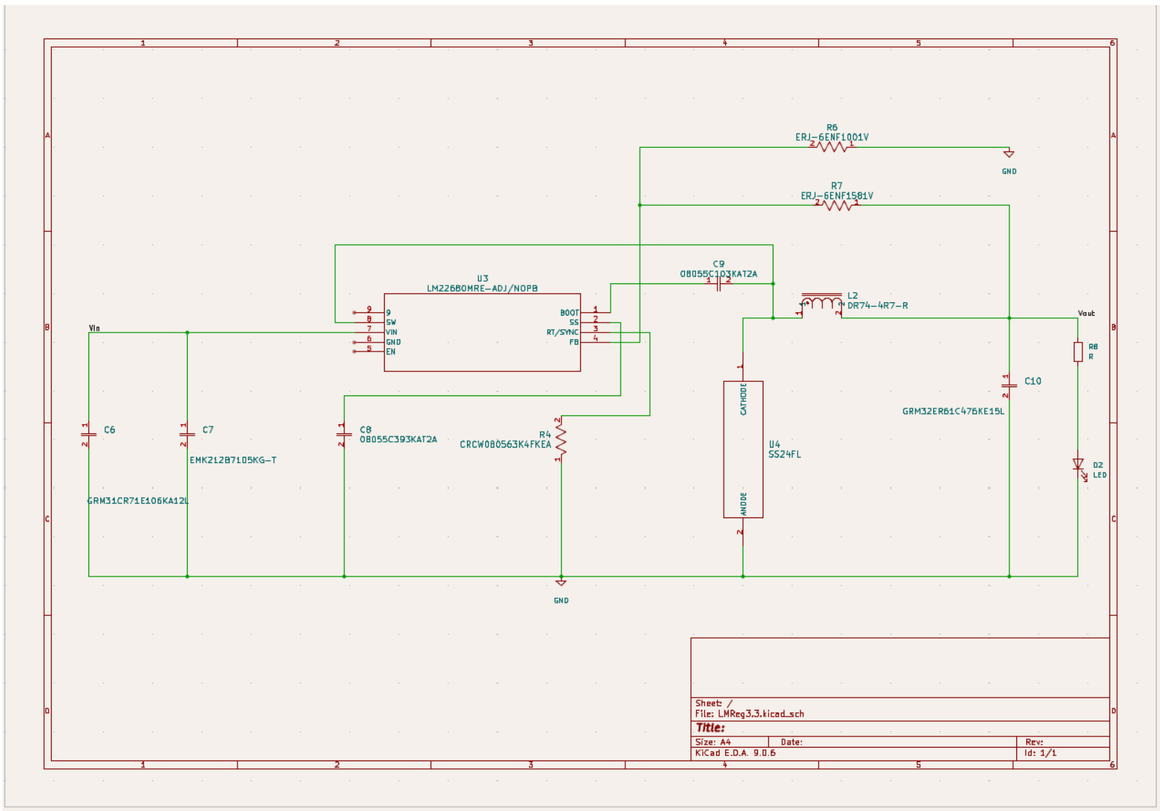

Figure 6.4.1 3.3V Regulator Schematic

6.4.2 5V Regulator

In the typical input range with an output of 5V at 2A, the regulator circuit will need 5 capacitors (labeled C1-C4 and C6), 3 resistors (labeled R_{FBB}, R_{FBT}, and R3), an inductor, and a diode. The inductor is found using equation 12 in the datasheet, using this equation the inductor value is found to be 470uH. Using equation 14 the input capacitor value can be found. From this equation, the input capacitor must be 10uF and 1uF. To find the output capacitor equation 16 is used, from this we find that the output capacitance must be 10uF, this value meets the requirement from the datasheet of the output capacitor of being at least 100uF or more. A voltage divider is used to find the values of R_{FBT} is found using equation 19 and a 1K value for R_{FBB}, the sum of these two resistor values should be at a maximum of 10K to maintain an accurate output voltage.

These values are consistent with the values shown in the WEBENCH design of the LM22680. The CAD schematic created in KiCad of this design is shown below.

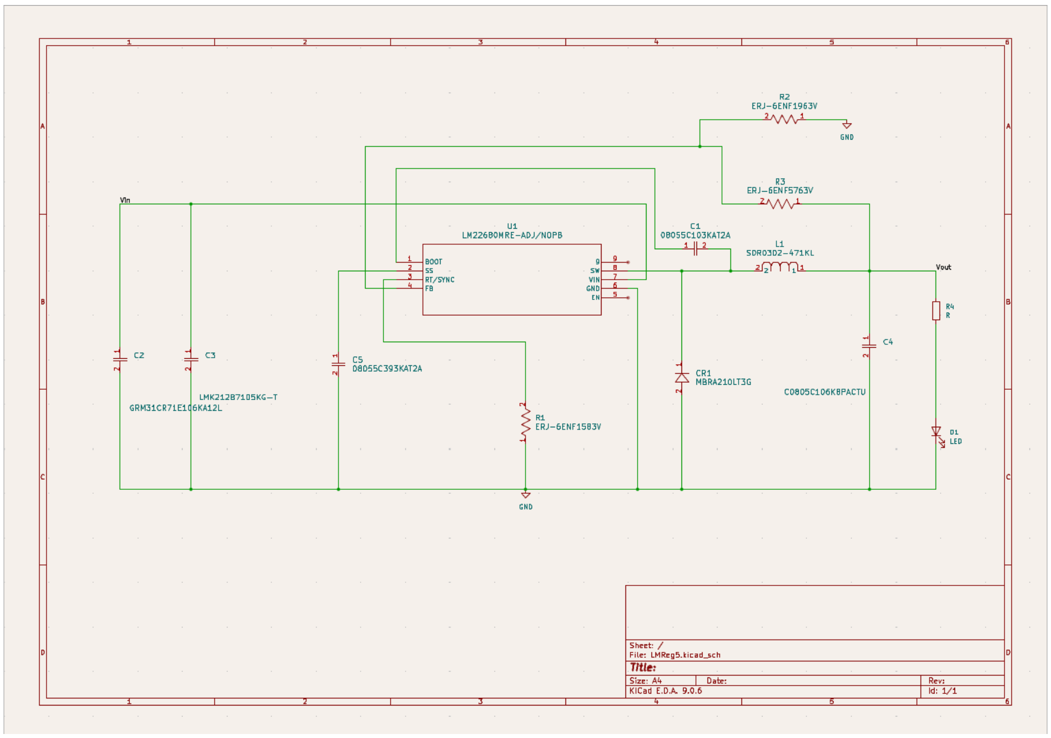

Figure 6.4.2 5V Regulator Schematic

6.5 ESP32 Pinout

This pinout is designed in Fusion 360 using the ESP32-WROOM-32E CAD. The connections shown are those which will be used to connect to our peripherals on the PCB board. Connections to the LCD screen, SD card connector, the amplifier, and 3.3V regulator input.

In the figure below the PINOUT schematic is shown, below that the tables show a closer look at the wiring and data flow that will be used in the final PCB design.

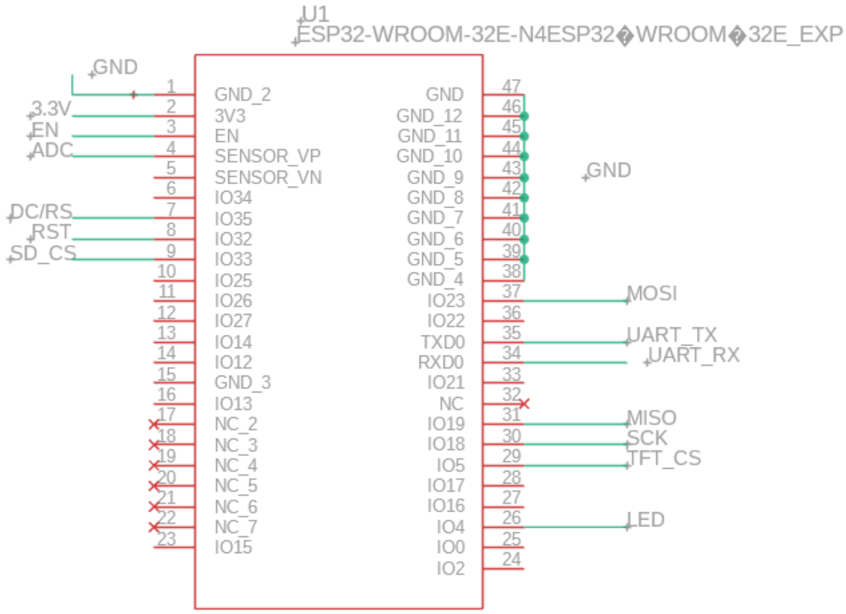

Figure 6.5.1 ESP32 PINOUT

Table 6.5.2 ESP32 Pin Connections

System	Connection	ESP32 Pin	Function
Photodiode Amplifier	ADC	SENSOR_VP	Input from filter/ diode sensor
LCD Screen	TFT_CS	GPIO5	LCD Chip Select
	DC/RS	GPIO35	Data/Command Select
	RST	GPIO32	Hardware Reset
	MOSI	GPIO23	Shared SPI Bus
	MISO	GPIO19	Shared SPI Bus
	SCK	GPIO18	Shared SPI Clock
SD Card Connector	SD_CS	GPIO33	SD Chip Select
	MOSI	GPIO23	Shared SPI Bus
	MISO	GPIO19	Shared SPI Bus

	SCK	GPIO18	Shared SPI Clock
Programming	UART_TX	TXD0	USB-UART
	UART_RX	RXD0	
Power	3.3V	3V3	Regulator
	GND	GND	Common Ground
	EN	EN	Enable Pin
Testing	LED	GPIO4	Used to show functionality

Table 6.5.3 ESP32 Peripherals

Signal	ESP32 Pin	Connected Devices
SCK	GPIO18	LCD and SD
MOSI	GPIO23	LCD and SD
MISO	GPIO19	LCD and SD

Chapter 7 Software Design

This project incorporates heavy software in two areas. The first is the LCD application, which displays the real-time dose rate readings and is able to visualize the results graphically. The other is the embedded software programmed onto the ESP32 which processes the data received from the photodiode to calculate the dose rates. The ESP32 is able to communicate this information to the display. These 2 components are foundational for the system and working together is imperative for capturing, processing and presenting the measurements in a clear way. Each part serves its own purpose but is working in tandem for accuracy, reliability, and use in the design.

7.1 LCD Application Design

The LCD part of the project is quintessential for allowing the user to be able to visualize and read the real-time dose rates coming from the x-ray. The goal of this software is as follows:

1. Process and transmit data: Successfully obtain and process the dose rate data from the ESP32 microcontroller, ensuring accurate conversion from the photodiode signal to measurable values.

2. Display and visualization: Present the calculated dose rates on the LCD display in real time, while also graphing the data to show trends over the duration of X-ray testing.

3. User interaction: Allow users to customize how the dose rate information is displayed—choosing between numerical values, graphical plots, or other visual formats for improved clarity.

4. Educational objective: Provide a tool that helps educate laboratory personnel on accurate dosimetry techniques and enhances their understanding of the X-ray machine’s radiation output

These goals are set in place to serve as a reminder and guide to our team of how to create a tool that will display the work from the PCB and with this in mind, we can design the software inn way that not only shows the values but creates an impactful learning experience as well as a creative way to display dose rates.

The application will constantly update a real-time graph that visualizes the dose rate readings while simultaneously displaying the values onto the LCD. This provides the users both an immediate reference and also a dynamic visual of how the dose rates change over time. By seeing it on a graph users can better identify patterns and fluctuations in radiation intensity during testing time.

To accommodate different preferences, the display will include a mode to be able to view the graph and date or just the graph and data one at a time. This feature to be able to customize the data displayed is especially useful in scenarios where the user does not want to focus on reading the visuals without the distraction of a number or vice versa. This is also helpful when monitoring data trends over a period of time.

Overall this display is designed to be both informative and self explanatory. By offering multiple visualization modes, the application supports users with different levels of technical expertise to make the results clear and easy to interpret in real time. This will allow us to accomplish our broader goal which is improving usability and promoting a better understanding of dose rate behaviors in the X-ray testing environment.

7.1.1. LCD Application Design Flowchart

This section consists of the flowcharts showing how the LCD operates from start-up to visualization and finally, user interaction. Each flow specifically illustrates how a specific function of the application works and how it interfaces alongside the ESP32.

In the figure below, we can see how the system is initialized. When the LCD is powered on, it interfaces with the MCU to then verify the connection and baud rate, then the initial UI layout is loaded and then the display waits for incoming data from the ESP32.

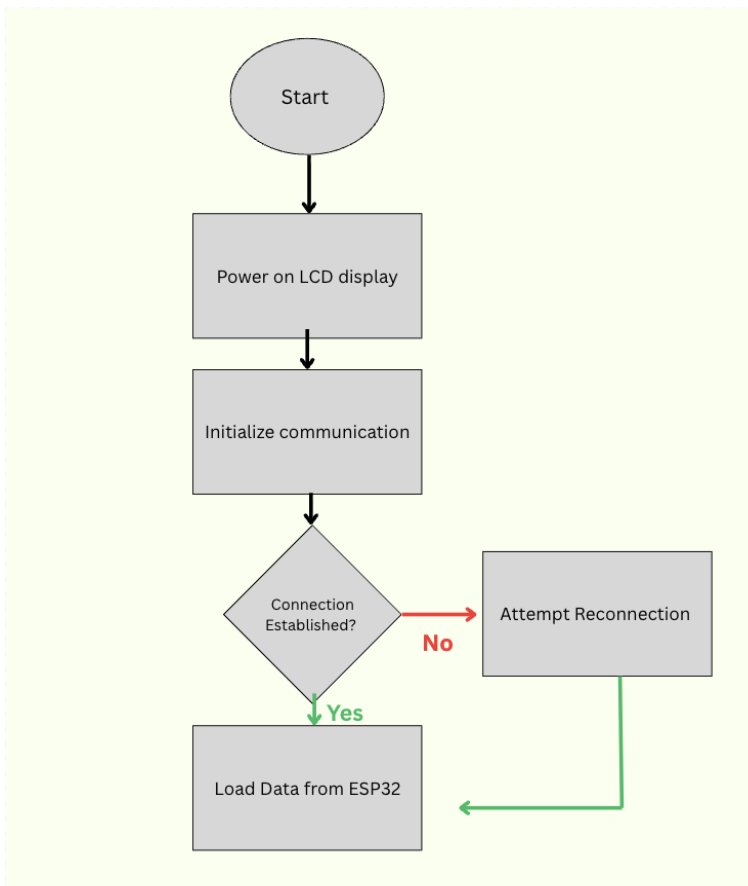

Figure 7.1.1.1 LCD Display Initialization

In the figure below, the ESP32 collects the dose rate from the photodiode and sends the data packet. The LCD then receives the packet and validates the format to which the data is then parsed. It is parsed through the payload to then numeric value and timestamp and then the data will store and buffer for graphing and then display values in real time. The system can then loop continuously at a set refresh rate.

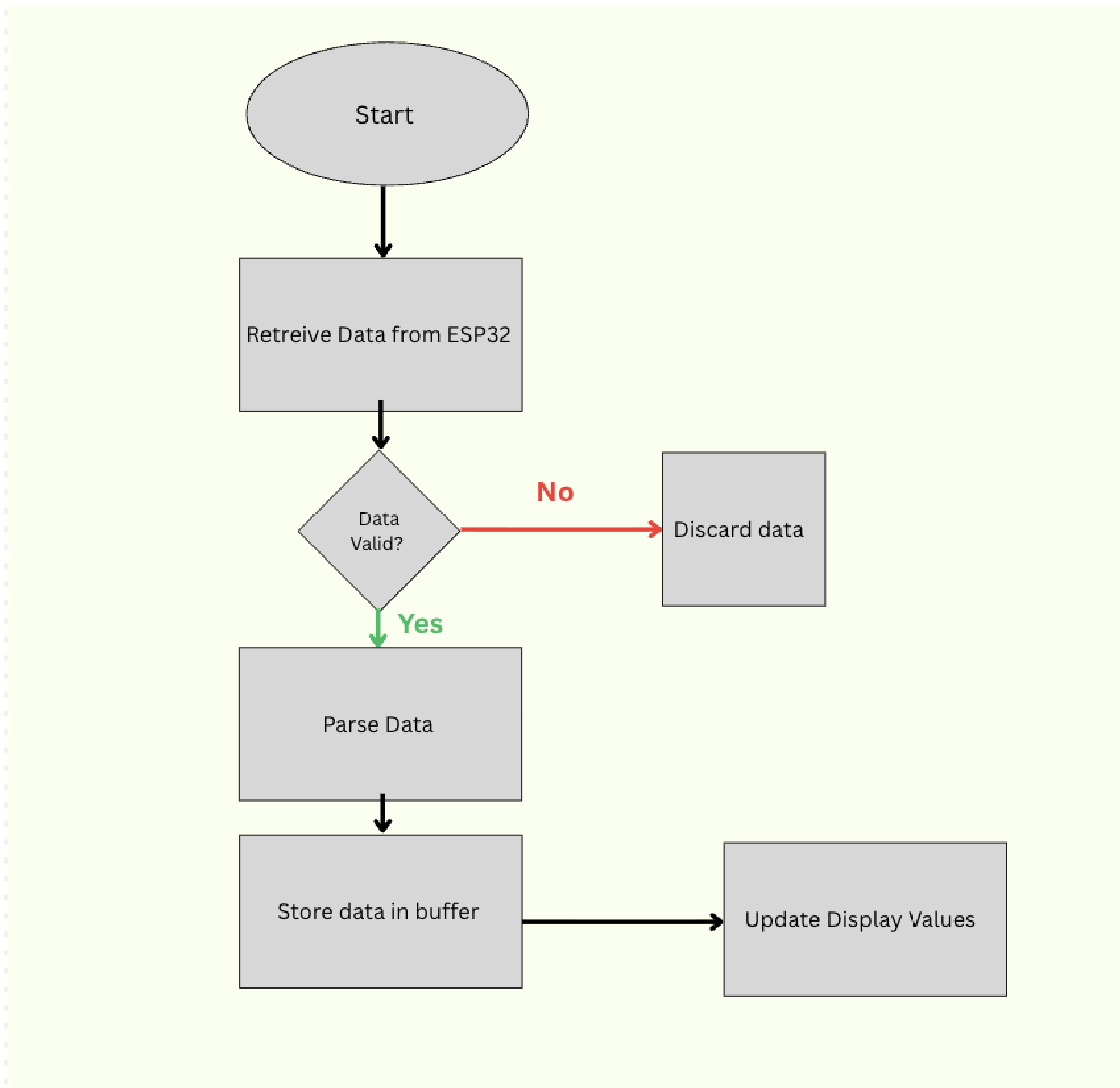

Figure 7.1.1.2 Data Processing Flow

In the figure below, it will be going over displaying and graphing the updates. First it will retrieve the latest buffered data, and then plot the data on a graph.

The screen will then have a numeric dose rate. Then there will be the option to scroll on the graph and refresh the axis dynamically. Then the graph is outputted to the LCD controller for rendering.

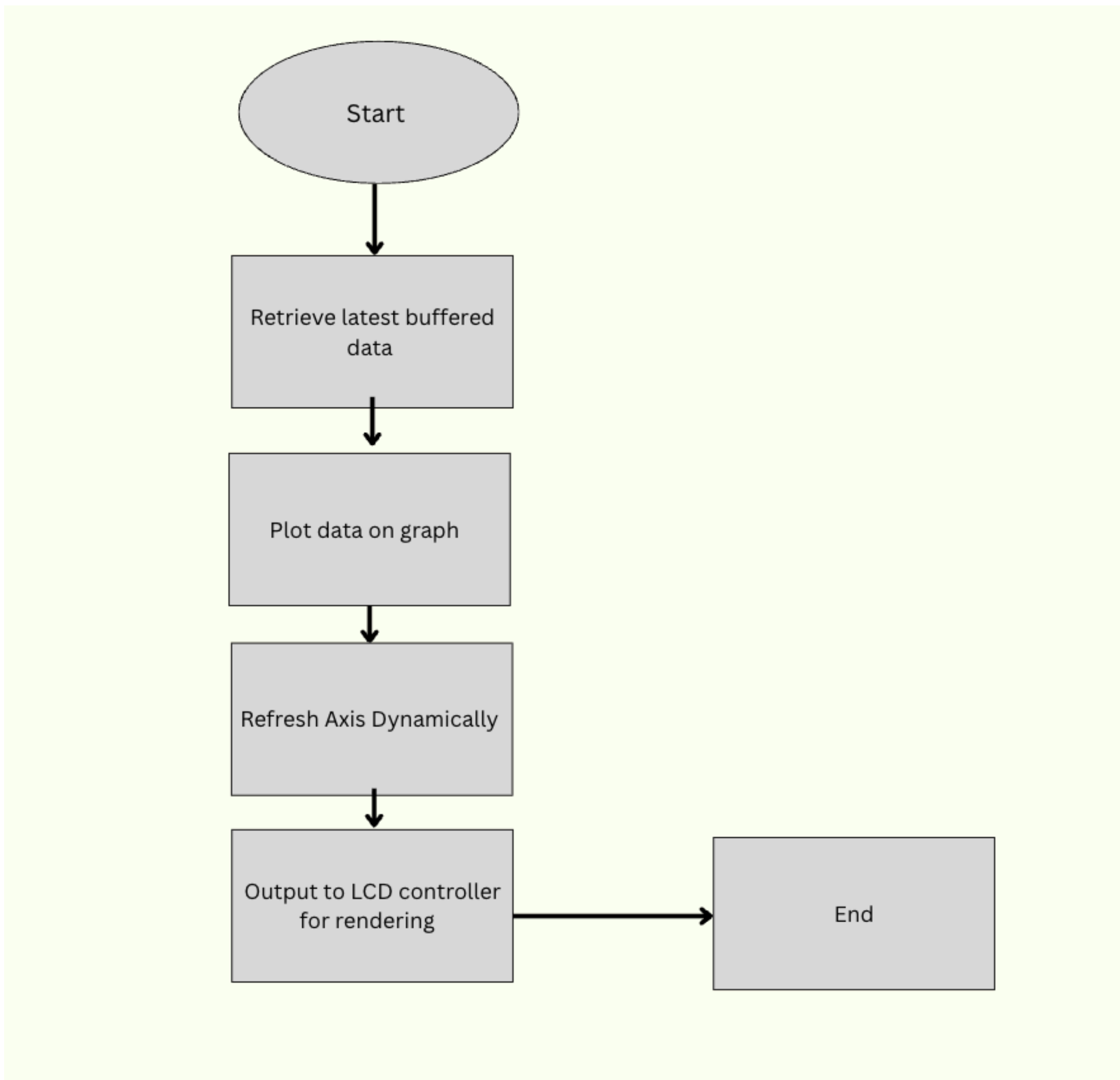

Figure 7.1.1.3 Graph Rendering Process

In the figure below, the user is given the option “Display Mode” from there a menu will appear to display either the numeric data or graphic data or a combined view.

Options:

1. Numeric Only
2. Graph Only
3. Combined View

The application will then update the UI layout accordingly and provide the option to export. Below can also be found a drawing of what the Application UI will look like when providing these options to the researcher.

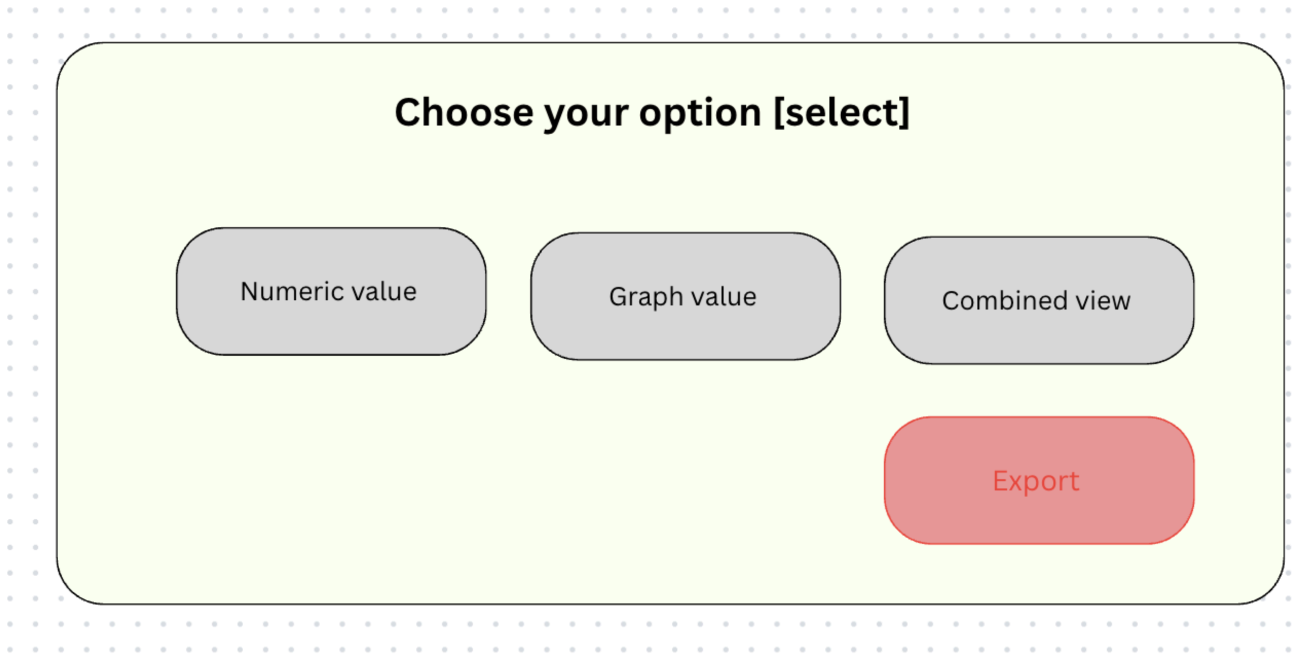

Figure 7.1.1.4 Display View

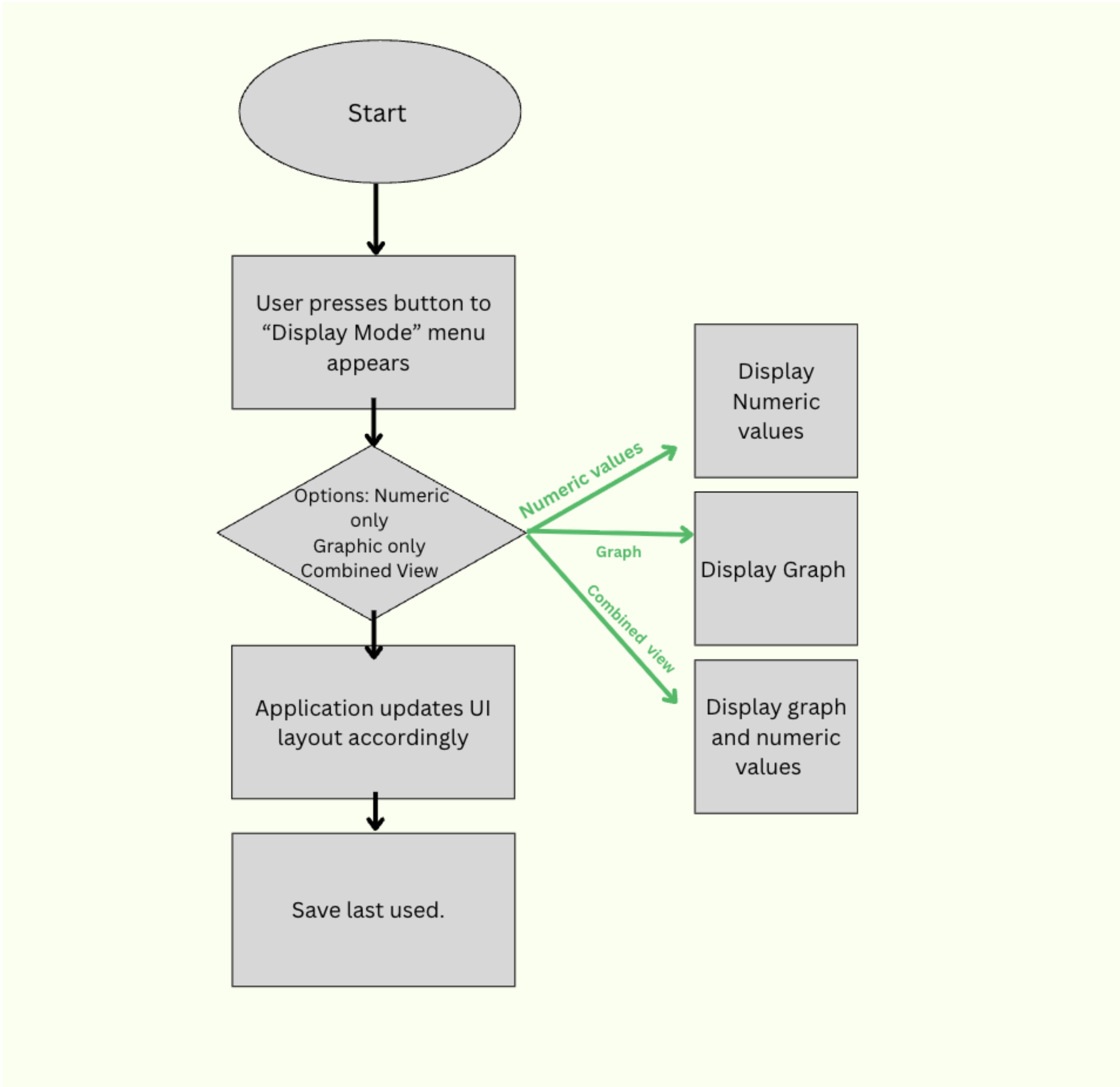

Figure 7.1.1.5 UI Mode Control

The figure below shows the process of error detection and reconnection handling within the system. Although this software operation is happening primarily on the inside of the software, it is crucial for making sure that the software is reliable and useful. When there is a timeout or data is lost from the x-ray, the software will signal the LCD to display a "Connection Error" message. The system will attempt to re-establish its communication with the MCU. The system will then attempt to communicate once more with the ESP 32. If the reconnection is successful,the application will log the error and resume normal operations. If the reconnection fails the system will stay in standby until the connection is restored.

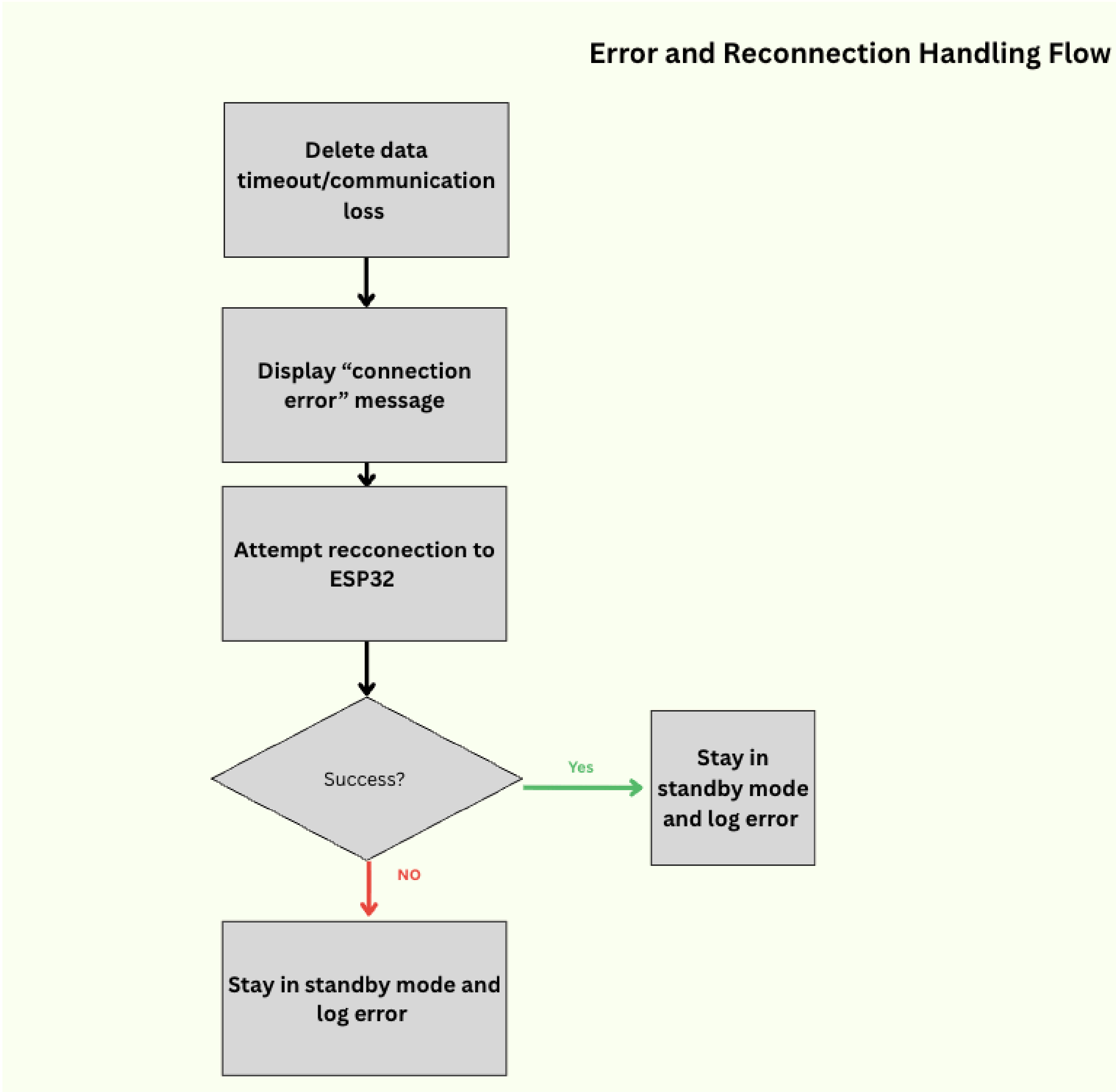

Figure 7.1.1.6 Error and Reconnection Handling Flow

7.2 ESP32 Software Integration and Data Processing

The second major software component of this system is programmed into the ESP32 microcontroller. This portion of the software is responsible for collecting sensor data from the photodiode, processing the signal into dose rates that are measurable, and communicating that information to the LCD. The ESP32 acts as the central control unit of the detector system, bridging the circuitry from the hardware and the user interface to ensure that data is accurately captured and then successfully displayed in real time.

The software is written in C/C++ using the Arduino IDE. This was chosen for its simplicity, compatibility with the ESP-IDF framework, and broad support for peripheral libraries such as SPI, I²C, and ADC. The program executes a continuous loop that reads analog voltage levels from the transimpedance amplifier, converts them to digital values using the onboard ADC, and processes the data using a calibration algorithm derived from X-ray test results. This processed information is then formatted into a dose rate value (in unit Gy/min) and transmitted to the LCD to display.

In addition to real-time measurements, the ESP32 software includes data filtering techniques to minimize signal noise and make sure the measurement is stable. Averaging algorithms are implemented to reduce fluctuations due to environmental noise or interference with electrical components, and threshold conditions are used to trigger warning indicators on the LCD when the dose rates exceed any limitations.

The ESP32 also manages communication protocols with peripheral devices. For this project, the LCD module is interfaced via SPI, allowing high-speed data transmission for updates via graph. In the future we would like this software to expand to include wireless connectivity, and make sure the system can log and transmit the dose-rate data over Wi-Fi or a PC.

Overall, the ESP32 software's main functions can be summarized as follows:

1. Acquiring sensor data: Continuously read the analog signal from the photodiode and convert it to digital values using the ESP32 ADC.

2. Data Processing: Apply calibration equations and averaging filters to convert sensor data into accurate, stable dose-rate readings.

3. Display Control: Format and transmit dose-rate values to the LCD for real-time visualization and graph plotting.

4. Error Handling: Detect abnormal readings, manage timeout conditions, and initiate corrective routines to maintain data integrity.

5. Communication and Expansion: Manage data transfer with the LCD and prepare for future integration of wireless data logging and remote monitoring capabilities.

This firmware ensures that the system operates reliably and continuously, supporting the larger goal of delivering accurate and accessible X-ray dosimetry in a user-friendly way. The ESP32’s performance and flexibility make it an essential component in bridging the hardware that will detect the x-ray and user-facing software interface, ensuring a smooth measurement and visualization system in real time.

7.2.1 ESP 32 Integration and Data Processing Flowchart

This section consists of the flowcharts that illustrate how the ESP32 firmware operates from system start-up through sensor data acquisition, processing, and transmitting the information to the LCD. Each flowchart specifically outlines how a major function of the microcontroller works and how it interacts with the display to provide accurate and real-time dosimetry results.

This flowchart outlines how the ESP32 boots up and prepares the system for operation. When powered on, the ESP32 initializes its ADC, SPI/I^2C communication, internal timers, and required tasks. It then verifies communication with the LCD and confirms that the data link is active. Once all modules are configured, the ESP32 transitions into its main sensing loop.

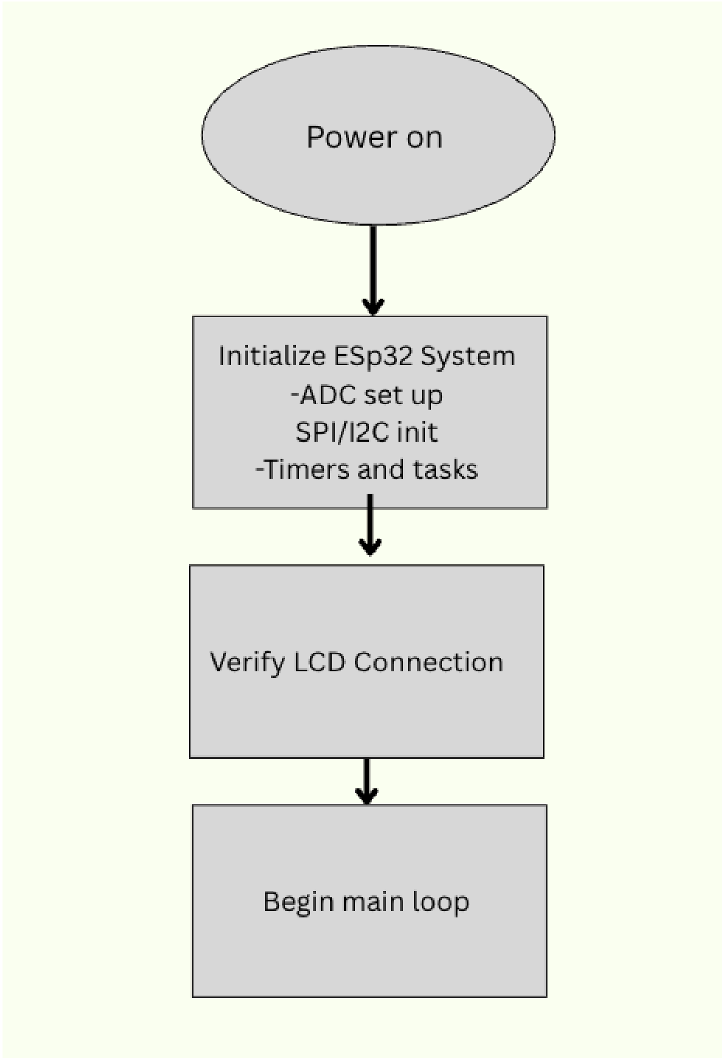

Figure 7.2.1.1 ESP32 initialization flow

This flowchart illustrates how the ESP32 continuously reads the photodiode output and converts it into a usable dose rate. The microcontroller samples the amplified voltage through the ADC, translates it into a digital value, and applies the calibration curve along with smoothing or averaging filters. After processing, the dose rate is stored and prepared for transmission to the LCD.

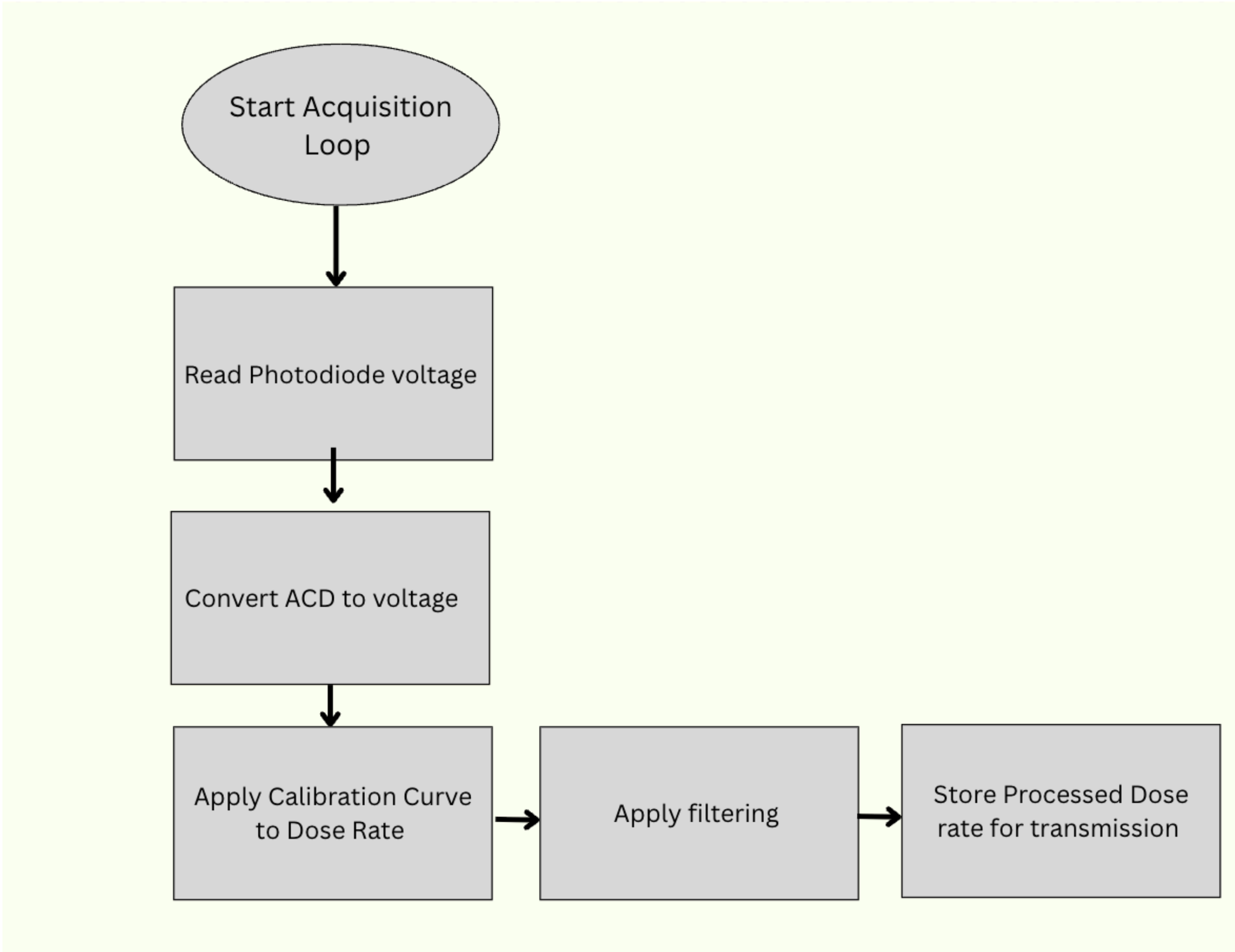

Figure 7.2.1.2 Sensor Data Acquisition and processing flow

This flowchart shows how processed data moves from the ESP32 to the LCD. Once a new dose-rate value is ready, the ESP32 packages the data and sends it over the selected communication protocol. The LCD acknowledges receipt, updates either the numerical view, graphical plot, or both, and the ESP32 resumes its loop to continue sending new measurements in real time.

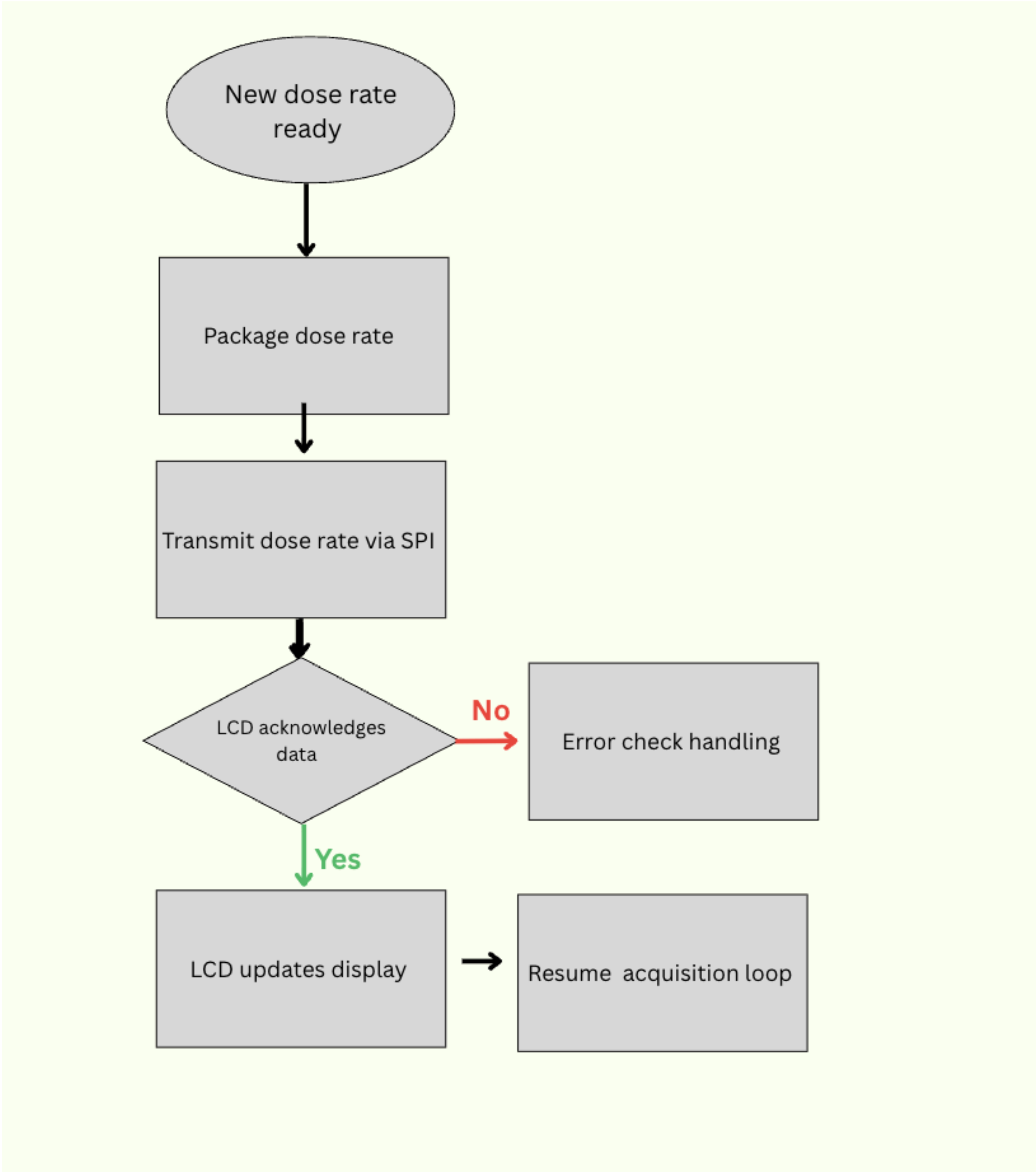

Figure 7.2.1.3 ESP 32 to LCD communication

This chart demonstrates how the ESP32 handles abnormal sensor or communication conditions. If the ADC detects invalid readings, excessive noise, or if communication with the LCD fails, the ESP32 enters an error-handling routine. It retries the action, attempts reconnection, and if recovery is successful, returns to normal operation. If the issue persists, it flags an error for display until stable data is restored.

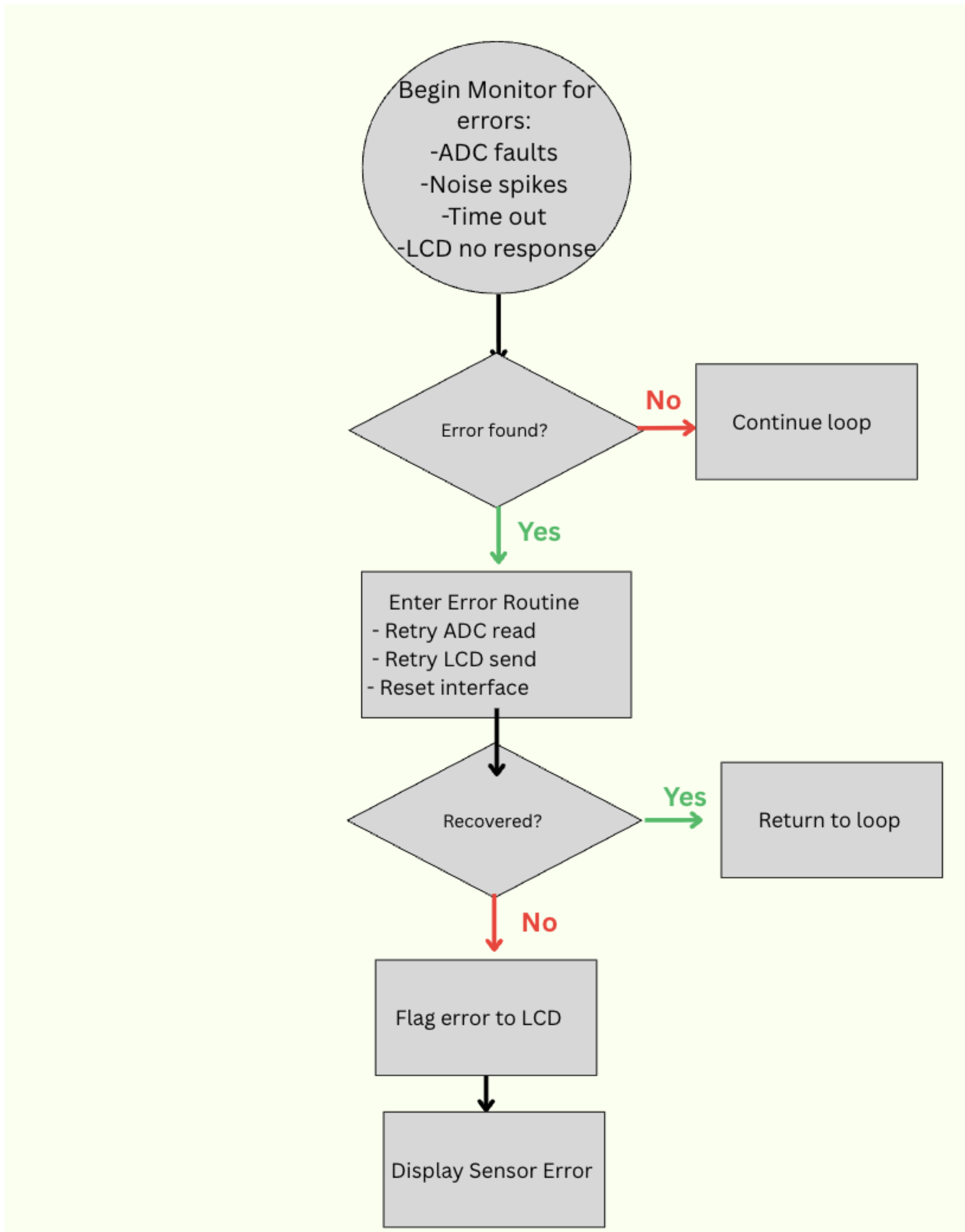

Figure 7.2.1.4 Error handling

7.3 Design Components

The implementation of the ESP32 and LCD software required planning the major firmware modules, defining communication requirements, and organizing the development schedule. This section outlines the core components that make up the embedded software and how they interact to provide real-time dose rate measurements on the LCD display.

7.3.1 System Components

The table below summarizes the primary software components used in the ESP32 firmware and LCD application, along with their roles in the system.

Table 7.3.1.1 Software Components

Component	Description
ADC reading module	Configures and reads analog voltage from the photodiode through the ESP32 ADC. Handles sampling timing and resolution control.
Dose Calculation Module	Converts raw ADC values into voltage and applies the project's calibration curve to compute dose rate in Gy/min.
Filtering and Averaging Module	Reduces measurement noise through averaging windows and smoothing algorithms to produce stable dose-rate readings.
Communication Handler	Packages processed dose-rate data and transmits it to the LCD using SPI or I^2C. Manages acknowledgments and retry logic for reliability.
LCD display handler	Updates the numerical dose-rate readout, refreshes graph frames, and switches between display modes selected by the user.
Display mode controller	Allows the LCD to toggle between showing the graph only, the numerical reading only, or both simultaneously.

Error Detection Module	Detects invalid ADC values, communication failures, or signal outliers. Initiates corrective routines and triggers on-screen warnings when necessary.

All of these components work together to enable the ESP32 to acquire, process, and send radiation data to the LCD in real time. The integration of each module ensures stable readings, fast updates on the UI, and reliability in terms of system behavior.

7.3.2 Integration

The integration stage focuses on synchronizing the ESP32 firmware with the LCD application to ensure proper data transmission and visualization. This includes validating the communication protocol, defining a consistent data format, and confirming that the LCD updates correctly with incoming dose-rate values.

To ensure proper alignment between components, an interface control description (ICD) was developed to outline the expected message structure, timing requirements, and error-handling behavior. During integration, the ESP32 was tested to confirm that calibration, filtering, and communication occurred within real-time constraints.

Once data transfer was validated, the LCD UI integration was performed to ensure that numerical updates, graphical plots, and mode selection functions behaved as intended. After full integration, end-to-end testing confirmed that the ESP32 could continuously compute and transmit dose rates while the LCD responded accurately to incoming data and user selections.

Chapter 8: System Fabrication/Prototype Construction

8.1 Photodiode Sensor PCB – AXUV20HS1 Interface Board

Below is the 2D model photodiode PCB. This board is responsible for hosting the AXUV20HS1 photodiode and providing a low-noise interface to the transimpedance amplifier (TIA) stage located on a separate PCB.

The photodiode is mounted using an SMD footprint oriented so the active window faces the incident X-ray beam from the X-rad 320 X-ray machine.

Through careful routing and isolation, this PCB ensures that the raw photocurrent reaches the op-amp input with minimal distortion, enabling accurate X-ray flux and dose-rate measurements.

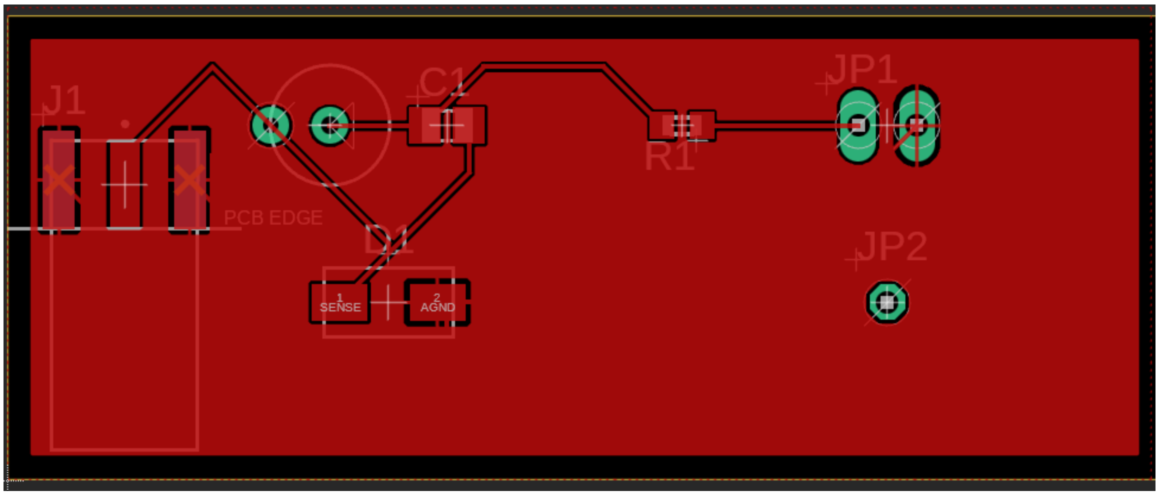

Figure 8.1 Diode PCB

The photodiode trace is kept as short as possible and placed on the top layer only, with no vias. The guard ring is implemented on the same layer to ensure effective isolation. Mounting holes are insulated from ground to prevent the X-ray machine's chassis from creating unintended current paths. This PCB was designed using Fusion 360 Electronics.

8.2 Op-Amp and Filter PCB

This PCB contains the OPA141 op-amp configured as a transimpedance amplifier to convert the photodiode's current into a usable voltage. The feedback resistor and capacitor are placed directly next to the op-amp to keep noise and parasitics low. After the TIA, a simple RC low-pass filter shapes the output and removes high-frequency noise before the signal goes to the ESP32's ADC.

The layout separates the sensitive analog area from any digital noise sources and uses a dedicated analog ground plane to avoid ground loops. Power pins are decoupled close to the op-amp, and the output header provides both the filtered signal and a clean ground reference to the microcontroller.

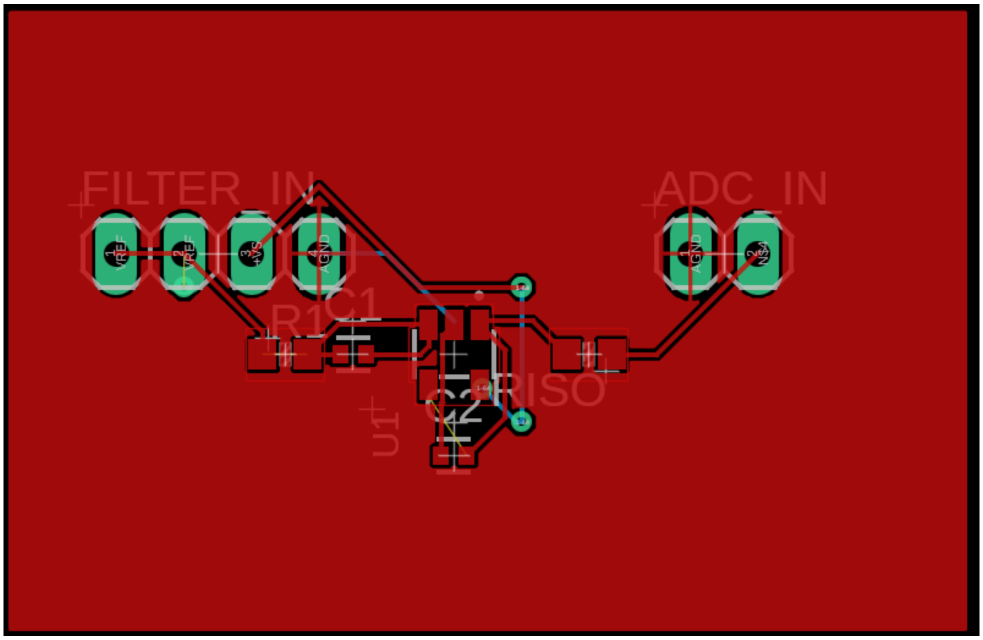

Figure 8.2 Op-Amp and Filter PCB

This PCB was also designed in Fusion 360 Electronics.

8.3 Main PCB

This report details the design of an embedded system project. The system is built around an ESP32-WROOM-32 microcontroller module, which serves as the central processing unit. A 5V switching regulator, the LM22676MR-5, and a 3.3V linear regulator, the MCP1727-3302xMF, were implemented for power management. A microSD card slot was integrated to provide data logging functionality. For the user interface, a TFT LCD display, the EA eDIPTFT43-A model, was included. The design is supported by various passive components, such as resistors and capacitors, alongside necessary connectors and protection elements. The complete design process, from component selection to final layout, will be described in the following sections.

The design process was very detailed. It started with choosing the right components. Then, I created the schematic diagram. The regulator circuits were designed using the official datasheets. After that, I assigned physical footprints to every part. Next, I designed the Printed Circuit Board (PCB). This involved placing the parts and routing the copper traces. This document will explain all these steps.

8.3.1 Overview

The entire system gets power from a battery pack. The pack has four 1.5V batteries connected in series. Together, they provide about 6 volts. This 6V power is not used directly by the components. Instead, it goes to two different voltage regulators.

The first regulator makes a stable 5V supply. It is a switching regulator called LM22676MR-5. This 5V power is used for the LCD display. It can also power other parts that need 5V.

The second regulator makes a clean 3.3V supply. It is a linear regulator called MCP1727-3302xMF. This 3.3V power is very important. It powers the ESP32 module. It also powers the microSD card and other low-voltage parts.

The ESP32 is the main controller. It does many important jobs. It communicates with the microSD card using a protocol called SPI. It talks to the TFT screen using serial communication. It also controls what is shown on the display. Furthermore, it can read external analog signals. These signals come through a 2-pin connector. An external filter circuit can be attached to this connector.

All these components are built onto a single PCB. This makes the system compact and reliable. It is also designed to be easy to manufacture.

8.3.2 Components

ESP32-WROOM-32

The ESP32-WROOM-32 is a powerful module. It has a dual-core processor inside. This means it can handle multiple tasks at once. It has built-in Wi-Fi and Bluetooth for wireless communication. It also includes its own flash memory to store programs. It offers many interfaces like SPI, UART, I2C, ADC, and PWM. These are used to connect to other parts of the system.

The module has specific needs for reliable operation. It must be supplied with a stable 3.3V regulated power. Small capacitors must be placed very close to its power pin. These are called bypass capacitors. Typical values are 0.1uF and 10uF. Good decoupling and a solid ground connection are also essential.

LM22676MR-5

The LM22676MR-5 is a DC-DC buck converter. Its output is fixed at 5V. It can supply a lot of current, up to 5 Amps. This is enough for the display and other peripherals. It is more efficient than a linear regulator for this job.

However, it needs several external parts to work correctly. It requires an input capacitor to smooth the incoming power. It needs a Schottky diode for the switching action. An inductor is needed to store and release energy. An output capacitor is used to smooth the 5V output. The physical layout of these parts on the PCB is critical. The parts must be close together to keep the switching loop small.

MCP1727-3302xMF (3.3V)

The MCP1727 is a Low-Dropout Regulator (LDO). It generates a very clean and quiet 3.3V output. This is perfect for noise-sensitive circuits like the ESP32. It is not as efficient as a switcher, but it provides a cleaner voltage.

Its design is simpler. I followed the guidelines from its datasheet. It needs an input capacitor, typically 1uF. It needs an output capacitor, typically 2.2uF. These should be ceramic capacitors. It is also important to provide a good thermal connection for heat dissipation. This means using enough copper on the PCB for its ground and input pins.

MicroSD Card

The microSD card slot allows for data storage. This is called data logging. The system can save information to the memory card. The slot operates on 3.3V power. It communicates with the ESP32 in SPI mode.

The connections are straightforward. The MOSI pin goes to ESP32 GPIO23. The MISO pin goes to ESP32 GPIO19. The SCK pin goes to ESP32 GPIO18. The CS (Chip Select) pin can be connected to any free GPIO pin, like GPIO5 or GPIO4.

EA DIPTFT43-A LCD Display

This is a smart color TFT display module. It requires a 5V power supply to operate correctly. The display can show text, graphics, and user interfaces. It communicates with the ESP32. The communication can be UART, I2C, or SPI. This depends on how we configure it.

Besides power and communication, it might need other connections. An optional reset pin can be used to restart the display. Other configuration pins might be needed to set its mode.

Passive components:

Many small passive components are used throughout the design.

- Capacitors: Different types are used for different jobs. Small 0.1uF capacitors are used for decoupling near ICs. Larger 10uF to 47uF capacitors are used for bulk storage to handle sudden power demands. Special capacitors are chosen for the regulators based on their datasheets.
- Resistors: These are used for many purposes. They are used as pull-up or pull-down resistors to keep signals stable. They are used in voltage divider circuits. They can also be configuration resistors for some components.
- Inductor: This is a critical part for the switching regulator. It stores energy and helps in converting the voltage efficiently.
- Schottky diode: This diode is used in the switching regulator circuit. It provides a path for the current when the regulator switches off. This is called a freewheeling diode.

The 3.3V regulator was designed carefully. I followed the instructions in the MCP1727 datasheet from Microchip. This ensures the regulator works properly and reliably.

For the input capacitor selection, the datasheet is very clear. It requires a minimum of a 1uF ceramic capacitor. This capacitor must be placed close to the VIN pin of the regulator. A 1uF capacitor was chosen in a small 0603 package. This capacitor helps to stabilize the input voltage. It also reduces noise coming into the regulator from the battery.

The output capacitor is also very important. The datasheet specifies a minimum of a 2.2uF ceramic capacitor. We used a 2.2uF capacitor in a 0603 package. It was placed very close to the VOUT pin of the regulator. This capacitor ensures the output voltage remains stable. It provides the quick bursts of current that the ESP32 might need when it starts processing.

The physical layout on the PCB is critical for performance. I followed these rules from the datasheet. The traces were made from VIN to the regulator and from the regulator to VOUT very short. We placed the input and output capacitors within 2–3 mm of the regulator chip. A solid, continuous ground plane was used on the PCB. I also made sure that no high-current or switching traces from the 5V regulator run near this LDO. This prevents electrical noise from affecting the clean 3.3V supply.

The schematic is the drawing of all the electrical connections. It is like a map for the circuit. We used KiCad software to draw the schematic.

The flow of power in the system is organized in a tree structure. It starts from the battery source which is approximately 6V. This 6V input goes directly to the input of the LM22676 5V switching regulator. The output of this regulator is a clean 5V rail. This 5V rail powers the LCD display. The same 6V battery input also goes to the input of the MCP1727 3.3V linear regulator. The output of this regulator is a clean 3.3V rail. This 3.3V rail powers the ESP32 module and the microSD card. The ESP32 was connected to the module carefully. The EN (Enable) pin is pulled up to 3.3V with a 10k resistor. This allows the chip to start up when power is applied. Decoupling capacitors were added to every power pin on the module. The SPI pins (GPIO23, GPIO19, GPIO18) were assigned for communication with the SD card. Other GPIO pins were routed to the LCD interface for control and data.

The SD card was wired to the ESP32 using the SPI protocol. The MOSI, MISO, and SCK lines were connected directly to the corresponding ESP32 SPI pins. The Chip Select (CS) line was connected to a user-selected GPIO pin. The SD card's power pin is connected to the 3.3V rail from the MCP1727 regulator. This power trace is filtered to keep it clean.

A 2-pin connector was added to the board. This connector is for an external analog input signal. A wire can be plugged in here. This wire carries an analog signal from an external sensor or circuit. This signal is connected to one of the Analog-to-Digital Converter (ADC) pins on the ESP32. The ESP32 can then read the voltage of this signal.

Each regulator section on the schematic is complete. This means all the parts they need to work were placed on the schematic. For the LM22676, this includes the input capacitor, the inductor, the Schottky diode, and the output capacitor. For the MCP1727, this includes its input and output capacitors. All values were chosen based on the official datasheet recommendations.

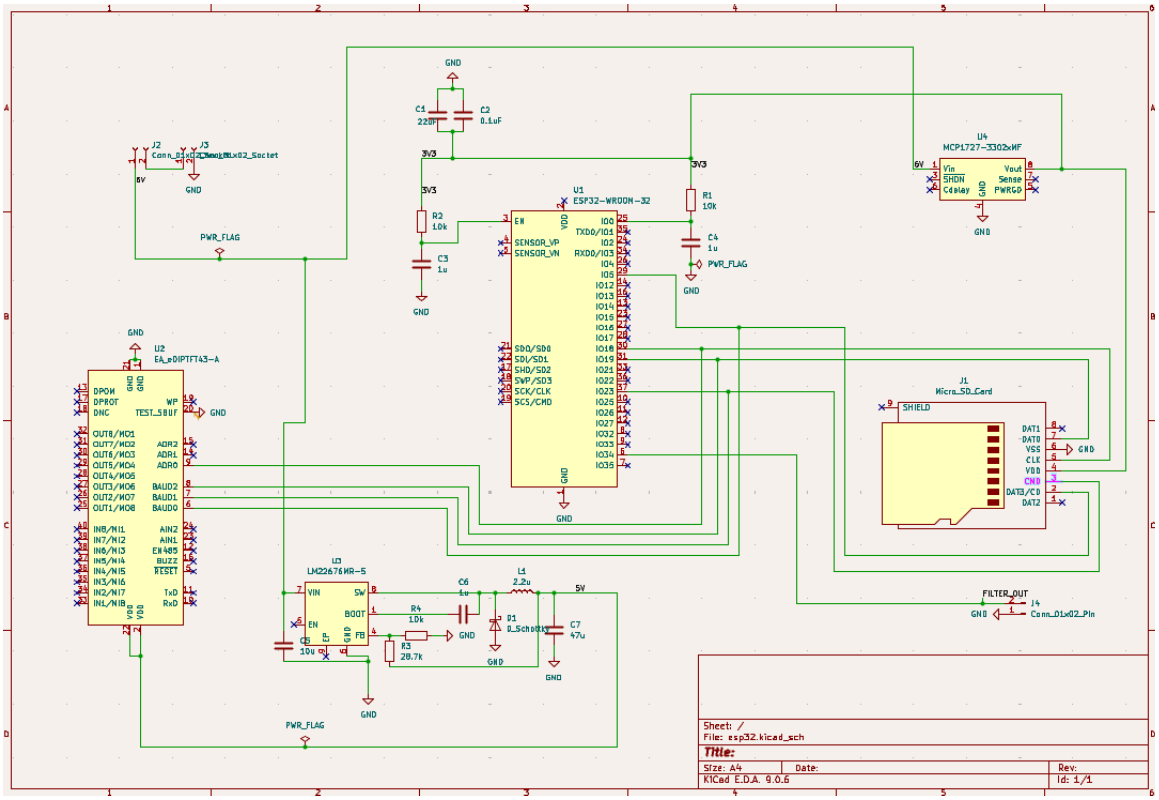

Figure 8.3.1: PCB schematic

A footprint is the physical pattern on the PCB where a part is soldered. Every symbol in the schematic must have a correct footprint.

Footprint assignment:

For most of the small resistors and capacitors, we used standard footprints. All resistors use the R_0603 footprint. All capacitors use the C_0603 footprint. The 0603 size is a good balance between size and ease of soldering.

The regulators need special footprints. The MCP1727-3302xMF comes in a DFN-8 package that measures 3x3mm. I used a footprint that matches this. The LM22676MR-5 comes in a SOIC-8 package with a special thermal pad on the bottom. This pad is called a PowerPAD. It helps to remove heat. We used a footprint that includes this large thermal pad.

I used different connectors. For the battery input and the external analog input, we used 2-pin headers. For potentially connecting other devices, I used 4-pin headers. We used standard pin header footprints or JST-style footprints for these.

The big modules also need accurate footprints. The ESP32-WROOM-32 footprint was taken from the official KiCad RF library. The microSD card slot footprint was found from a trusted library. The LCD display footprint was either provided by the manufacturer or created by us based on its dimensions.

We had to check for errors. We made sure every symbol on the schematic had a footprint assigned. We then ran the Electrical Rules Check (ERC) again to find any problems.

Table 8.3.1: Components in PCB

Ref Des	Value	Footprint / Part
C1	22uF	SD1:C_0603_1608Metric_Pad1.08x0.95mm_HandSolder
C2	0.1uF	SD1:C_0603_1608Metric_Pad1.08x0.95mm_HandSolder
C3	1u	SD1:C_0603_1608Metric_Pad1.08x0.95mm_HandSolder
C4	1u	SD1:C_0603_1608Metric_Pad1.08x0.95mm_HandSolder
C5	10u	SD1:C_0603_1608Metric_Pad1.08x0.95mm_HandSolder
C6	1u	SD1:C_0603_1608Metric_Pad1.08x0.95mm_HandSolder

C7	47u	SD1:C_0603_1608Metric_Pad1.08x0.95mm_HandSolder
D1	D_Schottky	SD1:D_2114_3652Metric_Pad1.85x3.75mm_HandSolder
J1	Micro_SD_Card	SD1:SD_Card_Device_16mm_SlotDepth
J2	Conn_01x02_Socket	SD1:PinSocket_1x02_P2.54mm_Horizontal
J3	Conn_01x02_Socket	SD1:PinSocket_1x02_P2.54mm_Horizontal
J4	Conn_01x02_Pin	SD1:PinHeader_1x02_P2.54mm_Vertical
L1	2.2u	SD1:L_0603_1608Metric_Pad1.05x0.95mm_HandSolder
R1	10k	SD1:R_0603_1608Metric_Pad0.98x0.95mm_HandSolder

R2	10k	SD1:R_0603_1608Metric_Pad0.98x0.95mm_HandSolder
R3	28.7k	SD1:R_0603_1608Metric_Pad0.98x0.95mm_HandSolder
R4	10k	SD1:R_0603_1608Metric_Pad0.98x0.95mm_HandSolder
U1	ESP32-WROOM-32	RF_Module:ESP32-WROOM-32
U2	EA_eDIPTFT43-A	Display:EA_eDIPTFT43-XXX
U3	LM22676MR-5	Package_SO:TI_SO-PowerPAD-8
U4	MCP1727-3302xMF	Package_QFN:DFN-8-1EP_3x3mm_P0.65mm_EP1.55x2.4mm

8.3.3 PCB Layout

The PCB layout is the process of arranging the parts and drawing the copper traces on the board.

A standard 2-layer PCB was used. This means the board has a top layer and a bottom layer. This is the most cost-effective option for manufacturing. It is perfect for a project of this complexity.

Power traces carry more current than signal traces. So, they need to be wider. I used thick traces for the battery input and the 5V rail. I placed the switching regulator (LM22676), its inductor, and its diode very close together. This makes the high-current switching loop very small. A small loop produces less electrical noise and works more efficiently.

The ESP32 layout requires attention. The area around its antenna must be kept clear. This means no copper pours or traces should be underneath that part of the module. This allows the Wi-Fi and Bluetooth signals to be strong and reliable. All the decoupling capacitors were placed directly next to the module's power pins. I also placed a solid ground plane under the module to provide a stable reference.

The signals for the SD card are relatively fast. Consequently, the SPI traces (MOSI, MISO, SCK, CS) were routed to be as short as possible. It was also ensured that the 3.3V power trace to the SD card is direct and is accompanied by a good ground return path nearby.

The LCD display requires 5V power. The trace carrying 5V to the display was made wide enough to handle the required current without overheating. The control pins for the display were grouped together on the connector, resulting in neat and organized wiring.

After all the footprints were placed on the board, the routing process was started. Routing involves drawing all the copper traces that connect the pins together. KiCad's interactive router tool was utilized for this purpose, as it facilitates easier trace drawing.

The final board is well organized. The power sections are clearly defined and separated from the sensitive digital parts. A clear separation was maintained between digital circuits, analog circuits, and the noisy switching power supply. The placement of all parts was optimized to minimize electrical noise and interference.

A Design Rule Check (DRC) was run upon completion. The DRC ensures that all traces are the correct width and that all parts are spaced appropriately. All DRC checks were passed by the final design.

The result is a clean and professional-looking PCB. All functions are integrated into the board, including power regulation, the microcontroller, the display interface, data logging, and external input. The design is now ready to be sent to a PCB manufacturer for production.

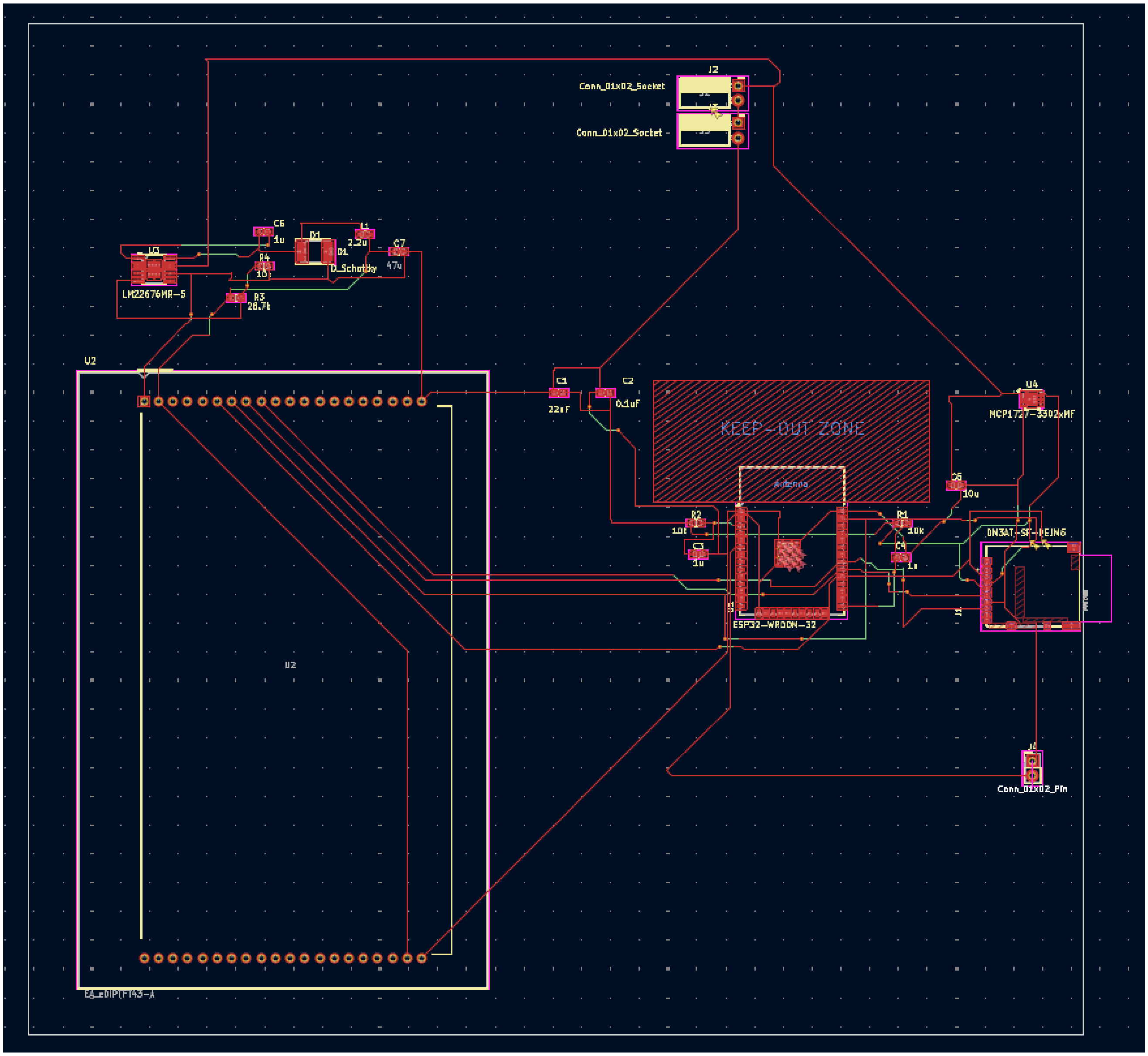

Figure 8.3.2: PCB layout

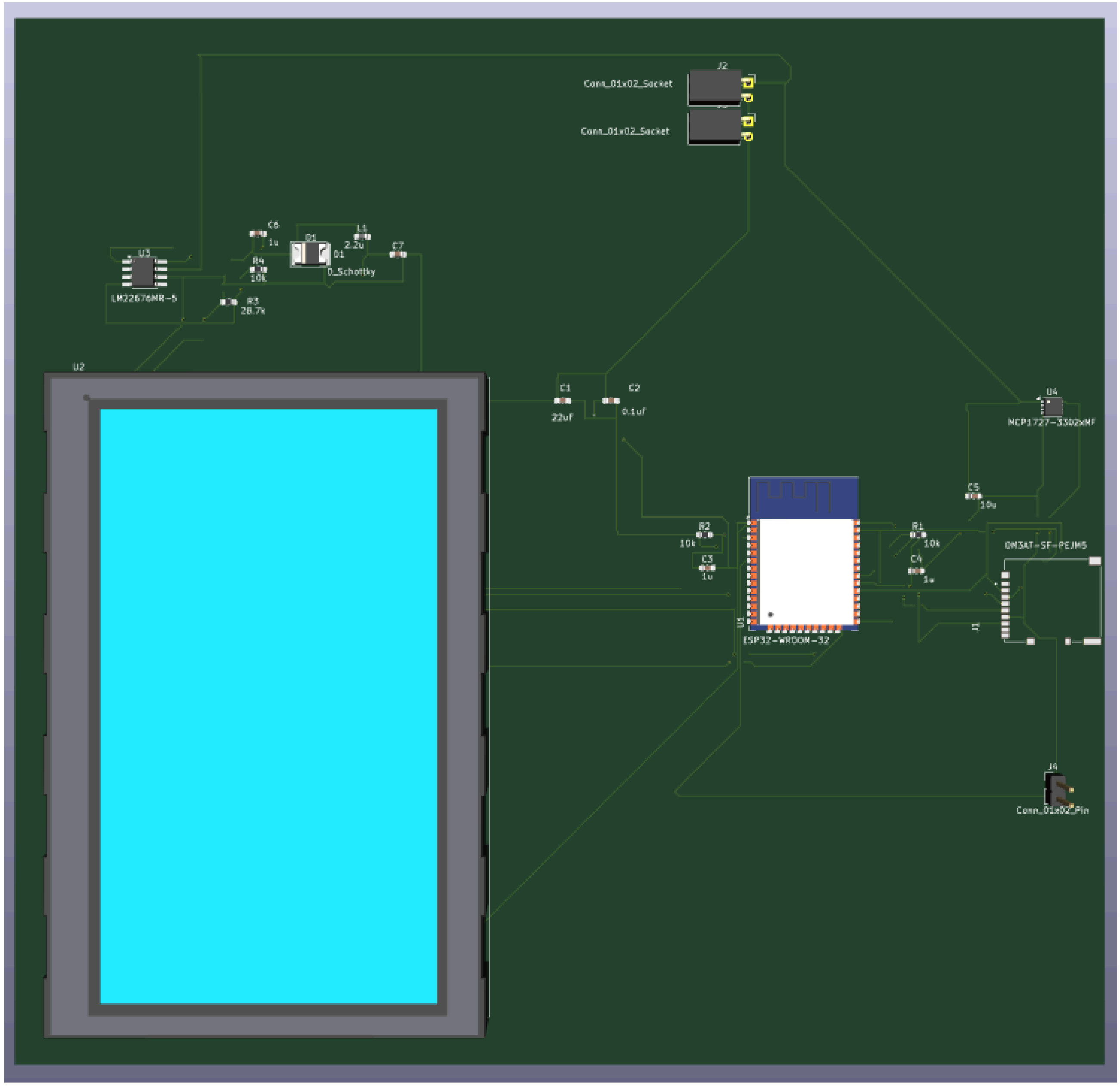

Figure 8.3.3: Final PCB

Chapter 9: System Testing and Evaluation

Testing and evaluation is critical in validating the performance of the X-ray dose detection system. This part of the process is important because it ensures that the hardware and software components of the system perform properly individually and together when they are integrated. This chapter outlines the planned testing procedures for each major subsection, what we plan to extract from testing, and how we will interpret that data to evaluate performance.

9.1 Diode PCB

The Diode PCB is the first stage of the system and it is designed to serve as the initial sensing stage. It converts incident X-ray waves into a measurable electrical signal. The purpose of testing this board will be to verify that the photodiode and TIA that is on the board will operate as expected and that the output signal is suitable for the next stage of amplification and filtering.

We aim to test multiple parts of the PCB starting with verifying basic electrical functionality and connectivity. We will be using a digital multimeter (DMM) to measure the supply voltage applied through the SMA connector to confirm that the photodiode receives the correct bias. The DMM will also be helpful in checking connections between the SMA terminals, photodiode pins, and ground plane of the board to ensure proper routing and to detect any shorts.

We also want to test for dark-current through the photodiode. This will be conducted by putting the photodiode in a light-shielded environment. This will simulate the X-ray chamber when it is off. Upon placing the board in a light-shielded environment the output current will be measured to confirm it falls within the expected range specified in the AXUV20HS1 datasheet. This test will validate that the diode is functioning properly and that there are no significant leakage or contamination issues. [4]

We also want to ensure the photodiode is functioning under illumination. So we will be exposing the diode to a fixed light source. The light source will be an iPhone flashlight at 10 cm away and we will vary the brightness and record the current output from the SMA port to verify a linear relationship between illumination level and output. This will confirm that the photodiode's responsivity is consistent and that the PCB traces are intact.

9.2 Op-Amp and Filter PCB

The op-amp and filter PCB will be tested to verify that it properly amplifies and conditions the signal received from the photodiode stage before it is fed into the ESP32. We want to test that the chosen operational amplifier provides the expected gain, that the low-pass filter effectively attenuates high-frequency noise so the overall output remains stable.

Similar to the diode PCB board, we will begin by testing the basic power and connectivity verification. The supply voltage rails will be measured at the op-amp pins to confirm that the OPA141 is receiving the correct operating voltage from the power supply and that no shorts exist on the board.

Moving further, we want to verify that the op-amp stage provides the correct amplification. By connecting an AC signal using a waveform generator at the input, we will simulate output current from the diode PCB. The output voltage will then be measured using an oscilloscope to ensure that the gain matches the theoretical value determined by the feedback resistor network. We will be testing multiple input amplitudes and frequencies to confirm that the amplifier operates consistently within its designed bandwidth and that no distortion or clipping occurs.

Once the amplification stage is validated, the filter portion of the circuit will then be tested and evaluated. This test will be done to make sure the filter section of the circuit works as intended and removes unwanted noise from the signal. A range of input frequencies will be applied to the circuit using a function generator and the output will be observed on an oscilloscope to see how the signal strength changes at different frequencies. From this, we will determine where the filter begins to reduce higher-frequency signals, confirming that it matches the designed cutoff point.

9.3 Power Testing

The power for our design can be tested by checking to ensure proper functionality of the regulators. For regulator testing we will be checking to ensure there is current flowing through the regulators and that the correct 3.3V and 2A are being outputted from the first regulator and that the second has a 5V and 1.8mA output. This can be done using two main approaches, visually testing and testing in the lab. For the regulator design an LED with a 100 ohm resistor will be added at the output load. When breadboarding we will be able to visually see if there is a current flowing to the output of the regulator if the LED is turned on, if the LED is not turned on, we will know that the regulator is not designed correctly. We will also use this approach for the actual PCB design by adding an LED to the regulator output to easily verify the power to the device. This will prove that the regulator does have current flowing through the circuit. Using an LED with a however it will not prove that the output voltage and current match the requirements.

When testing the actual output voltage and current we will use laboratory testing with a breadboarded circuit. By following the circuit design from WEBENCH the regulator will be designed. The testing will begin by measuring the ohmic value of the load resistor which is in series with the LED. Using a power supply found in the lab an input supply of 6V and .5A to act as our battery we will be using in our final design. The output voltage from the regulator will then be measured as well as the voltage across the LED. Using the ohms law with the ohmic value of the resistor (R_{LED}), the output voltage (V_o), and the voltage across the LED (V_f), the LED current can be calculated.

We will also need to use an electronic load to apply a load to the regulator. This load can be set to the exact output values we need, it will also be able to set the load values we need to use. With this load turned on the output values from the regulators can be measured. Adding together the current from this load and the LED current, the total output current is found. This current should match the desired 2A and 1.8mA for each regulator.

The efficiency of the regulators will also be calculated by finding both the input and output power (multiplying the voltage by the current). Efficiency is calculated with the output power divided by the input power and multiplied by 100. This efficiency should be close to the efficiency from WEBENCH for the regulator designs, however we will expect some differences between these values due to real world issues and imperfect parts.

In summary, for regulator testing we will use an LED at the output to visually ensure the regulator is being powered and has current flowing through. We will also use the breadboarded regulators with an output load resistor and LED to measure the output current from the LED. Then with an electronic load set to our design requirements, we will measure the output voltage and current. The two currents will be added together to ensure the total output current meets our design needs. The output voltage measured with this load will be compared with our expected output to verify that the regulator will perform to our needs. Using all of these values we will be able to find the input and output powers to then calculate the efficiency. The efficiency can be compared to the expected efficiency from the WEBENCH design.

9.4 Software Testing and Evaluation

The software component of the X-ray dose detection system is responsible for acquiring ADC measurements, processing the data into dose-rate values, updating the LCD in real time, and finally, maintaining stable communication between these modules. Since the accuracy of the system depends equally on firmware performance and hardware correctness, a thorough software testing must be completed. This section outlines the planned procedures for validating the ESP32 firmware, LCD display routines, communication stability, timing behavior, and system-wide data integrity.

9.4.1 Firmware Functional Testing

Firmware testing ensures that each module of the software performs as intended before being fully integrated.

9.4.1.1 ADC Sampling Verification

The ESP32's ADC is used to digitize the processed analog output from the op-amp/filter stage. Testing will include using a precise DC source to apply known voltages, logging the raw ADC values and comparing measurements against ESP32 ADC calibration to make sure we are getting the expected resolution.

This verifies that digital readings correctly represent the analog signal from the hardware chain.

9.4.1.2 Data Processing and Dose-Rate Calculation

The firmware converts ADC measurements to current and then to dose rate through calibration constants and simple filtering. To validate correctness we must simulate the ADC inputs to verify that the calculated dose rate values match the expected numerical results. We must also do edge-case testing which will help us ensure the algorithm is behaving properly. Finally, we will check the filtering to make sure our output is smooth and stable.

This confirms that digital processing maintains accuracy across the full operating range.

9.4.2 LCD Display and User Interface Testing

The LCD is the primary output for the user, so it must be reliable and reflect the real-time outputs.

To test, we can do a static display verification. This will take the known values and send them to the LCD to check for correctness, spacing, decimal placement, and clarity in terms of text. Additionally, we can do real-time update testing. To evaluate responsiveness, a script will rapidly change ADC inputs and the display's refresh rate will be monitored. We will verify the absence of any flickering, freezing, or any re-draw issues during the updates.

To handle error messaging, fault conditions will be introduced strategically. Some examples of this are disconnecting the photodiode board, simulating an ADC failure, or introducing out-of-range numerical values. In liu, the LCD must correctly display messages like “connection error”, “invalid reading”, or “signal lost”.

This ensures the display can communicate abnormal system conditions clearly.

9.4.3 System Communication and Timing Tests

The ESP32 uses multiple tasks for sampling, processing, and displaying data. Because of this, the timing and communication tasks must be verified.

FreeRTOS task behavior will be monitored using a debugging output. We will also ensure that tasks do not block indefinitely or cause a priority inversion. Queue sizes will be tested under sampling rates that are high to verify that the data is not lost in transmission. We will also perform testing for buffer integrity and timing stability. These tests include stress testing queues with maximum sampling loads, measuring time stamps to confirm consistent sampling intervals, and evaluating jitter and update delays under different CPU load conditions. These tests ensure reliable scheduling and timing accuracy during real-time operation.

9.4.4 Software-Hardware Integration Testing

After validating individual modules, testing will be performed on the integrated hardware-software chain. A function generator or DC source will sweep the voltages into a photodiode or TIA chain and the output on the LCD will be recorded and compared to expected dose-rate values. It will confirm that the hardware and firmware calibrations are aligned.

If the final design includes a reset or calibration button, we will perform repeated button presses to test correct interrupt triggering and debouncing. The system should not freeze or miss interrupts for optimum functionality.

To verify reliability during a continuous operation. The system will run for 4-8 hours with input levels that are representative of the project. We will then monitor for leaks, watchdog resets, or any timing drifts. Finally we will use a heap in the ESP-IDF tools and record to make sure there are no fragmentation issues.

9.4.5 Acceptance Criteria

Software validation is considered successful when the ADC readings are consistent, dose rates match the calibration model, the LCD updates smoothly without any freezing or lag, all tasks are running without timing issues missed updates or overflows, the firmware handles errors smoothly, and when the system is stable during a long duration test without any memory or watchdog failures. Meeting these requirements confirms that the software is reliable, accurate, and ready for integration with the full radiation-testing environment.

Chapter 10 Administration

10.1 Budget

The budget for this project is set at $3,000, as agreed upon by our team and faculty sponsor, to ensure financial feasibility for the radiation lab while providing flexibility for replacement parts and prototyping. This budget covers a wide range of components, including our core circuit elements, PCB fabrication costs, and the high-cost photodiode at the center of our design. Additionally, funds are allocated to account for potential replacements or design modifications, allowing us to address unforeseen expenses without jeopardizing project progress. A detailed breakdown of cost is provided in the Bill of Materials table below.

10.2 Bill of Materials

As seen by the table above, we are below the goal limit of $3000 by exactly $1,473.39 allowing for prototyping and replacement parts.

Table 10.2.1 Bill of Materials

Component Part Name	***Quantity***	***Unit Price (USD)***	***Total Price (USD)***
Core Circuit Components			
LM22680 Regulator IC	4	$4.83	$19.20
MicroSD Card Breakout Board+	2	$7.50	$15.00
SMA-J-P-H-ST-EM1 SMA Connector	4	$2.47	$9.72
Amphenol RF SMA Coaxial Cable Assemblies 135101-03	1	$34.99	$34.99
OPA141AID Op-Amp	3	$3.07	$9.21
ESP32 Dev Kit	1	$10.00	$10.00
ESP32-WROOM-32E-N4 MCU Module	3	$4.87	$14.52
LR6XWA/BXU 1.5V AA	10	$4.50	$45.00

Battery			
OLIREXD 2 AA Battery Holder (2-slot)	5	$8.00	$40.00
AXUV20HS1 Opto Diode	2	$627.06	$1254.12
Additional Components			
2.8" TFT Resistive Touch Shield (LCD Display	3	$24.95	$74.85
Total			
Grand Total	–	–	$1526.61

Chapter 11 Conclusion

During SD1, our team focused on completing the system design and preparing all documents needed before fabrication. One of our major accomplishments was finishing the final PCB layout. The board includes all essential circuits for power regulation, signal conditioning, microcontroller communication, and data logging. We also checked all traces, clearances, and footprints to make sure the design meets electrical and manufacturing requirements.

We completed the bill of materials (BOM) for all components needed for the detector. This includes resistors, capacitors, microcontrollers, connectors, and supporting circuitry. The BOM helps us stay organized and ensures that we can order parts quickly at the start of SD2. We also reviewed part availability to avoid delays from long lead times.

Our team has created a clear plan for SD2. The main goal is to order the PCBs before the semester begins. This is important because we need enough time for manufacturing, delivery, and assembly. By receiving the boards early, we can start soldering and testing right away. This gives us more time for debugging, calibration, and design changes if they are needed.

In SD2, our focus will shift from design to building and testing the hardware. Once the PCBs arrive, we will begin soldering the components and checking for power and connectivity issues. After assembling the main hardware, we will continue with firmware development. This includes programming the ESP microcontroller, setting up the LCD display, and creating the data logging system with the SD card.

We will also complete the design and ordering of any additional PCBs, such as the diode PCB and filter PCB. These boards are essential for the X-ray detection path and need to be ready for integration. When all hardware is assembled, the team will run system tests, measure signals from the diode, and validate the detector’s performance.

Each team member has a set of tasks that support the project goals. These roles help us stay organized and make steady progress in SD2.

In conclusion, Project Hulk—developed in partnership with the Radiation Effects and Reliability Lab (RERL)—will deliver a compact, accurate, and reliable system capable of measuring and graphing radiation dose rates in real time. The device captures current generated by a PIN diode located inside the X-Rad 320, serving as the system’s primary radiation-sensing component. When exposed to x-rays, the PIN diode produces a current proportional to the dose rate, which is then routed through a carefully designed low-pass filter. This filtering stage removes unwanted electrical noise and stabilizes the signal, ensuring that only clean, usable data is passed to the ESP32 microcontroller. Once received, the ESP32 uses equations and calibration models provided by RERL’s research team to convert this analog current into an accurate digital dose-rate value. The processed data is then transmitted to the TFT LCD display, where it is graphed in real time to give operators immediate, intuitive visual feedback during X-ray operation.

The core components of this system include the ESP32 microcontroller, the TFT LCD module for real-time graphical output, the microSD card interface for optional data logging and archival, and the op-amp-based analog front end responsible for amplification, filtering, and overall signal conditioning. During the research and system-design phase, each component was selected with careful consideration of electrical performance, stability, noise susceptibility, radiation-environment compatibility, and ease of integration. These design choices allowed us to effectively meet all of our project goals and engineering requirements. Project Hulk is programmed using the Arduino IDE, which serves as the primary development environment for the firmware. This platform facilitates data acquisition, mathematical conversion of current to dose rate, graphical rendering on the LCD, timing management, and any potential data storage or communication tasks.

The final design of Project Hulk provides a practical and user-friendly device for monitoring the radiation output of the X-Rad 320. Its real-time update capability allows users to immediately observe fluctuations or trends in dose rate, improving situational awareness during testing procedures and offering more confidence in experimental repeatability. The custom-designed PCB housing increases durability, supports safer cable management, and improves portability, while also presenting the system in a clean, professional format appropriate for regular laboratory use or demonstration settings.

This documentation reflects the complete design process of Project Hulk, detailing the underlying concepts of the project, the goals and constraints we established, the rationale for part selection, and the plans for electrical, software, and mechanical implementation. It also includes our testing methodologies, safety and standards considerations, final schematics, firmware architecture, and design verification steps. With continued support from our sponsor, the RERL, along with the University of Central Florida's Senior Design instructional team, we are confident that Project Hulk will successfully meet its performance targets and contribute a meaningful improvement to dose-rate monitoring within radiation research environments such as the RERL and beyond.

Appendix A

[1] J. Abramovitch, "Development of a Silicon PIN Diode X-Ray Detector," *SMU Scholar Undergraduate Research*, Southern Methodist University, Apr. 15, 2014. [Online]. Available: https://scholar.smu.edu/cgi/viewcontent.cgi?article=1031&context=upjournal_research

[2] Nazififard M;Suh KY;Mahmoudieh. "Experimental Analysis of a Novel and Low-Cost Pin Photodiode Dosimetry System for Diagnostic Radiology." The Review of Scientific Instruments, U.S. National Library of Medicine, pubmed.ncbi.nlm.nih.gov/27475554/. Accessed 4 Sept. 2025.

[3] Feng, Hua, et al. "Double-Layer Silicon Pin Photodiode X-Ray Detector for a Future X-Ray Timing Mission." ADS, ui.adsabs.harvard.edu/abs/2006NIMPA.564..347F/abstract. Accessed 4 Sept. 2025.

[4] OpenAI, *ChatGPT* [Large language model]. San Francisco, CA, USA: OpenAI, 2025. [Online]. Available: https://chat.openai.com/

[5] DeepSeek-V3, *DeepSeek Chat* [Large language model]. [Online]. Available: https://chat.deepseek.com/

[6] M. Nazififard, K. Y. Suh, and A. Mahmoudieh, "Experimental analysis of a novel and low-cost pin photodiode dosimetry system for diagnostic radiology," *Review of Scientific Instruments*, vol. 87, no. 7, Jul. 2016, doi: https://doi.org/10.1063/1.4955170.

[7] "X-RAD 320: 320 kVp Orthovoltage Energy X-ray Unit" brochure, Precision X-Ray Inc., North Branford, CT, USA, Feb. 2019. [Online]. Available: https://cancer.wisc.edu/research/wp-content/uploads/2019/02/X_RAD_320_Brochure.pdf

[8] "X-RAD 320 Facility Requirements," Precision X-Ray Inc. (North Branford, CT, USA), [Online]. Available: https://s3.amazonaws.com/ssllc_public_images/01tQh000004RmhOIAS-a1vQh0000007sdBIAQ-Precision%20X-RAD%20320%20Facility%20Requirements

[9] "X-RAD Biological Irradiator User Manual, Rev 2.1," Precision X-Ray Inc., North Branford, CT, USA, Nov. 2015. [Online]. Available: https://www.img.cas.cz/files/2020/01/X-Rad-User-Manual-Rev-2.1.pdf

[10] "AXUV Series Photodiodes for Extreme Ultraviolet and X-Ray Detection." Opto Diode Corporation, 2023, https://www.optodiode.com/pdf/AXUVHS.pdf.

[11] Hamamatsu Photonics. "Characteristics and Use of Photodiodes." Hamamatsu Photonics Technical Note, 2023, https://www.hamamatsu.com/resources/pdf/ssd/si_pd_handbook_v3a_e.pdf.

[12] Rieke, G. H. Detection of Light: From the Ultraviolet to the Submillimeter. 2nd ed., Cambridge University Press, 2003.

[13] "ADA4530-1: Ultra-Low Bias Current, Electrometer-Grade Amplifier." Analog Devices, 2023, https://www.analog.com/en/products/ada4530-1.html

[14] "LTC6268: 500 MHz, Low Bias Current FET Input Op Amp." Analog Devices, 2023, https://www.analog.com/en/products/ltc6268.html

[15] "OPA141: Precision, Low Noise, Low Input Bias Current, 36-V, JFET-Input Operational Amplifier." Texas Instruments, 2023, https://www.ti.com/lit/ds/symlink/opa141.pdf

[16] Sedra, Adel S., and Kenneth C. Smith. Microelectronic Circuits. 8th ed., Oxford University Press, 2020.

[17] Texas Instruments. "Active Filter Design Techniques." Analog Engineer's Circuit Cookbook: Op Amps, 2023, https://www.ti.com/lit/an/sloa088b/sloa088b.pdf

[18] "ESP32-WROOM-32 Datasheet." Espressif Systems, 2024, https://www.espressif.com/sites/default/files/documentation/esp32-wroom-32_datasheet_en.pdf

[19] "ESP-IDF Programming Guide." Espressif Systems Documentation, 2024, https://docs.espressif.com/projects/esp-idf/en/latest/esp32/

[20] "Arduino Uno Rev3." Arduino Official Documentation, 2024, https://docs.arduino.cc/hardware/uno-rev3

[21] "MSP430FR6989 LaunchPad Development Kit." Texas Instruments, 2024, https://www.ti.com/tool/MSP-EXP430FR6989

[22] "Raspberry Pi 4 Model B Product Brief." Raspberry Pi Foundation, 2024, https://www.raspberrypi.com/products/raspberry-pi-4-model-b/

[23] "A Guide to SD Card Types," *CDW.com*, Aug. 20, 2021. https://www.cdw.com/content/cdw/en/articles/hardware/types-of-sd-cards.html

[24] "A Guide to SD Card Types," *CDW.com*, Aug. 20, 2021. https://www.cdw.com/content/cdw/en/articles/hardware/types-of-sd-cards.html

[25] https://www.facebook.com/vizmohanan, "Interfacing Catalex Micro SD Card Module with Arduino - CIRCUITSTATE Electronics," *CIRCUITSTATE Electronics*, May 10, 2021. https://www.circuitstate.com/tutorials/interfacing-catalex-micro-sd-card-module-with-arduino/

[26] Adafruit Industries, "MicroSD card breakout board+," Adafruit.com, 2020. https://www.adafruit.com/product/254?gad_source=1&gad_campaignid=21079227318&gbraid=0AAAADx9JvSIV2M5KJkqpriLTfAIvCmGG&gclid=Cj0KCQjw9obIBhCAARIsAGHm1mQ-inS3VGZI1hh56_34MT2NROVoDE-NIVgvIm7z9AmUen_Vd-Jt6jIaAvI3EALw_wcB

[27] Adafruit Industries, "Adafruit Micro SD SPI or SDIO Card Breakout Board - 3V ONLY!," Adafruit.com, 2024. https://www.adafruit.com/product/4682

[28] "Energizer E91 Alkaline AA Battery: Product Datasheet," Energizer Corporate, [Online]. Available: https://data.energizer.com/pdfs/e91.pdf

[29] "Energizer E92 Alkaline AAA Battery: Product Datasheet," Energizer Brands, LLC. [Online]. Available: https://data.energizer.com/pdfs/e92.pdf

[30] "Energizer E93_AP Product Datasheet," Energizer, 1.5 V Alkaline Battery, [Online]. Available: https://data.energizer.com/pdfs/e93_ap.pdf

[31] "Energizer E95 Alkaline D-Cell Battery: Product Datasheet," Energizer Brands, LLC. [Online]. Available: https://data.energizer.com/pdfs/e95.pdf

[32] "ENERGIZER 522 9 V Product Datasheet," Energizer Holdings, Inc., [Online]. Available: https://data.energizer.com/pdfs/522.pdf

[33] "The Importance of Voltage Regulation," Voltagecorrection.com, Apr. 15, 2024. https://www.voltagecorrection.com/the-importance-of-voltage-regulation

[35] “1-7. Principle of operation of series regulators | Toshiba Electronic Devices & Storage Corporation | Americas – United States,” Semicon-storage.com, 2025. https://toshiba.semicon-storage.com/us/semiconductor/knowledge/e-learning/basics-of-low-dropout-ldo-regulators/chap1/chap1-7.html

[35] “Linear and Switching Voltage Regulators – An Introduction,” PREDICTABLE DESIGNS, Nov. 28, 2016. https://predictabledesigns.com/linear-and-switching-voltage-regulators-introduction/

[36] “Efficiency Formula - Keysight Technologies,” Keysight.com, 2025. https://www.keysight.com/used/hk/en/knowledge/formulas/efficiency-formula

[37] “Buck Converters (Step-Down Converter),” www.monolithicpower.com. https://www.monolithicpower.com/en/learning/mpscholar/power-electronics/dc-dc-converters/buck-converters

[38] “LM25575,” LM25575 data sheet, product information and support | TI.com, https://www.ti.com/product/LM25575?utm_source=google&utm_medium=cpc&utm_campaign=app-null-null-GPN_EN-cpc-pf-google-ww_en_cons&utm_content=LM25575&ds_k=LM25575&DCM=yes&gclsrc=aw.ds&gad_source=1&gad_campaignid=1767856010&gbraid=0AAAAAC068F28SIG9_hjsZK_aIAmayXyXZ&gclid=CjwKCAiA_orJBhBNEiwABkdmjN71NT14M34QxHN3qfoMNx16PgNbrege5_zaWjxB5WfYmZcBPNk_BxoC7-IQAvD_BwE (accessed Nov. 23, 2025).

[39] “LM2592HV,” LM2592HV data sheet, product information and support | TI.com, https://www.ti.com/product/LM2592HV?utm_source=google&utm_medium=cpc&utm_campaign=app-null-null-GPN_EN-cpc-pf-google-ww_en_cons&utm_content=LM2592HV&ds_k=LM2592HV&DCM=yes&gclsrc=aw.ds&gad_source=1&gad_campaignid=1767856010&gbraid=0AAAAAC068F28SIG9_hjsZK_aIAmayXyXZ&gclid=CjwKCAiA_orJBhBNEiwABkdmjK5MjTw1CPBywVp72oN46jWPirnxb-7Hh3HOrsGgTax5o8awhLyO1RoCmGEQAvD_BwE (accessed Nov. 23, 2025).

[40] “LM20242,” LM20242 data sheet, product information and support | TI.com, https://www.ti.com/product/LM20242?utm_source=google&utm_medium=cpc&utm_campaign=app-null-null-GPN_EN-cpc-pf-google-ww_en_cons&utm_content=LM20242&ds_k=LM20242&DCM=yes&gclsrc=aw.ds&gad_source=1&gad_campaignid=1767856010&gbraid=0AAAAAC068F28SIG9_hjsZK_aIAmayXyXZ&gclid=

CjwKCAiA_orJBhBNEiwABkdmjC4ZUYyXL6rkFVf042JyH35hCXb7DC6LnWPvgjVjlzwgoysZthV2uBoCkscQAvD_BwE (accessed Nov. 23, 2025).

[41] "LM22680," LM22680 data sheet, product information and support | TI.com, https://www.ti.com/product/LM22680?utm_source=google&utm_medium=cpc&utm_campaign=app-null-null-GPN_EN-cpc-pf-google-ww_en_cons&utm_content=LM22680&ds_k=LM22680&DCM=yes&gclsrc=aw.ds&gad_source=1&gad_campaignid=1767856010&gbraid=0AAAAAC068F28SIG9_hjsZK_aIAmayXyXZ&gclid=CjwKCAiA_orJBhBNEiwABkdmjGfJWKdWGy_5kP_4LaJ2VyY-BDFag3klNCmqg0fK6jtLYSETiM5gbRoCDKkQAvD_BwE (accessed Nov. 23, 2025).

[42] "Board Level Connectors," *DigiKey*, 2025. https://www.digikey.com/en/product-highlight/a/amphenol-rf-division/board-level-connectors#edge (accessed Nov. 07, 2025).

[43] PE3184-6 pasternack | cable assemblies | DigiKey, https://www.digikey.com/en/products/detail/pasternack/PE3184-6/22163993 (accessed Nov. 23, 2025).

[44] "Amphenol RF 135101-03 amphenol RF SMA Coaxial Cable assemblies," DX Engineering, https://www.dxengineering.com/parts/aml-135101-03?seid=dxese1&utm_source=chatgpt.com (accessed Nov. 23, 2025).

[45] "SMA male to SMA male .141 hand formable cable using RG402 aluminum coax, 6 inches," HASCO COMPONENTS, https://www.hasco-inc.com/cable-assemblies/sma-male-to-sma-male-141-semi-rigid-cable-using-rg402-aluminum-coax-6-inches/?srsltid=AfmBOoo1O4hfqEcAb-xHFuCiy48B-cb8u_TTCYUCSnS2jpw_qrieU8Hm (accessed Nov. 23, 2025).

[46] Occupational Safety and Health Administration (OSHA). "Electrical Standards." U.S. Department of Labor, 2024, https://www.osha.gov/electrical

[47] IEEE Standards Association. "About IEEE Standards." Institute of Electrical and Electronics Engineers, 2024, https://standards.ieee.org/

[48] IEEE Std 315-1975. Graphic Symbols for Electrical and Electronics Diagrams (Including Reference Designation Letters). IEEE, 1975.

[49] IEEE Std 1057-2017 / IEEE Std 1241-2011. Standards for ADC Performance Characterization. IEEE, 2017.

[50] IPC-2221B: Generic Standard on Printed Board Design. IPC Association Connecting Electronics Industries, 2023.

[51] "IPC-2221A Generic Standard on Printed Board Design," 2003. Available: https://www-eng.lbl.gov/~shuman/NEXT/CURRENT_DESIGN/TP/MATERIALS/IPC-2221A(L).pdf

[52] "ChatGPT," *ChatGPT*, 2017. https://chatgpt.com/c/68fbbf5d-ae78-8328-83ac-425486028542 (accessed Nov. 07, 2025).

[53] "SD Standard Overview | SD Association," *www.sdcard.org*, Dec. 11, 2020. https://www.sdcard.org/developers/sd-standard-overview/

[54] "Capacity (SD/SDHC/SDXC/SDUC) | SD Association," *www.sdcard.org*, Dec. 11, 2020. https://www.sdcard.org/developers/sd-standard-overview/capacity-sd-sdhc-sdxc-sduc/

[55] Motorola, Inc. *"SPI Block Guide V03.06."* Document No. S12SPIV3/D, Original Release 21 Jan 2000, Revised 04 Feb 2003. Available: https://opencores.org/usercontent/doc/1499360489

[56] Texas Instruments. *"Serial Peripheral Interface (SPI) – Reference Guide, Literature Number SPRU059E."* Texas Instruments Incorporated, June 2002 (Revised Feb 2009). Available: https://www.ti.com/lit/pdf/spru059

[57] STMicroelectronics. "AN4041: Using the SPI Interface with STM32 Microcontrollers." Application Note AN4041, Doc ID 022706 Rev 2, January 30 2012. Available: https://www.st.com/resource/en/application_note/an4041-using-the-spi-interface-with-stm32-microcontrollers

Appendix E

Case Study 1 ChatGPT:

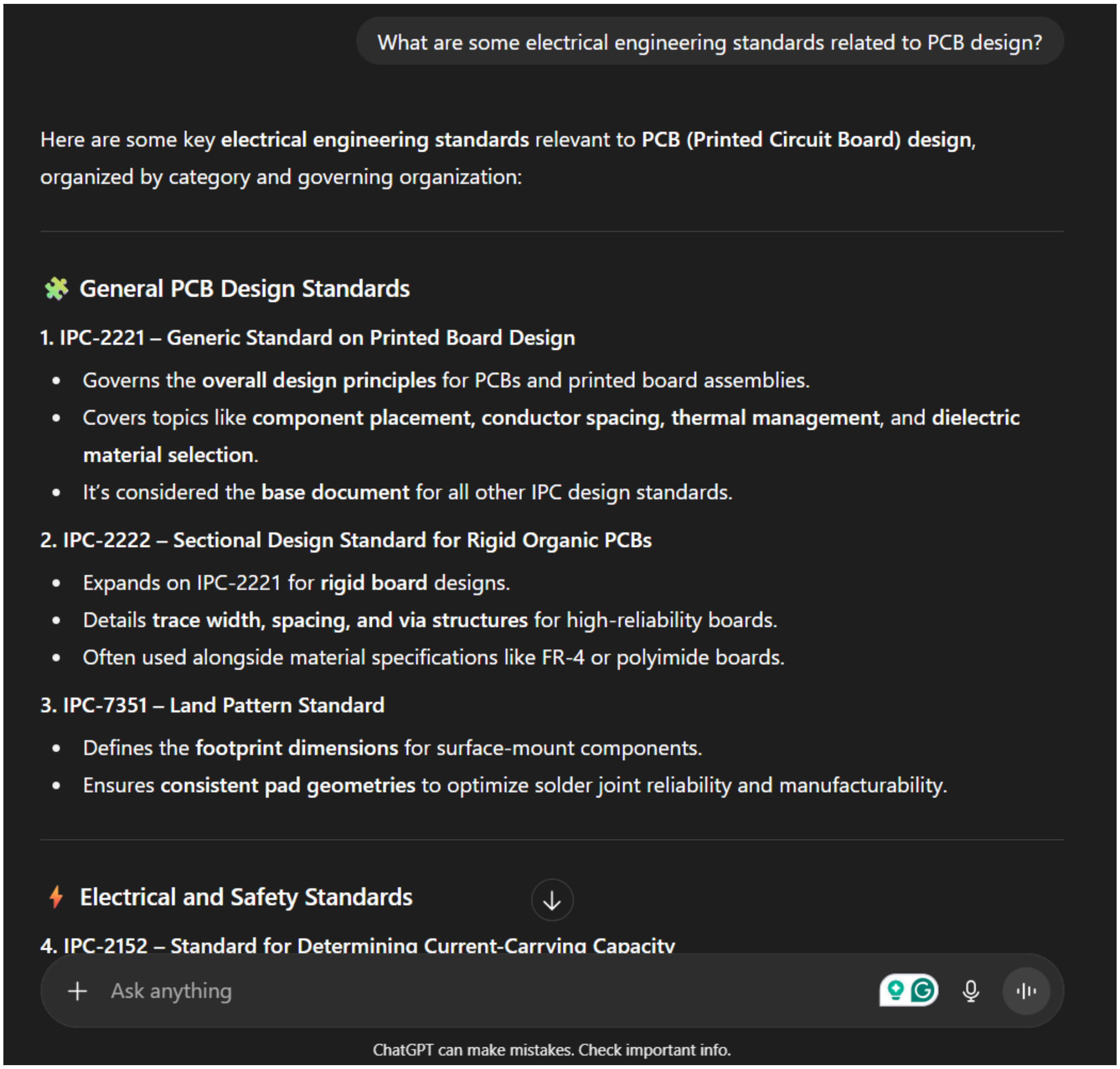

What are some electrical engineering standards related to PCB design?

Here are some key **electrical engineering standards** relevant to **PCB (Printed Circuit Board) design**, organized by category and governing organization:

General PCB Design Standards

1. IPC-2221 – Generic Standard on Printed Board Design

- Governs the **overall design principles** for PCBs and printed board assemblies.
- Covers topics like **component placement, conductor spacing, thermal management**, and **dielectric material selection**.
- It's considered the **base document** for all other IPC design standards.

2. IPC-2222 – Sectional Design Standard for Rigid Organic PCBs

- Expands on IPC-2221 for **rigid board** designs.
- Details **trace width, spacing, and via structures** for high-reliability boards.
- Often used alongside material specifications like FR-4 or polyimide boards.

3. IPC-7351 – Land Pattern Standard

- Defines the **footprint dimensions** for surface-mount components.
- Ensures **consistent pad geometries** to optimize solder joint reliability and manufacturability.

Electrical and Safety Standards

4. IPC-2152 – Standard for Determining Current-Carrying Capacity

Ask anything

ChatGPT can make mistakes. Check important info.

Case Study 1 Microsoft Copilot:

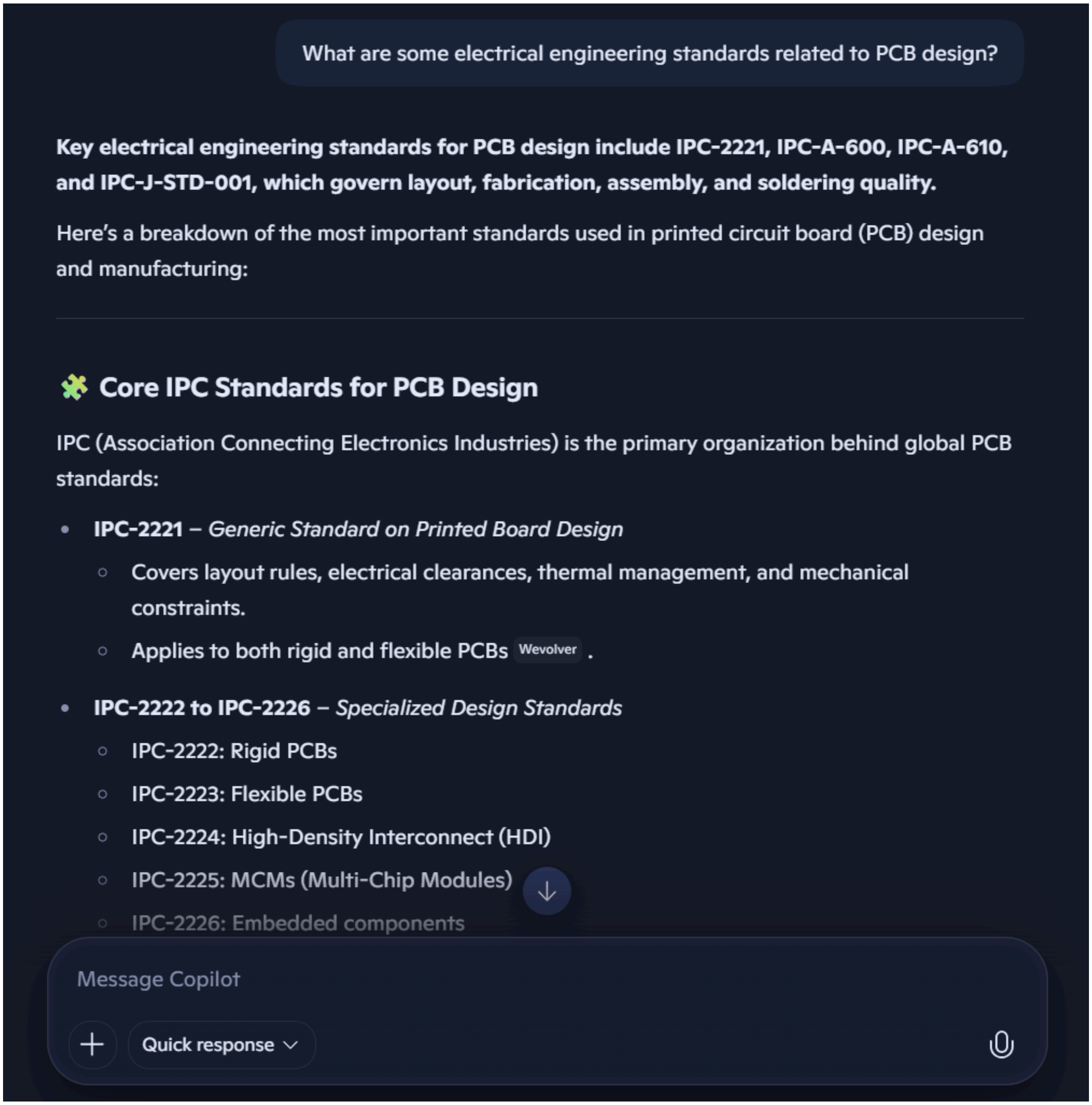

Case Study 1 Deepseek:

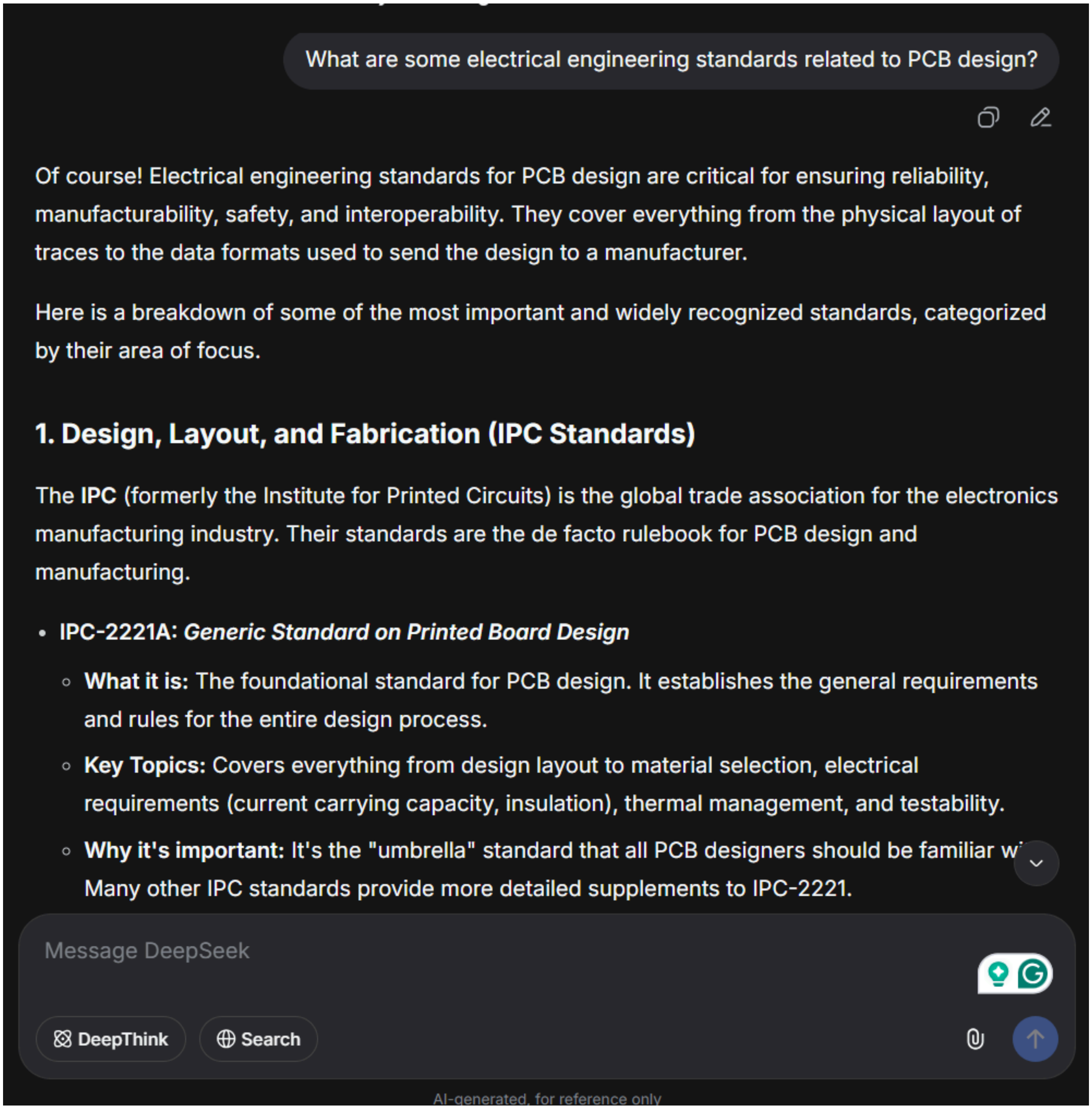

What are some electrical engineering standards related to PCB design?

Of course! Electrical engineering standards for PCB design are critical for ensuring reliability, manufacturability, safety, and interoperability. They cover everything from the physical layout of traces to the data formats used to send the design to a manufacturer.

Here is a breakdown of some of the most important and widely recognized standards, categorized by their area of focus.

1. Design, Layout, and Fabrication (IPC Standards)

The **IPC** (formerly the Institute for Printed Circuits) is the global trade association for the electronics manufacturing industry. Their standards are the de facto rulebook for PCB design and manufacturing.

- **IPC-2221A:** ***Generic Standard on Printed Board Design***
  - **What it is:** The foundational standard for PCB design. It establishes the general requirements and rules for the entire design process.
  - **Key Topics:** Covers everything from design layout to material selection, electrical requirements (current carrying capacity, insulation), thermal management, and testability.
  - **Why it's important:** It's the "umbrella" standard that all PCB designers should be familiar w
    Many other IPC standards provide more detailed supplements to IPC-2221.

Case Study 2 ChaptGPT:

An **MCU (Microcontroller Unit)** is essentially the "brain" of an embedded system. It's a small computer on a single chip that includes a **processor (CPU)**, **memory (RAM and Flash)**, and **peripherals** (like timers, ADCs, and communication interfaces). Its job is to **control** other components in the circuit and execute the program instructions you write.

Here's a breakdown of what it does:

- 🧠 **Processing:** The CPU executes code — performing logical and mathematical operations, making decisions, and running control loops.
- 💾 **Memory Management:** It stores your program (firmware) and any temporary data needed during execution.
- 🔌 **Peripheral Control:** The MCU interfaces with external devices (like sensors, actuators, displays, or communication modules) through digital I/O pins, analog inputs, or communication buses (I2C, SPI, UART, etc.).
- ⚙️ **Automation:** It continuously monitors inputs, processes data, and adjusts outputs accordingly — for example, reading a sensor value and turning on an LED when it exceeds a threshold.
- ⚡ **Timing & Control:** Built-in timers and interrupts allow precise timing control for events, PWM signal generation, and multitasking operations.

In your **X-ray dose rate detector project**, the MCU (like an ESP32) would:

- Read analog data from the **op-amp circuit** connected to the photodiode.
- Process that data to calculate the dose rate.
- Display the readings on the **LCD screen**.
- Log the data to an **SD card**.
- Potentially communicate wirelessly for data transfer or monitoring.

Case Study 2 Microsoft Copilot:

A **Microcontroller Unit (MCU)** is a compact integrated circuit designed to perform specific tasks in embedded systems. Think of it as a tiny computer that controls devices and processes in everything from kitchen appliances to industrial machines.

🧠 Core Functions of an MCU

- **Processing**: Executes instructions using its built-in CPU.
- **Memory**: Includes RAM (for temporary data) and flash memory (for storing programs).
- **Input/Output (I/O)**: Interfaces with sensors, buttons, displays, motors, and other peripherals.
- **Timing**: Uses internal timers and counters for precise control (e.g., blinking LEDs, generating PWM signals).
- **Communication**: Supports protocols like UART, SPI, I2C, CAN for talking to other devices.

🛠️ Common Applications

- **Consumer electronics**: Remote controls, washing machines, smart thermostats.
- **Automotive systems**: Engine control units, airbag sensors, infotainment.
- **Industrial automation**: Motor controllers, robotic arms, process monitoring.
- **Medical devices**: Glucose meters, heart rate monitors.
- **IoT gadgets**: Smart home devices, wearables, environmental sensors.

MCUs are prized for their low power consumption, small size, and cost-effectiveness. If you're curious about how MCUs differ from microprocessors or want help choosing one for a project, I can dive deeper!

Message Copilot

Quick response

Case Study 2 Deepseek:

Of course! This is a fundamental question in electronics.

In simple terms, an **MCU (Microcontroller Unit)** is a tiny, self-contained computer on a single chip designed to control a specific task or a set of tasks in an embedded system.

Think of it as a **dedicated brain for everyday devices.**

The Core Idea: The "All-in-One" Computer

Unlike the general-purpose CPU (Central Processing Unit) in your laptop or phone that handles many different tasks (browsing, videos, games), an MCU is designed to execute one specific program repeatedly and efficiently. It integrates all the essential components of a computer into one chip:

1. **Processor Core (CPU):** The "brain" that executes instructions from the program.
2. **Memory (RAM & Flash):**
   - **Flash Memory:** Stores the program you write (like its permanent "hard drive").
   - **RAM (Random Access Memory):** Provides temporary storage for data while the program is running.
3. **Peripherals:** This is the key to its usefulness. These are built-in circuits that allow the MCU to interact with the outside world. Common peripherals include:
   - **GPIO (General-Purpose Input/Output) Pins:** These are the physical pins on the chip that can

Message DeepSeek

DeepThink Search

Case Study 3 ChatGPT:

If I want an output voltage of 2.5V and the AXUV20HS1 photodiode produces 2.5 microamps of photocurrent at any given x-ray intensity, what feedback resistor should I use when constructing the TIA?

We'll use the **transimpedance amplifier equation** again:

$$V_{out} = -I_{photo} \times R_f$$

You want:

$$|V_{out}| = 2.5\,\text{V}$$

and

$$I_{photo} = 2.5\,\mu A = 2.5 \times 10^{-6}\,A$$

Now solve for R_f:

$$R_f = \frac{V_{out}}{I_{photo}} = \frac{2.5}{2.5 \times 10^{-6}} = 1.0 \times 10^{6}\,\Omega$$

✅ **Answer:**

You should use a **1 MΩ feedback resistor** to achieve a 2.5 V output at 2.5 µA photocurrent.

> Note: If your circuit inverts the signal (as TIAs normally do), the output will be –2.5 V. To obtain a positive 2.5 V instead, you could use a non-inverting stage after the TIA or reverse the diode orientation depending on your bias configuration.

Case Study 3 Microsoft:

If I want an output voltage of 2.5V and the AXUV20HS1 photodiode produces 2.5 microamps of photocurrent at any given x-ray intensity, what feedback resistor should I use when constructing the TIA?

To determine the appropriate feedback resistor R_f for your transimpedance amplifier (TIA), you can use the basic relationship:

$$V_{\text{out}} = I_{\text{photo}} \cdot R_f$$

Where:

- $V_{\text{out}} = 2.5\,\text{V}$ (desired output voltage)
- $I_{\text{photo}} = 2.5\,\mu\text{A} = 2.5 \times 10^{-6}\,\text{A}$

Solving for R_f:

$$R_f = \frac{V_{\text{out}}}{I_{\text{photo}}} = \frac{2.5}{2.5 \times 10^{-6}} = 1 \times 10^{6}\,\Omega = 1\,\text{M}\Omega$$

✅ Recommended Feedback Resistor: 1 MΩ

This will convert the 2.5 μA photocurrent into a 2.5 V output voltage. Make sure to consider bandwidth and noise implications when selecting such a high resistance—higher resistances can reduce bandwidth and increase thermal noise. Let me know if you'd like help optimizing for speed or noise performance too.

Case Study 3 Deepseek:

Important Practical Considerations for Your Design

While the calculation is simple, building a stable and accurate TIA, especially for a sensitive detector like the AXUV20HS1, requires a bit more attention.

1. **Op-Amp Selection:** This is critical. You must choose an operational amplifier with:
   - **Very Low Input Bias Current:** The op-amp's input bias current should be significantly smaller than your 2.5 µA photocurrent. A FET-input or CMOS-input op-amp is essential (e.g., OPA140, ADA4622-2, LMC6081).
   - **Low Input Offset Voltage:** This error will be multiplied by the non-inverting gain of your circuit.
   - **Sufficient Gain-Bandwidth Product (GBP):** The TIA circuit has a limited bandwidth, and a higher GBP op-amp will help achieve the desired bandwidth and stability.
2. **Stability and Bandwidth:** A large feedback resistor like 1 MΩ creates a significant time constant with the op-amp's input capacitance and the photodiode's capacitance. This can lead to oscillation.
   - You will almost certainly need a **feedback capacitor (C_f)** in parallel with the 1 MΩ resistor to compensate for this. Its value is typically in the picofarad range.
   - The value of C_f is chosen to provide phase margin and set the bandwidth. The bandwidth (f_{-3dB}) can be approximated by:
     $f_{-3dB} \approx \frac{1}{2\pi R_f C_f}$
   - Start with a small, variable capacitor (or a fixed capacitor in parallel with a smaller variable one) to tune for a clean output signal on an oscilloscope.
3. **Resistor Specifications:** Use a high-quality, low-noise, low-drift resistor for Rf, such as a metal film type. The tolerance (e.g., 1%) will directly affect your output voltage accuracy.
4. **Photodiode Biasing:** The AXUV20HS1 is a silicon photodiode that can be used in either photovoltaic (0V bias) or photoconductive (reverse bias) mode. Your TIA circuit is inherently a **photovoltaic mode** circuit, which is fine for many applications as it minimizes dark current.

In summary: Your calculated value of Rf = 1 MΩ is correct. For a practical circuit, be prepared to add a small feedback capacitor (e.g., 1-5 pF) in parallel with this resistor to ensure stability.

Case Study 4 ChatGPT:

1. Shot Noise (Photodiode and Dark Current)

Source:
Shot noise arises from the discrete nature of charge carriers flowing through the photodiode. It depends on the total diode current (signal + dark current).
Equation:

$$i_{n,shot} = \sqrt{2qI_D\Delta f}$$

where q is the electron charge, I_D is the diode current, and Δf is bandwidth.

Minimization:

- Use a **low-dark-current photodiode** (e.g., cooled or large-area devices with good surface passivation).
- Operate the photodiode in **photovoltaic (zero-bias)** mode to minimize dark current (though this slightly reduces speed).
- **Shield the detector** from stray light or background radiation.

---

2. Johnson (Thermal) Noise

Source:
Thermal agitation in resistors, especially the **feedback resistor** R_f in a transimpedance amplifier (TIA).
Equation:

$$v_{n,R} = \sqrt{4kTR_f\Delta f}$$

Minimization:

- Use the **lowest feasible feedback resistor value** consistent with the desired gain (balance against signal level).
- **Limit the bandwidth** using a feedback capacitor C_f to filter high-frequency noise.
- Use **metal-film resistors** with low excess noise.

---

3. Op-Amp Input Noise

Source:
The op-amp contributes both **voltage noise density** (e_n) and **current noise density** (i_n), both of which convert into output noise through the feedback network.

Minimization:

- Choose an **ultra-low input bias current op-amp** (e.g., OPA140, LTC6268, ADA4530-1 for femtoamp input currents).
- For high R_f designs, **current noise** dominates; choose a **JFET or CMOS-input** op-amp.
- Minimize op-amp **input capacitance** and **parasitic capacitance** between inverting input and ground.
- **Stabilize the TIA** using C_f across R_f to compensate for the photodiode capacitance.

---

4. Parasitic Capacitance and Leakage

Source:
Leakage currents and stray capacitances at PCB traces, solder flux residue, or between op-amp pins can add noise or cause instability.

Minimization:

- Use a **guard ring** around the op-amp input node connected to the same potential as the non-inverting input.
- Use **short traces**, minimize surface contamination, and clean the PCB to reduce leakage.
- Choose a **low-leakage PCB substrate** (e.g., FR4 may suffice, but PTFE or ceramic are better for ultra-low current).
- **Avoid solder mask** near the high-impedance input trace.

---

5. Electromagnetic Interference (EMI) and Ground Noise

Source:
External fields, switching power supplies, and digital traces coupling into the sensitive analog node.

Minimization:

- **Star grounding** to isolate analog and digital grounds.
- **Shield the circuit** in a metal enclosure (Faraday cage).
- Place **bypass capacitors** (e.g., 0.1 μF ceramic) near op-amp power pins.
- Separate analog and digital traces and add **ground planes** under the photodiode and op-amp.

Summary Table

Noise Source	Primary Cause	Mitigation Techniques
Shot noise	Photodiode current fluctuations	Low-dark-current diode, zero-bias mode
Johnson noise	Thermal noise in R_f	Reduce R_f, add feedback capacitor
Op-amp voltage/current noise	Op-amp input characteristics	Use low-noise JFET/CMOS op-amp
Leakage/parasitic capacitance	PCB contamination, long traces	Guard rings, clean PCB, short traces
EMI and ground loops	External coupling, shared return paths	Shielding, star ground, decoupling capacitors

---

Case Study 4 Microsoft Copilot:

🔊 Primary Noise Sources

1. **Thermal (Johnson) Noise**
   - Originates from resistors, especially the feedback resistor in the TIA.
   - **Formula:** $V_n = \sqrt{4kTR}$, where k is Boltzmann's constant, T is temperature, and R is resistance.
   - *Higher resistance = more noise.*
2. **Shot Noise**
   - Caused by the discrete nature of charge carriers in the photocurrent.
   - **Formula:** $I_n = \sqrt{2qI}$, where q is electron charge and I is photocurrent.
   - *Inherent to photodiode operation; cannot be eliminated but can be minimized by increasing signal strength.*
3. **Flicker (1/f) Noise**
   - Dominates at low frequencies and comes from the op-amp and other active components.
   - *More prominent in CMOS op-amps and poorly designed biasing circuits.*
4. **Op-Amp Voltage and Current Noise**
   - Voltage noise appears across the feedback resistor.
   - Current noise flows through the photodiode and input impedance.
   - *Critical in low-current applications where even picoamp-level noise matters.*

🛠️ Minimization Techniques

Op-Amp Design Choices

- **Low Input Bias Current:** Choose op-amps with femtoamp-level bias currents to avoid corrupting the photocurrent.
- **Low Input Voltage and Current Noise Specs:** Prioritize op-amps designed for precision and low-noise applications (e.g., OPA129, ADA4530-1).
- **Low 1/f Noise Corner:** Select op-amps with low flicker noise for DC or low-frequency applications.

Circuit Design

- **Optimize Feedback Resistor:** Balance between gain and thermal noise. Use lower resistance if thermal noise dominates, but ensure sufficient output swing.
- **Add Feedback Capacitor:** A small capacitor (pF range) in parallel with the feedback resistor stabilizes the TIA and limits bandwidth, reducing high-frequency noise.
- **Shielding and Guard Rings:** Use guard rings around sensitive nodes to prevent leakage currents and capacitive coupling.

PCB Layout Best Practices

- **Short Traces:** Minimize trace length from photodiode to op-amp to reduce parasitic capacitance and inductance.
- **Ground Plane:** Use a solid ground plane to reduce EMI and provide a low-impedance return path.
- **Isolate Analog and Digital Sections:** Prevent digital switching noise from coupling into the analog readout.
- **Clean Power Supply:** Use low-noise regulators and decoupling capacitors close to op-amp power pins.

📘 Additional Insights

- According to Texas Instruments, photodiode noise performance is highly sensitive to layout and component selection.
- Thorlabs emphasizes the importance of minimizing Johnson noise and using low-noise measurement instruments.
- Stanford's EE392B notes that modeling noise as current sources helps in accurate simulation and design.

Would you like help simulating a low-noise TIA circuit or selecting specific op-amps for your application?

Case Study 4 Deepseek:

Main Sources of Noise

Here are the primary noise sources, from typically most significant to least for a low-current TIA:

1. Johnson (Thermal) Noise of the Feedback Resistor

- **What it is:** The fundamental noise generated by the random thermal motion of electrons in any resistor. It sets the theoretical noise floor for a perfect circuit.
- **Formula:** $V_{n,R_f} = \sqrt{4kTR_f \cdot BW}$
  - k is Boltzmann's constant, T is temperature in Kelvin, R_f is the feedback resistance, and BW is the system bandwidth.
- **Key Point:** This noise voltage appears directly at the output. When referred to the input (RTI), it becomes a current noise: $I_{n,R_f} = \frac{\sqrt{4kTR_f \cdot BW}}{R_f} = \sqrt{\frac{4kT \cdot BW}{R_f}}$. This shows that a larger R_f actually gives lower current noise from the resistor, which is good for current-sensitive measurements.

2. Op-Amp Voltage Noise

- **What it is:** A noise source internal to the op-amp, modeled as a voltage source in series with the non-inverting input.
- **Impact:** This voltage noise appears directly at the output, but it's gain-boosted by the TIA's non-inverting gain at higher frequencies. The noise gain of a TIA is not 1; it peaks at high frequencies due to the photodiode capacitance (C_d) and feedback capacitance (C_f).
- **Key Point:** This is often the dominant noise source at higher frequencies, especially with large R_f values. The peak in the noise gain curve can amplify the op-amp's voltage noise significantly.

3. Op-Amp Current Noise

- **What it is:** A noise source internal to the op-amp, modeled as a current source flowing into each input terminal.
- **Impact:** The current noise flowing into the inverting input interacts with the feedback impedance (Z_f). The resulting voltage noise is $V_{n,out} = I_n \times Z_f$.
- **Key Point:** For a TIA with a large R_f, this is a critical specification. FET-input and CMOS-input op-amps have exceptionally low current noise (often in the fA/√Hz range), making them ideal for low-current applications like photodiode readouts. Bipolar op-amps have much higher current noise and are generally unsuitable.

4. Shot Noise from the Photodiode

- **What it is:** The fundamental quantum noise arising from the discrete nature of charge carriers (electrons and holes). It's present in both the photocurrent and the dark current.
- **Formula:** $I_{n,shot} = \sqrt{2q(I_{photo} + I_{dark}) \cdot BW}$
  - q is the electron charge, I_{photo} is the signal current, and I_{dark} is the diode's dark current.
- **Key Point:** For the AXUV20HS1 in photovoltaic mode (0V bias), the dark current is very low (picoamps), so this is usually a minor contributor compared to the Johnson and voltage noise in a well-designed circuit.

How to Minimize Noise through Op-Amp Design and PCB Layout

A. Op-Amp Selection and TIA Design (The "Design" Part)

1. **Choose the Right Op-Amp:**
   - **Input Bias Current:** Must be << your signal current. Choose a FET/CMOS op-amp (e.g., OPA141, ADA4610-1, LTC6268).
   - **Voltage Noise:** Select an op-amp with low voltage noise density (nV/√Hz). However, there's often a trade-off with power supply current.
   - **Current Noise:** As stated, a FET/CMOS op-amp is the correct choice here, as its current noise is negligible compared to other sources in this application.
2. **Bandwidth Limitation is Your Friend:**
   - The total integrated noise is proportional to the square root of the bandwidth ($\sqrt{BW}$). **Only use as much bandwidth as your signal requires.**
   - Use the feedback capacitor (C_f) not just for stability, but to set a precise bandwidth. The -3dB bandwidth is $f_{-3dB} = \frac{1}{2\pi R_f C_f}$. This filter dramatically reduces the integrated noise by cutting off the high-frequency noise peak.
3. **Optimize the Feedback Resistor:**
   - While a larger R_f gives more sensitivity, it also increases the Johnson noise voltage and the sensitivity to op-amp voltage noise (due to higher noise gain). There is an optimal value for a given bandwidth and photodiode capacitance. For your 1 MΩ requirement, this is a good value, but don't arbitrarily make it larger than needed.

B. PCB Layout (The "Art" Part - Crucial for Success)

A poor layout can ruin the performance of a perfect schematic.

1. **Guard Ring (The Most Important Technique):**
   - **What it is:** A conductive trace that completely surrounds the sensitive inverting input node (the photodiode connection and the op-amp's inverting input) and is driven at the same potential.
   - **How it works:** It actively diverts leakage currents from the high-impedance node to the guard ring, preventing them from flowing into the input. It also drastically reduces parasitic capacitance to other traces.
   - **Implementation:** Connect the guard ring to a low-impedance point at the same DC voltage as the inverting input. In a standard TIA, this is circuit ground. The guard ring should be on the same layer as the input traces and should also be implemented on inner layers if possible.
2. **Proper Grounding and Supply Decoupling:**
   - Use a solid ground plane to provide a low-impedance return path.
   - Place decoupling capacitors (typically a 100 nF ceramic and a 1-10 µF tantalum) as close as physically possible to the op-amp's supply pins. Their job is to shunt high-frequency noise on the supply lines directly to the ground plane.
3. **Minimize Capacitance at the Inverting Input:**
   - This node is extremely high-impedance. Keep the connection between the photodiode, the op-amp input, and the feedback components as small as possible. This minimizes parasitic capacitance, which improves stability and reduces the high-frequency noise gain.
4. **Use Surface-Mount Components (SMD):**
   - SMD components have much lower parasitic inductance and leakage than through-hole parts.
5. **Cleanliness (Conformal Coating):**
   - After assembly and testing, clean the board with a solvent suitable for removing flux residues. For extreme environments (high humidity), consider applying a conformal coating to prevent leakage currents across the board's surface, especially across the guard ring break.

By combining a carefully selected low-noise, low-I_b op-amp with a judiciously chosen C_f to limit bandwidth, and implementing a meticulous PCB layout centered around a proper guard ring, you can build a photodiode readout circuit whose performance is limited by fundamental physics (resistor Johnson noise and photodiode shot noise) rather than by design or layout artifacts.

Case Study 5 Chat GPT:

Key Factors in Selecting and Integrating Software for an Embedded System

When developing an embedded system in an engineering project, software choices play a crucial role in determining the system's performance, scalability, and reliability. The following factors should be considered when selecting and integrating software:

---

1. Hardware Compatibility

The software must align with the hardware platform's capabilities and constraints. Factors such as processor speed, available memory, communication protocols, and power consumption determine which programming languages, frameworks, and operating systems can be supported. For example, low-level languages like C or C++ are often used for microcontrollers due to their efficiency and control over hardware resources.

---

2. Real-Time Performance

Embedded systems often need to perform time-critical tasks. The software must ensure deterministic execution and minimal latency for processes such as data acquisition, control loops, or sensor monitoring. Choosing a real-time operating system (RTOS) or frameworks optimized for embedded use can help achieve these performance goals.

---

3. Development Tools and Environment

Selecting an appropriate integrated development environment (IDE), compiler, and debugging tools can significantly affect productivity. Consider the tool's compatibility with target hardware, available libraries, and ease of debugging. Popular options include platforms that support firmware frameworks, real-time task management, and integrated simulation or testing capabilities.

---

4. Software Architecture and Stack Design

The architecture should be modular and scalable. This includes decisions such as whether to use a layered architecture, which separates hardware abstraction from higher-level logic, or whether to integrate web-based interfaces for data visualization or control. If the system interacts with external networks or servers, the choice of software stack (e.g., for communication or web applications) should prioritize efficiency, security, and maintainability.

---

5. Resource Efficiency

Embedded devices have limited memory, processing power, and storage. The software must be optimized to use these resources efficiently. Code efficiency, memory management, and minimizing overhead from unnecessary libraries or services are key to maintaining performance and battery life.

---

6. Reliability and Safety

Reliability is paramount in embedded applications. Error handling, exception management, and watchdog mechanisms should be integrated into the software design to ensure system stability under unexpected conditions. For safety-critical systems, adherence to relevant safety standards and thorough testing procedures is essential.

---

7. Security

If the embedded system communicates with external devices or networks, software security becomes a critical consideration. Encryption, authentication protocols, and secure data handling practices help prevent unauthorized access or data breaches. It is also important to manage firmware updates securely to prevent exploitation.

---

8. Compliance with Standards and Constraints

Software should comply with applicable engineering and industry standards for communication protocols, data formats, and quality assurance. In addition, design must consider real-world constraints—such as economic limits, environmental factors, manufacturability, and sustainability—that affect software and hardware integration.

9. Maintainability and Scalability

A modular and well-documented codebase simplifies updates, debugging, and future improvements. Version control systems, structured documentation, and clear interface definitions allow new engineers to understand and expand the software as the project evolves.

10. Integration and Testing

Integration planning should begin early in development. Hardware-in-the-loop (HIL) testing, simulation, and validation procedures ensure the software performs correctly once deployed on physical hardware. Continuous integration and testing help identify compatibility issues early in the project timeline.

Summary

Selecting and integrating software for an embedded system involves balancing technical performance, compatibility, and long-term maintainability. The best solutions are those that are efficient, reliable, and scalable—capable of meeting real-time operational requirements while remaining flexible for future updates and improvements.

Case Study 5 Microsoft Copilot:

Selecting and integrating software for an embedded system is a critical step in engineering projects, especially where performance, reliability, and resource constraints are paramount. Here's a comprehensive breakdown of the key factors to consider:

🧠 1. System Requirements and Constraints

- **Real-time performance:** Does the system need hard or soft real-time capabilities?
- **Resource limitations:** Consider CPU speed, memory (RAM/ROM), and power consumption.
- **Latency and throughput:** Ensure the software meets timing and data processing needs.

🧩 2. Hardware Compatibility

- **Processor architecture:** Ensure the software supports the target microcontroller or processor (e.g., ARM, RISC-V).
- **Peripheral support:** Check for drivers and libraries for sensors, communication interfaces (SPI, I2C, UART), etc.
- **Board support packages (BSPs):** Availability of BSPs can significantly reduce integration effort.

🛠️ 3. Development Tools and Ecosystem

- **Toolchain support:** Availability of compilers, debuggers, and IDEs (e.g., GCC, Keil, IAR).
- **Simulation/emulation tools:** Useful for early testing and debugging.
- **Community and vendor support:** A strong ecosystem can accelerate development and troubleshooting.

🔐 4. Reliability and Safety

- **Fault tolerance:** Support for watchdogs, error detection, and recovery mechanisms.
- **Certifications:** Compliance with standards like ISO 26262 (automotive), DO-178C (aerospace), or IEC 61508 (industrial).
- **Testing frameworks:** Built-in support for unit testing, integration testing, and code coverage.

🧩 5. Software Architecture and Modularity

- **RTOS vs. bare-metal:** Decide based on complexity, timing, and multitasking needs.
- **Middleware availability:** Protocol stacks (e.g., TCP/IP, CAN, Modbus) and abstraction layers.
- **Scalability and portability:** Can the software be reused or scaled for future projects?

🔒 6. Security Considerations

- **Secure boot and firmware updates**
- **Data encryption and authentication**
- **Vulnerability management and patching mechanisms**

💰 7. Licensing and Cost

- **Open-source vs. proprietary:** Consider licensing terms, support, and long-term viability.
- **Total cost of ownership:** Include development, maintenance, and potential licensing fees.

🔄 8. Integration and Interoperability

- **APIs and interfaces:** Well-defined APIs simplify integration with other software modules.
- **Communication protocols:** Ensure compatibility with other system components (e.g., CAN, Ethernet, BLE).
- **Version control and CI/CD:** Support for modern development workflows.

📈 9. Performance Monitoring and Diagnostics

- **Logging and tracing tools**
- **Remote diagnostics and telemetry**
- **Profiling and optimization support**

Case Study 5 Deep Seek:

Category 1: Technical & Architectural Factors

These factors relate to the core technical capabilities and how the software fits into the system's architecture.

1. **Hardware Compatibility & Constraints:**
   - **CPU Architecture (ISA):** ARM (Cortex-A/M/R), RISC-V, x86, etc. The software must be compiled for the target ISA.
   - **Microcontroller/Microprocessor (MCU/MPU):** Specific chip variants and their capabilities (e.g., STM32, ESP32, NXP i.MX).
   - **Memory (RAM & Flash):** The software's memory footprint must fit within the available physical memory. This is often the most stringent constraint.
   - **Peripherals:** Does the software have drivers for the required peripherals (e.g., UART, I2C, SPI, USB, Ethernet, CAN, GPIO, ADC/DAC)?
   - **Real-Time Clock (RTC), Watchdog Timer (WDT):** Essential for many embedded systems; software must support their use.
2. **Real-Time Requirements:**
   - **Hard vs. Soft Real-Time:** Does a missed deadline cause a catastrophic failure (hard) or just degraded performance (soft)?
   - **Determinism:** The system must be predictable. This heavily influences the choice of **Real-Time Operating System (RTOS)** or even a bare-metal approach.
   - **Worst-Case Execution Time (WCET):** The software's tasks must have a known and acceptable WCET.
3. **Operating System & Kernel:**
   - **Bare-Metal (Super Loop):** Simple, low-overhead, full control. Best for very simple systems.
   - **Real-Time Operating System (RTOS):** e.g., FreeRTOS, Zephyr, VxWorks. Provides task scheduling, IPC, and resource management for complex applications.
   - **Embedded Linux:** e.g., using Yocto Project or Buildroot. For powerful MPUs with rich feature sets, networking, and GUI requirements.
   - **Proprietary OS:** For specific, high-reliability domains (e.g., aerospace, medical).
4. **Performance & Footprint:**
   - **CPU Load:** Can the processor handle the software's computational demands while running all other tasks?
   - **Memory Usage:** Code size (Flash) and runtime memory (RAM). Minimizing this is a key goal.
   - **Power Consumption:** Software directly impacts power use (e.g., sleep modes, clock speeds, peripheral management). Critical for battery-operated devices.

peripheral management). Critical for battery-operated devices.

5. **Software Ecosystem & Dependencies:**
   - **Libraries & Middleware:** What third-party libraries are needed (e.g., communication stacks like MQTT, CoAP; security libraries like mbed TLS; graphics libraries like LVGL)?
   - **Compiler & Toolchain:** Availability and quality of the toolchain (e.g., GCC, Clang, IAR, Keil).
   - **Hardware Abstraction Layers (HALs):** Does the vendor provide a good HAL? This can drastically reduce porting effort.

Category 2: Development & Lifecycle Factors

These factors impact the engineering team's ability to develop, test, and maintain the software.

1. **Development Tools & Debugging:**
   - **IDE & Editor Support:** Is there a good development environment?
   - **Debugging Capabilities:** Support for JTAG/SWD, printf debugging, kernel logs, and profiling tools.
   - **Simulation/Emulation:** Can the software be tested without physical hardware? This accelerates early development.
2. **Licensing & Cost:**
   - **Open Source (e.g., GPL, Apache, MIT):** Understand the obligations (e.g., GPL may require releasing your source code). MIT/BSD licenses are very permissive.
   - **Commercial/Proprietary:** What are the licensing fees (per-unit royalty, one-time fee)? Does it fit the project's budget?
   - **Total Cost of Ownership (TCO):** Includes initial cost, development time, maintenance, and royalty fees.
3. **Documentation & Community Support:**
   - **Quality of Documentation:** Is it complete, accurate, and has good examples?
   - **Community & Forums:** A vibrant community is invaluable for troubleshooting.
   - **Vendor Support:** For commercial software, the quality and responsiveness of technical support is crucial.
4. **Long-Term Viability & Roadmap:**
   - **Is the software actively maintained?** You don't want to rely on abandoned software.
   - **Update & Patch Policy:** How are security vulnerabilities and bugs addressed?
   - **Long-Term Support (LTS):** Important for products with long lifecycles.
